SAPIENZA
UNIVERSITÀ DI ROMA

PHD IN BIOCHEMISTRY

CYCLE XXXI (A.A. 2015-2018)

Impairment of insulin signaling cascade favors the development of Alzheimer disease pathology by altering APP processing in the brain

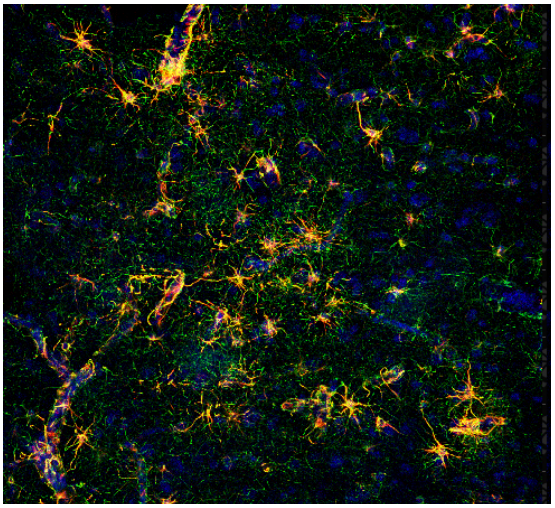

Supervisor

Dr. Eugenio Barone

Coordinator

Prof. Stefano Gianni

PhD Candidate

Francesca Triani

SAPIENZA
UNIVERSITÀ DI ROMA

PHD IN BIOCHEMISTRY

CYCLE XXXI (A.A. 2015-2018)

Impairment of insulin signaling cascade favors the development of Alzheimer disease pathology by altering APP processing in the brain

Supervisor

Dr. Eugenio Barone

Coordinator

Prof. Stefano Gianni

PhD Candidate

Francesca Triani

E senti allora, se pure ti ripetono che puoi,
fermati a mezza via o in alto mare,
che non c'è sosta per noi,
ma strada, ancora strada,
e che il cammino è sempre da ricominciare.

Eugenio Montale

INDEX

List of Abbreviations:

3-NT: 3-nitrotyrosine

4E-BP: 4E-binding protein

AD: Alzheimer disease

AICD: amyloid intracellular C-terminal fragments

aMCI: amnistic MCI

AP-1: Activator protein 1

APLP1/2: APP-like protein 1/2

ApoE4: ApolipoproteinE-4

APP: amyloid precursor protein

Aβ: amyloid b (Ab)-peptide

BACE-1: beta-site amyloid precursor protein-cleaving enzyme 1

BBB: Blood brain barrier

BIR: Brain Insulin resistance

BR: Bilirubin

BV: Biliverdin

BVR-A: Biliverdin reductase-A

CK1: casein kinase 1

CNS: Central Nervous System

CSF: cerebrospinal fluid

CTF: carboxyl terminal fragment

DIAD: Dominant inherited AD

DM: diabetes mellitus

DNPH: dinitrophenylhydrazine

EAD: early AD

ER: endoplasmic reticulum

ERK1/2: Signal-regulated kinases 1/2

FAD: Familial AD

FOXO3: Forkhead box O3

GDP: guanosine diphosphate

GLUT4: glucose transporter type 4

GPX: Glutathione peroxidase

GRB2: growth factor receptor-bound protein 2

GSK3β: glycogen synthase kinase 3β

GTP: guanosine triphosphate

H2O2: hydrogen peroxide

HNE: 4-hydroxy-2-nonenal

HO-1: Heme oxygenase 1

HO•: hydroxyl radical:

IAPP: islet amyloid polypeptide

IGF-1R: Insulin-like growth factor receptors

INI: Intranasal insulin

IR: Insulin receptor

IRS: Insulin receptor substrate

JNK1: c-Jun N-terminal kinases

LAD: Late-stage AD

MAPK: Mitogen-activated protein kinases

MCI: mild cognitive impairment

mTOR: mammalian target of rapamycin

NFTs: neurofibrillary tangles

NO•: nitric oxide

O2−•: superoxide radical anion

ONOO−: peroxynitrite

OS: Oxidative stress

P70S6K: Ribosomal protein S6 kinase beta-1

PC: protein carbonyls

PCAD: preclinical AD

PDK1: phosphoinositide-dependent kinase 1

PH: pleckstrin homologe

PI3K: Fosfoinositide 3-chinasi

PIKK: phosphatidylinositol 3-kinase-related kinase protein

PIP_3: phosphatidylinositol (3,4,5)-triphosphate

PKB: protein kinase B /AKT

PKC: protein kinase C

PKR: protein kinase R

PS1/PS2: Presenil-1/2

PTB: phosphotyrosine-binding

PTEN: phosphatase and tensin homolog

PUFAs: Polynsatured fatty acid

rER: rough endoplasmic reticulum

RNS: Reactive nitrogen species

ROS: Reactive oxygen species

SAD: Sporadic AD

sAPPα/β: soluble APP α/β

SH2: Src Homology 2

SHIP: SH2 domain containing inositol-5-phosphatase

siRNA: Small-interfering RNA

SOCS: suppressor of cytokine singalling

SOD1: Superoxide dismutase

SOS: Son of seven less

SPs: senile plaques

SRP: signal recognition particles

T2D: type 2 diabetes

TGN: Trans-Golgi network

TNFα: Tumor necrosis factor α

1. INTRODUCTION

1. Alzheimer's Disease

In 1907, Aloïs Alzheimer related in the article "On an unusual Illness of the Cerebral Cortex" the uncommon case of a 51-year-old patient who was suffering from memory loss, disorientation, hallucinations and cognitive impairment. After the death of the patient, *post mortem* examination showed an atrophic brain with "striking changes of the neurofibrils" and "minute military foci" caused by the "deposition of a special substance in the cortex" [1]. One century later, this "unusual illness" named Alzheimer's disease (AD) has become the most widespread neurodegenerative disease whose etiology is still unknown [2].

AD is an age-related neurodegenerative disorder and is the most common form of dementia in the elderly people, accounting for 50% to 70% of cases. Approximately 10–30% in the population over 65 years of age, 15-20% over age 75, and 25-50% over age 85 are affected by dementia. The major prevalence is in Asia (22.9 million people) while Europe and the Americas account for 10.5 and 9.4 million people, respectively [3]. According to the World Alzheimer Report, 46.8 million people worldwide are afflicted with AD; this number is expected to increase to 131 million people by the year 2050 [4, 5].

It is characterized by a progressive deterioration of cognitive functions that can be linked to a significant reduction of the volume of the brain in AD patients as compared to healthy patients. The atrophy results from the degeneration of synapses and the death of neurons, in particular in

hippocampus, the brain region playing a role in memory and spatial orientation. The age is the highest risk factor for AD, the risk of developing the disease reaching 50% for individuals beyond age 85 [3]. Interesting, because of higher life expectancy and the decrease in estrogen levels due to menopause, women are more susceptible than men to develop AD [6].

Pathologically, apart a loss of synapses, AD is identify by an increase in the number of extracellular amyloid beta-peptide (Aβ)-rich senile plaques (SPs), derived from the cleavage of amyloid precursor protein (APP), and an increase in intracellular neurofibrillary tangles (NFTs) composed of aggregated hyper phosphorylated Tau, a microtubule stabilizing protein [7, 8].

There are two major forms of AD: the sporadic (SAD) and the familial (FAD). Most patients with Alzheimer's disease (>95%) have the SAD, which is characterized by a late onset (80–90 years of age), and it is the consequence of the failure to clear Aβ peptide from the interstices of the brain. A small subset (<10%) of AD cases have autosomal dominant inherited Alzheimer's disease (DIAD) and have an early age of onset (mean age of ~45 years). Individuals living with Down's syndrome (also called trisomy 21) have an increased risk of early-onset AD because they carry an extra copy of chromosome 21 in which is located the gene responsible for APP formation [9]. Mutations of several genes encoding APP, PS1 and PS2, which cause overproduction or formation of an aberrant form of Aβ, have been found to cause mainly early-onset AD [10, 11], while apolipoprotein E4 (ApoE4) (involved in Aβ clearance) is considered as being the most common high genetic risk factor for late-onset AD [12].

From a clinical point of view, AD is characterized by a decline in episodic memory that is often mistaken for normal cognitive deficiencies due to aging. Because the pathology remains hidden within the brain tissue and the high presence of co-morbidities, such as cerebrovascular disease and hippocampal sclerosis, clinical diagnosis remains inherently error prone and subjective. The National Institute of Neurological and Communicative Disorders and Stroke in conjunction with the Alzheimer's Disease and Related Disorders Association (NINCDS-ADRDA) have established valid clinical and research criteria, based on the use of conventional clinical, laboratory, and imaging techniques, for the diagnosis of probable, and possible AD [13]. Even if, an accuracy diagnosis during life is as high as 85% due to modern imaging and laboratory techniques, a definite diagnosis of AD can only be made by biopsy or with specimens obtained at an autopsy [14].

The progression of this disease can be stratified into four main stages: preclinical AD (PCAD), mild cognitive impairment (MCI), early AD (EAD) and late-stage AD (LAD). PCAD is defined as the potential stage of AD in which the patient presents as a fully functional individual in cognitive exams, yet the growing pathology within the brain tissue is present [15]. MCI has been described as being the transition stage between normal cognition and EAD, and is subdivided intro both amnestic MCI (aMCI) and non-amnestic MCI [16]. Pathologically, each stage differs in that both amyloid plaques and NFTs increase in distribution and density from MCI to LAD.

1.1 Amyloid precursor protein

APP is a member of a family of related proteins that includes APP-like protein 1 (APLP1) and 2 (APLP2). They are single-pass transmembrane proteins with a large extracellular domain and a short cytoplasmatic region that undergo similar processing. The Aβ domain is unique to the APP, though the family shares several other conserved domain such as the E1 and E2 domains in the extracellular sequence [17]. Although the native biological role of this protein is obvious of interest to AD, APP is involved in several physiological functions such as neuritis outgrowth, synaptogenesis, neuronal protein trafficking, cell adhesion and calcium metabolism [18, 19].

The human APP gene, located on chromosome 21, was first identified in 1987 [20] and 8 isoforms arising from alternative splicing of that. The 3 isoforms most common are: APP695, which is expressed predominantly in the CNS, APP751 and APP770, which are more ubiquitously expressed. Mutations in critical regions of APP, including the region that generates Aβ, are causative of the hereditary form of familial AD and a related condition of hereditary cerebral amyloid angiopathy [21, 22].

Full-length APP is produced in large quantities in neurons and is metabolized very rapidly. It is synthesized in the endoplasmatic reticulum (ER) and then transported through the Golgi apparatus to the trans-Golgi-network (TGN), where can be transported to the cell surface or directly to an endosomal compartment. Crucial steps in APP processing occur at the cell surface and in the TGN. Sequential secretase cleavage of the APP occurs by two pathways: Non-amyloidogenic processing and Amyloidogenic processing. Both processes generate soluble ectodomains (sAPPα and sAPPβ) and identical amyloid intracellular C-terminal fragments (AICD).

Although under physiological conditions, the majority (≈ 90%) of APP processing undergoes non-amyloidogenic processing via α-secretase cleavage within the Aß domain, changes in the balance between amyloidogenic and non-amyloidogenic APP processing has the potential to affect dramatically Aß generation and accumulation.

Over to secretase cleavage, APP can be cleaved by caspases (predominantly caspase-3) at position Asp664 within the cytoplasmic tail during apoptosis to generate a potentially cytotoxic peptide containing the last 31 amino acids of APP (called C31). Additional γ-cleavage generates the fragment containing the region between γ – and caspase-cleavage sites called JCasp [23, 24], which has been reported to play a minor role in cytotoxicity.

Cleavage of APP by α-secretase precludes Aß generation, as the cleavage site is within the Aß domain, and releases a large soluble ectodomain of APP (sAPPα) and an 83-residue carboxy-terminal fragment (APP C-83). A-secretase is a zinco metalloproteinase, which cleaves APP primarily at the plasma membrane. Several members of the ADAM (a disintegrin and metalloproteinase) family possess α-secretase-like activity and three of them have been suggested as the α-secretase: ADAM9, ADAM10 and ADAM17. sAPPα has an important role in neuronal plasticity/survival and is protective against excitotoxicity. Moreover, it regulates neuronal stem cell proliferation and is important for early CNS development. The CFT, once formed, is cleaved by γ-secretase to generate p83 and the APP intracellular domain (AICD). The p83 fragment is rapidly degraded and widely believed to possess non-important function [25].

The first step in Aß generation is the cleavage of APP by beta-site amyloid precursor protein-cleaving enzyme 1 (BACE1), a β-secretase [26].

ß-cleavage releases a soluble APPβ fragment (sAPPβ) and a 99-residue carboxy-terminal fragment (APP C-99). Although sAPPβ only differs from sAPPα by lacking the Aß1-16 region at its carboxyl-terminus and it was reported to function as a death receptor 6 ligand, mediate axonal pruning and neuronal cell death [27]. After the ß-cleavage the βCTF remain membrane-associated and will be further cleaved by γ-secretase. Since these APP CTF is intermediate products, their functions have been less characterized. However, overexpression of APP βCTF was found to be cytotoxic and cause neuronal degeneration, perhaps by perturbing APP signal transduction [28]. γ-cleavage can yield both $Aß_{40}$, the majority species of Aß in the brain, and $Aß_{42}$, as well as release the intracellular domain of APP (AICD).

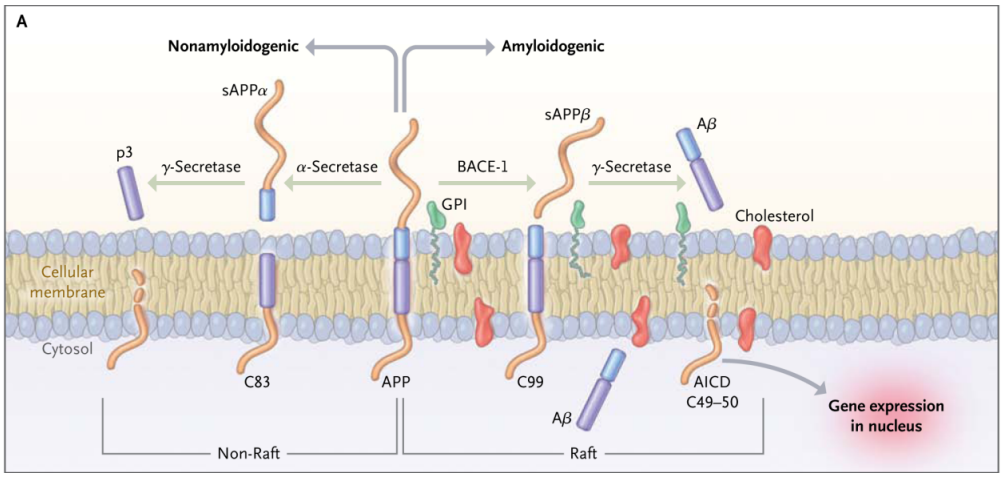

Figure 1. Schematic representation of APP processing. The APP processing occurs in two distinct pathways: non-amyloidogenic and amyloidogenic. The amyloidogenic pathway involves the sequential cleavage of APP by β-secretase, which releases a sAPPβ and the β-CTF. This is cleaved by γ-secretase, generating AICD and releasing Aβ. In the non-amyloidogenic pathway APP are cleaved at the α-secretase site within the Aβ-domain releasing sAPPα and the α-CTF. Proteolytic cleavage of α-CTF by γ-secretase releases AICD and p3 fragment.

1.1.1 BACE1

In 1999-2000, several groups identified BACE1 (called Asp2 or memapsin 2) as the major ß-secretase. BACE1 has two aspartic protease active site motifs, DTGS (residues 93-96) and DSGT (residues 289-292), and mutation of either aspartic acid renders the enzyme inactive [29]. Like other aspartic proteases, BACE1, has an N-terminal signal sequence (residues 1-21) and a pro-peptide domain (residues 22-45) that are removed by post-translational modification [30]. Moreover, it has a single transmembrane domain near its C-terminus (residues 455-480) and a palmitoylated cytoplasmic tail [31, 32].

The cell biology of BACE1 was investigated in order to further understand BACE1 regulation and to identify other potential therapeutic targets in the ß-secretase pathway. It is initially synthesized in the endoplasmic reticulum (ER) as an immature precursor protein (proBACE1) with a molecular weight of ≈ 60 kDa. ProBACE1 is short–lived and undergoes rapid maturation, in the Golgi, into a 70 kDa form, which involves the addition of complex carbohydrates and removal of the propeptide domain [33]. The majority of BACE1 molecules are localized within Golgi and endosomal compartments, where they co-localize with ßAPP [29, 34]. The acidic pH optimum of BACE1 indicates that it is predominantly active within late Golgi compartments and/or endosomes/lysosomes. This is consistent with previous findings demonstrating that ß-secretase cleavage of ßAPP can occur in all of these acidic compartments [35, 36].

Interesting, it has been reported that BACE1 is re-internalized from

the cell surfaces to early endosomes and can recycle back to the cell surface, where is available to cleave APP again. The intracellular trafficking is largely controlled by a dileucin motif in the cytoplasmic tail of BACE1 [37]. This signal is located close to a negatively charged domain, which contains a potential phosphorylation site. BACE1 is phosphorylated within its C-terminal and that the biological function of BACE1 phosphorylation resides in the regulation of the retrieval of re-internalized BACE1 from endosomes [38]. Walter et colleagues identified a single phosphorylation site on serine residue 498 in the C-terminal domain of BACE1 and that casein kinase 1 (CK1) can phosphorylate BACE1 at the serine residue [38]. The phosphorylation site, which is preceded by a stretch of acidic amino acid residues, represents a canonical recognition motif for CK1, but not for glycogen synthase kinase 3β or cyclin-dependent kinases. Even if the mechanisms through which this kinase influences BACE1 trafficking is still unknown, we cannot exclude the possibility that the phosphorylation may have subtle effects on βAPP processing and may be altered during the pathogenesis of AD.

CK1 consists of a family of eight genes, which appear to function as monomeric enzymes: α, γ1, γ2, γ3, δ, ε1, ε2, and ε3, but only CKIα, CKIδ and CKIε are elevated in human AD hippocampus. Family members contain a highly conserved N-terminal catalytic domain of ≈290 residues coupled to a variable C-terminal region that ranges in size from 40 to 180 aa. It is present in both the cytosol and the nucleus but the C-terminal region of that promote differential subcellular localization of individual isoforms (e.g., cellular membrane versus cytoplasm) [39, 40]. A number of proteins have been found to interact with CK1 isoforms in several tissues resulting in its targeting to specific signaling pathways [41, 42].

Moreover, several lines of evidence suggest that constitutively active CK1ε increases the formation of Aβ. The mechanism by which CK1ε activity leads to the regulation of Aβ formation is still unknown [43].

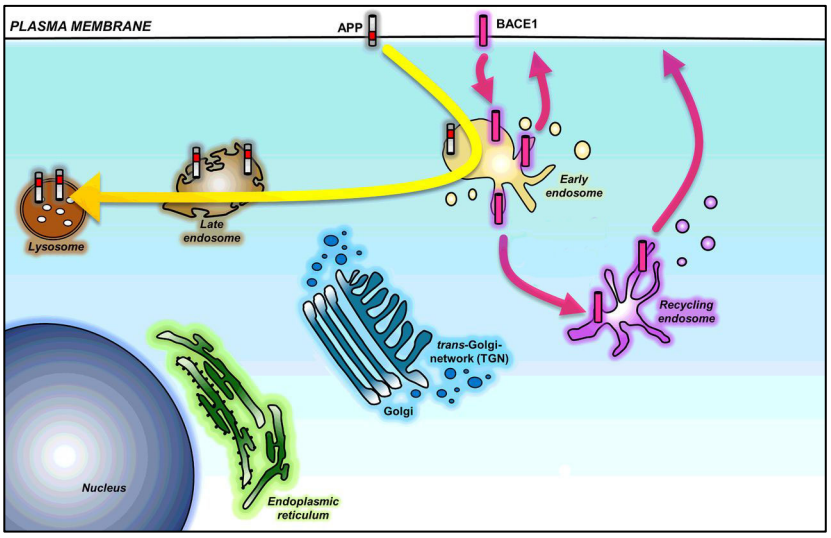

Figure 2. Intracellular trafficking of BACE1. BACE1 are internalized from the cell surface in the early endosomes. From the early endosomes, the intracellular trafficking itineraries of BACE1 is trafficked to the late endosome/lysosome and then it is transported to the recycling endosomes before being recycling back to the cell surface.

1.1.2 Amyloid beta function

The toxic effects of Aß have been explored widely but a few studies in the past decade have also highlighted its physiological roles in maintaining a healthy nervous system in a concentration-dependent manner [44]. The physiological processes positively influenced by Aß are neurogenesis, synaptic plasticity, memory formation, calcium homeostasis, metal sequestration and antioxidant properties [45].

There are two main toxic species of Aß, $Aß_{40}$ and $Aß_{42}$. The last one has two extra hydrophobic amino acids compared to $Aß_{40,}$ which promotes greater fibrilar formation in $Aß_{42}$ and is known to be more toxic. Once Aß is produced, individual amyloid peptides, ($Aß_{42}$ in particular) spontaneously self-aggregates to form small multiple coexisting physical forms. One forms consists of oligomers (2 to 6 peptides), which coalesce into intermediate assemblies [46]. ß-amyloid can also grow into fibrils, which arrange themselves into ß-plated sheets to form the insoluble fibers of advanced amyloid plaque. Soluble oligomers and intermediate amyloids are the most neurotoxic forms of Aß. Although the majority of Aß is secreted out of the cells, it can be generated in several subcellular compartments, such as the ER, Golgi/TGN, and endosome/lysosome. In addition, extracellular Aß can be internalized in the cell for degradation.

However, since Aβ has been found in healthy brain in soluble form but in aggregated form in AD patient brain [47], a hypothesis has been proposed to explain the formation of the senile plaques. The amyloid cascade hypothesis formulated in the early 1990s [48] has become a dominant model for AD pathogenesis [49]. The hypothesis proposed that an abnormal

extracellular increase of Aβ levels in brain could lead to Aβ aggregation into β-sheet rich structures. Aggregation starts with the formation of oligomers species that are reorganized into protofibrils and fibrils, found in amyloid plaques. Oligomers accumulated in AD patient brains are suggested to be the more toxic species for cells [50, 51], as they can in particular permeabilize cellular membranes, thus initiating a series of events leading to cell dysfunction and death .

1.2 Oxidative damage

Accumulation of Aβ impairs mitochondrial redox activity, increases the generation of reactive oxygen (ROS) and reactive nitrogen species (RNS). In AD and in the normal aging brain, they cause considerable oxidative stress (OS), which in turn contribute to lipid and protein damage [52, 53]. Mounting evidence suggests an important role played by biometals including iron, zinc and copper in Aβ and neurodegeneration [54]. In concordance with those findings, there are high affinity binding sites for copper and zinc on the N-terminal metal-binding domains of Aβ and its precursor APP while copper is a potent mediator of the highly reactive hydroxyl radical ($OH^{\bullet}$), and consequently contributes to the increase of oxidative stress characteristic of AD brain according to the high concentration of copper found in amyloid plaques [55]. This seems to be associated with the length of Aβ fragments, with $A\beta_{42}$ being more toxic than $A\beta_{40}$ and the most likely candidate to generate hydrogen peroxide and other ROS.

OS is induced by an imbalance in the redox state, involving the generation of excess reactive oxygen species (ROS) or the dysfunction of the antioxidant system. A major protective system of the cell is the “team” of antioxidant enzymes such as superoxide dismutase (SOD), glutathione peroxidase (GPx), glutaredoxins, thioredoxins and catalase. A reduction or a loss of function of the antioxidant enzymes, as indexed by decreased specific activity, has been reported in AD [56]. Proteins are highly susceptible to oxidative damage that inevitably affects secondary and tertiary structure resulting in irreversible modification of protein shape and, consequently, function. These modifications include dissociation of subunits, unfolding, exposure of hydrophobic residues, aggregation and backbone fragmentation among others [57] .

There are three major indices of protein oxidation that are detectable by standard methods: protein carbonylation (PC), protein nitration (3-NT) and protein bound-4 hydroxynonenal (HNE).

Protein carbonyl groups are generated from the direct oxidation by ROS of various side chains of amino acid residues (Lys, Arg, Pro, Thr, His and others) by the extraction of hydrogen atoms by alpha carbons and by cleavage of the peptide chain. This global oxidation process is referred to “primary protein carbonylation”, a product that could be detected by the reaction with 2,4-dinitrophenylhydrazine (DNPH), forming DNP-hydrazones [58].

Protein tyrosine nitration (3-NT) is a well-characterized chemical modification and normally is considered an irreversible form of protein damage, and therefore a robust biomarker of nitrosative stress [59]. Protein nitration occurs following formation of peroxynitrite (ONOO−) from superoxide (O2•−) and nitric oxide (NO•).

Lipid peroxidation is one of the main events causing redox imbalance

and subsequent build-up of oxidative damage within the cell. Lipid peroxidation is able to damage directly membranes, because ROS attack polyunsaturated fatty acids (PUFA) in the lipid bilayer. Neuronal membranes are particularly rich in PUFAs, that are broken down and release elevated levels of reactive electrophilic aldehydes, able to bind covalently proteins by forming adducts with specific amino acids. According to a number of factors, such as acyl chain length and degree of unsaturation, the lipid hydroperoxide that is formed by reaction of a carbon radical with oxygen, can form malondialde-hyde, 4-hydroxy-2- trans-nonenal (HNE) and acrolein, among other products of lipid peroxidation. Among these, HNE is a highly reactive and is produced primarily in the brain via lipid peroxidation of arachidonic acid, highly abundant omega- 6 PUFA components of neuronal membranes.

Increased damage to proteins, detected using proteomics approaches, show that specific proteins are modified by OS and that this alteration can contribute to the impairment of several key pathogenic pathways [60].

2. Insulin: structure and biosynthesis

Until the end of the 1950s, insulin was considered only as a hormone secreted by the β cells of the pancreatic islets of Langerhans and maintains normal blood glucose levels facilitating the absorption of cellular glucose, regulating the metabolism of carbohydrates, lipids and proteins and promoting cell division and growth through its mitogenic effects.

Insulin consists of two polypeptide chains: α, consists of 21 amino acids, and β, consists of 30 amino acids. The two chains are linked together by two disulfide bonds; an additional disulfide is formed within the α chain. The secreted insulin consists of 51 amino acids with a molecular weight of 5.8 kDa. However, the insulin gene encodes a 110-amino acid precursor known as preproinsulin. As with other secreted proteins, preproinsulin contains a hydrophobic N-terminal signal peptide, which interacts with cytosolic ribonucleoprotein signal recognition particles (SRP) [61]. SRP facilitates preproinsulin translocation across the rough endoplasmic reticulum (rER) membrane into the lumen. This process occurs via the peptide-conducting channel, where the signal peptide from preproinsulin is cleaved by a signal peptidase to yield proinsulin [62]. In the ER the proinsulin, after a conformation changing is transported to the trans-Golgi network (TGN) where it enters immature secretary vesicles and it is cleaved to yield insulin and C-peptide. Insulin and C-peptide are then stored in these secretory granules together with islet amyloid polypeptide (IAPP or amylin) and other less abundant β-cell secretary products [63, 64].

The β-cells respond to many nutrients in the blood circulation, including glucose, other monosaccharaides, amino acids and fatty acids. Glucose is the primary stimuli for insulin release in some animal species, because it is a principal food component and can accumulate immediately after food ingestion.

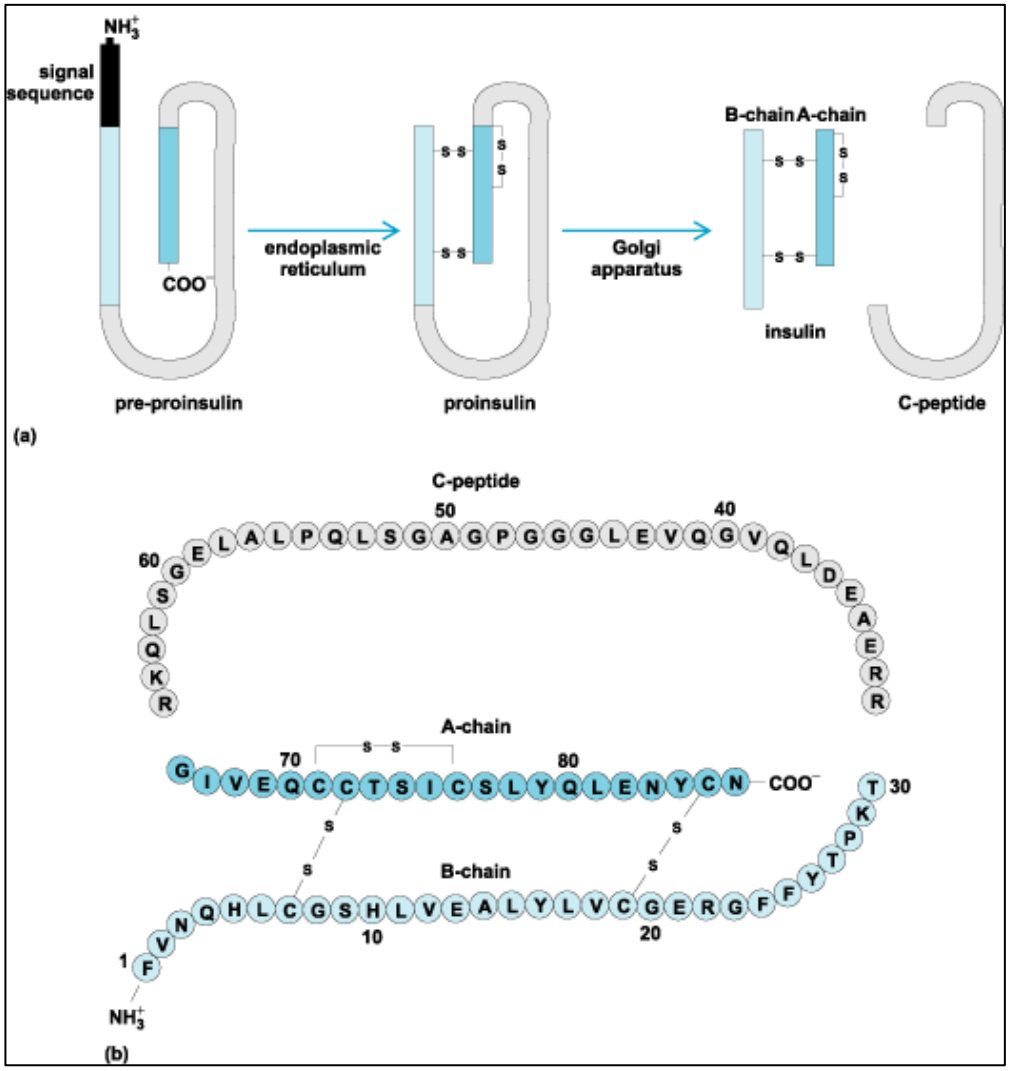

Figure 3. Insulin structure and biosynthesis

2.1 Cerebral Insulin

In the late 1970s, the central nervous system (CNS) was not considered an insulin-dependent tissue, but now it is well known that insulin plays a major physiologic role in this tissue and its disturbances, being involved in certain neurodegenerative states, such as Alzheimer's disease (AD). The presence of insulin in the brain was first detected by Havrankova, who used radioimmunoassay to determine high levels of insulin in brain extracts [65]. Likewise, they reported that insulin content in the brain was independent of the peripheral insulin, since circulating insulin levels had no effect on the brain's insulin concentration [66].

The notion that insulin could cross the Blood brain barrier (BBB) was first suggested by Margolis and Altszuler, who showed that insulin levels in the Cerebrospinal fluid (CSF) of rats increased slightly after peripheral infusions of this hormone suggesting that insulin crossed the BBB possibly by means of a saturable transport system [67]. These results were later confirmed in dogs after the intravenous administration of insulin [68]. They found a large, rapid increase in blood insulin, but a relatively small increase in the hormone in the CSF. These findings confirmed a non-linear correlation between plasma and CSF levels of insulin, providing the first evidence for a saturable transport system for this hormone from blood to the brain. Although there is no direct evidence on whether the insulin transport system and the Insulin receptor (IR) are the same protein, this seems to be widely assumed, as they have similar physicochemical properties (saturability, specificity, affinity, immune neutralization, cooperative interactions, and kinetics of dissociation) [67, 69]. On the other hand, differences in the activity of the BBB transporter system may be responding to regional

differences in insulin permeability, and also to the hormone concentration, recording the highest values in the pons, medulla, and hypothalamus, and the lowest in the occipital cortex and thalamus [70]. This insulin transport may be regulated by multiple factors, such as glucocorticoids, or by several pathophysiological situations, such as obesity, diabetes mellitus (DM), AD or the physiological aging process [71] .

Evidence also exists that insulin can be produced *de novo* in brain regions such as the hippocampus, prefrontal cortex, olfactory bulb and entorhinal cortex [65, 72, 73]. While the significance of this evidence is still debated, recent studies show that functional insulin signaling components in forebrain regions may exert a neuroprotective role in areas responsible for various functions of memory [74, 75].

2.1.1 Mechanisms of insulin signaling transduction in the brain

IR is tetrameric glycoproteins that belong to the receptor tyrosine kinase (Tyr) well studied with regard to its function in the regulation of peripheral glucose metabolism. Although expression of the insulin receptor in the brain was discovered decades ago [65, 76], insulin receptor function in this classic 'insulin-insensitive' organ remains largely unknown. Recent studies in neuronal cell culture suggest that insulin receptor signaling regulates several neuronal functions, including spine density and neurite growth [77, 78]. It is composed of two ligand-binding sites, disulfide-linked extracellular α subunits, which are linked by disulfide bonds to two

membrane-spanning β subunits. The α subunit is predominantly hydrophilic in nature, lacks membrane anchor regions, and contains 15 potential N-glycosylation sites and 37 cysteine residues. The β subunit contains a portion that is extracellular, a portion that comprises the transmembrane region of the receptor, and a portion that is intracellular, and which possess inherent tyrosine-protein-kinase activity [79]. Interestingly, two different isoforms of IR have been found in mammalian: IR-B (the longer isoform) is the most prominent isoform in classical insulin-sensitive tissues, skeletal muscle, adipose tissue, and liver; and IR-A prominent in the brain [80, 81]. These receptors are highly abundant in all the cerebral areas, especially in the hypothalamus, cerebellum, hippocampus and cerebral cortex and striatum.

Concerning intracellular localization, this receptors are more present in neurons (with high protein expression in cell bodies and synapses) than in glial cells and the levels of these decrease with the age, suggesting an involvement in the aging [82, 83].

Once bound to α subunits of neuronal IR, insulin promotes auto phosphorylation of the β subunits at Tyr residues 1158,1162 and 1163 triggering its intrinsic Tyr kinase activity and phosphorylating insulin receptor substrate (IRS) docking proteins (IRS1-4) at Tyr residues [84, 85], which initiate divergent signal transduction pathways [86]. Likewise, following the binding of insulin, aggregated IRs are rapidly internalized into the cell by a process that at least in part involves coated pits and vesicles [87]. It has been suggested that aggregation or internalization could be essential for insulin signaling [88]. The internalized IRs can then be degraded or recycled back to the cell membrane. In literature are described 6 isoforms of IRSs (IRS1, IRS2, IRS3, IRS4, IRS5 and IRS6) but the most insulin responses are mediated by IRS1 and IRS2. IRS1 controls body growth and

peripheral insulin action, while IRS2 regulates brain growth, body weight control, glucose homeostasis, and female fertility [84]. IRS proteins are composed of an NH_2-terminal pleckstrin homology (PH) domain adjacent to a phosphotyrosine-binding (PTB) domain, and followed by a tail containing numerous tyrosine and Ser/Thr phosphorylation sites (75). The Tyr phosphorylation sites coordinate down-stream signaling cascades by binding the SH2 domains present in common effector proteins, including enzymes (the phospho- inositide 3-kinase, PI3K; the phosphatase SHP2; or the tyrosine- kinase Fyn) or adapters (SOCS1, SOCS-3, GRB2, and others) [84, 89]. By contrast, the specific serine phosphorylation of the IRS1/2 by the c-Jun N-terminal kinase (JNK1) and other protein kinases inhibits insulin-stimulated tyrosine phosphorylation, which correlates closely with insulin resistance (76).

Two major cellular signaling pathways can be activated by the kinase activity of insulin receptor are: phosphoinositide-3 kinase (PI3K)/Akt and the Ras/mitogen-activated protein kinase (MAPK) pathways. These cascades regulate several cellular processes, such as gene expression, protein synthesis, vesicle trafficking, lipid and protein metabolism, cell growth and differentiation [90, 91]. The activation of the two pathways not necessarily occur simultaneously, especially in pathophysiological conditions, where one pathway can prevail over the other [92].

There are more proteins that can act a negative regulators strictly control on the intensity and duration of the insulin signal. Among these we know same phosphatases: (i) LAR and PTP1B which dephosphorylate the Tyr residues of IR and IRS, (ii) PP2A, PP2B and PP2C which regulate the activity of Akt and ERK by the Ser/Thr residues and (iii) PTEN and SHIP2

regulate the activity of PIP_3, antagonizing the PI3K/AKT pathway [93]. Interesting is the inhibitory modulation obtains through the phosphorylation of IRS on Ser/Thr residues by same kinases like PKC, JNK, IKK, MAPK and AKT. In particular AKT mediates the signal through the activation of mTOR, which inactive IRS. In details, mTOR-mediated inhibitory phosphorylation of IRS1 on a serine residue uncouples PI3K/Akt axis from insulin and IGF-1 receptor signals. Therefore, potentially leading to the development of insulin resistance. Other proteins, such as JNK or inflammatory components (e.g. TNFα), can switch off PI3K/Akt axis regulating IRS1 activity [94, 95].

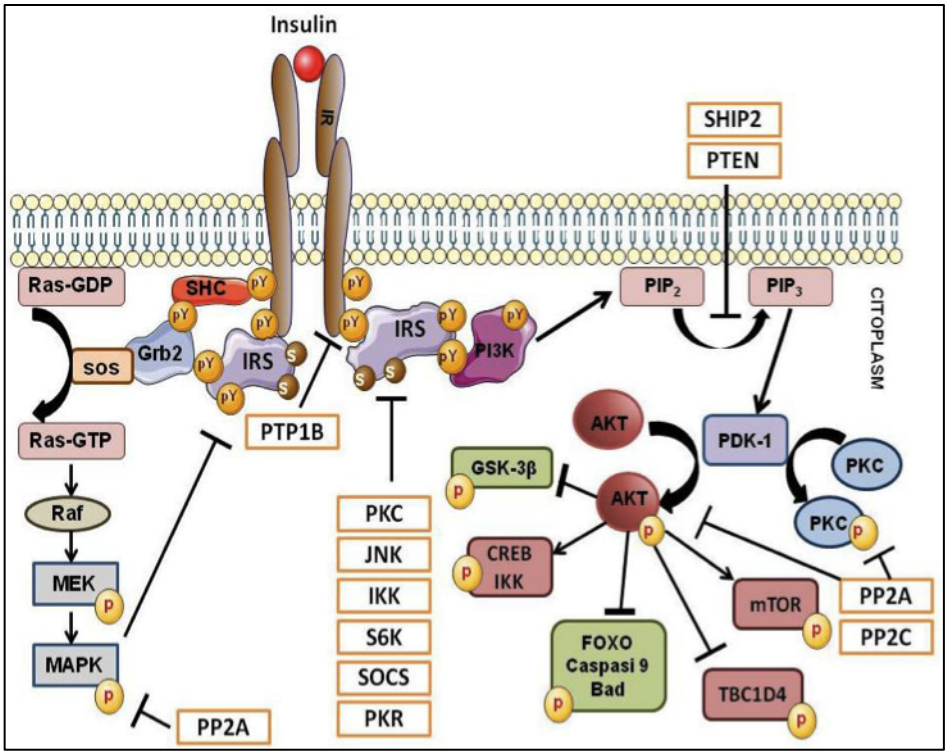

Figure 4. Mechanisms of insulin signalling in the brain. Under normal conditions binding of insulin to IR promotes its activation through IR dimerization and autophosphorylation of specific Tyr residues. Stimulation of IR kinase activity is then followed by Tyr phosphorylation of a variety of endogenous substrates, including IRS-1. These events lead the activation of multiple signaling pathway required for insulin's pleiotropic action, including: (i) PI3K/AKT axis and (ii) MAPK cascade. The first one has reached the crucial point in the activation of AKT, the main node of the signal cascade. It is a serine / threonine kinase that has several molecular targets: e.i. GSK3-β and mTOR. The second pathway sees the final activation of MAPK that culminate in the activation of several transcription factors that control gene expression. Insulin signalling is regulated by the action of several molecules, such as phosphatases (PP2A, PP2C, PTEN, SHIP2, PTB1B) which dephosphorylate IRS, IR, PKC, ERK, PIP3 and AKT; serine/threonine kinases that determine the inactivativeation of IRS1 and the stress kinases such as JNK, IKK and MAPK, along with PKC and S6K activated by mTOR.

2.1.1.1 PI3K/Akt axis

After binding of the p85 SH2 domain to the phosphorylated Tyr of active IRS, PI3K becomes active and p110 inhibition is relieved, allowing translocation of active PI3K to plasma membrane and subsequent transformation of phosphatidylinositol 4,5-bisphosphate (PIP2) to PI-3,4,5-trisphosphate (PIP_3). All of this pathway is negatively regulated by phosphatase and tensin homolog, PTEN [96]. Then, PIP_3 bind and recruit from the membrane, phosphoinositide- dependent kinase-1 (PDK-1), determining the activation. Consequently, activated PDK-1 in turn recruit and active form the plasma membrane some protein kinase: protein kinase C (PKC) and protein kinase B (PKB or Akt) [97] through the phosphorylation of Thr-308 and Ser-473 residues [98, 99]. Once activated, AKT, detaches from plasma membrane and translocate into cytosol and nucleus [99], where it phosphorylates target proteins at Ser and Thr residues, thus regulating numerous processes [100] : (i) *activation of mTOR,* which is associated with the regulation of genes involved in the control of protein synthesis, cell growth and neuronal glucose metabolism; (ii) *inhibition of FoxO3* (Forkhead box O), which cause the block of nuclear translocation of FoxO3 and its subsequent deleterious targeting of nuclear genes, thus promoting hippocampal and cerebrellar granular neuronal survival [101]; (iii) *inhibition of several proapoptotic proteins such as GSK-3β , caspasi-9 and Bad;* and (iv) *activation of CREB* (cAMP – responsive element-binding protein).

Once the activation of mTOR by AKT, several phosphorylates components of the protein synthesis machinery, including ribosomal S6 kinase 1 (S6K1), and the translation inhibitor eukaryotic translation initiation factor 4E-binding protein (4E-BP) are activated by it [102, 103]. S6K1 presents two different isoforms, the p70 (p70S6K) mainly cytoplasmic and the p85 (p85S6K) with 23 additional that allows its targeting to the nucleus [104]. 4E-BP exists in three isoforms (1, 2, and 3) that have similar functions but differs in their tissue distribution. 4E-BP3 expression is limited to few tissues, and is excluded from the nervous system while both 4E- BP 1 and 2 are expressed in nervous tissues but 4E-BP2 is the major isoform [105].

GSK-3β, Ser/Thr protein kinase, is inactive by Akt through a phosphorylation at the N-terminal Ser9, initiating multiple physiologic effects [106, 107]. GSK-3β is negatively regulated also by PKC and c-AMP-dependent protein kinase (PKA) (which are also activated by insulin) [108]. Depending on the cellular context, GSK-3β can be targeted to different intracellular locations (e.g., cytosol, mitochondria, or nucleus) to easily access its substrates: active GSK-3β (Ser9 dephosphorylated) appears mostly in nuclei, mitochondria, and membrane lipid rafts (detergent-resistant plasma membrane micro domains involved in signal transduction), while inactive GSK-3β is mostly cytosolic [109]. Besides Ser9 dephosphorylation, GSK- 3β can be also activated by phosphorylation at Tyr216, and, although this mechanism remains unclear, changes in intracellular Ca^{2+} or Fyn (a member of the Src Tyr kinase family) appear to be involved [110, 111]. The inhibition of GSK3β, occurring after PI3K inhibition, has been described to prevent apoptosis, while overexpression of a constitutively active GSK-3β resulted in PC12 cell death [112] .

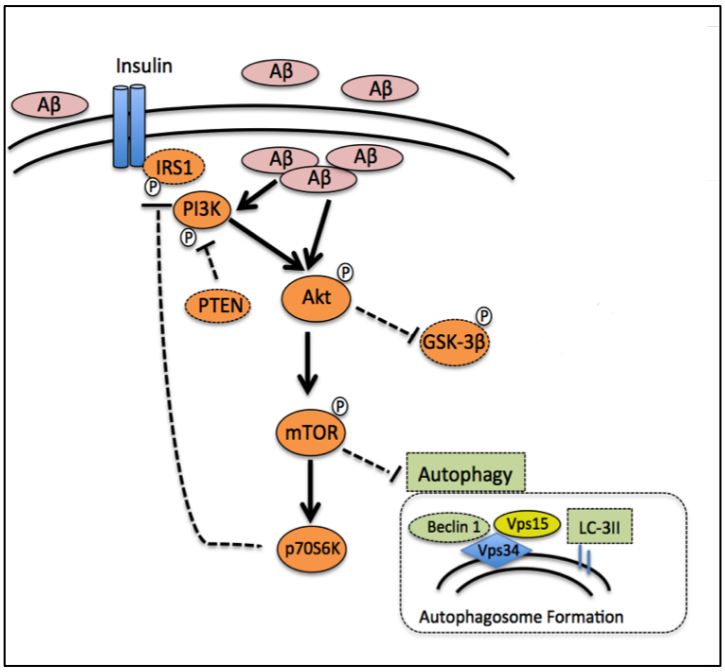

Figure 5. PI3K/AKT axis. mTOR and insulin signaling network. Growth factors, such as insulin, and nutrients, such as glucose, bind to membrane receptors to activate class I PI3K. This process generates PIP3, which recruits protein kinase B (PKB/Akt) and its activator PDK1 (phosphoinositide-dependent kinase 1) to the plasma membrane, resulting in activation of PKB/Akt. Active PKB/Akt indirectly activates mTOR through inhibition of negative regulators [tuberous sclerosis complex (TSC1/2)] of mTOR and activating the mTOR activator Rheb (Ras homolog enriched in brain). mTOR phosphorylates and activates S6 kinase 1 (p70S6K1), that in turn promote protein translation. In addition, mTOR phosphorylates and inactivates eukaryotic initiation factor 4E-binding protein (4E-BP). A primary negative-feedback inhibitory pathway exists whereby sustained activation ofmTOR/p70S6K suppresses Akt activity. This mechanism acts through mTOR-mediated serine phosphorylation of IRS-1, to induce IRS-1 inactivation and degradation, thus eliminating coupling of PI3-K/Akt to the insulin and IGF-1 receptors and other activating receptors.

2.1.1.2 ERK1/2 cascade

ERK1/2 forms a parallel branch to PI3K/Akt signaling. After phosphorylation of IR, the adapter protein SHC (Src homology-2 domain-containing) binds to IR and Grb2 (growth factor receptor-bound protein 2) is attracted to bind to SHC via its SH2 domains, thus activating the ERK1/2 signaling pathway; SH2 domains can also bind directly the phosphorylate tyrosine residues of IRS. Grb2 has other domains, SH3, that interact with the guanine nucleotide exchange Son of Sevenless (SOS) protein, stimulating the exchange of GDP for GTP at Ras, which becomes active and then recruits the Ser/Thr kinase Raf. Subsequent activation of MEK (or MAP2K, mitogen-activated protein kinase kinase) leads to phosphorylation (and activation) of ERK1/2 on Thr and Tyr residues [113, 114], culminating in activation of several transcription factors that control gene expression (e.g., Ets-like protein-1 (Elk-1) and c-Myc) [99].

2.2 Impairment of brain insulin signaling in AD

Brain insulin resistance (BIR) can be defined as the failure of brain cells to respond to insulin. Mechanistically, this lack of response could be due to down-regulation of insulin receptors, an inability of insulin receptors to bind insulin or faulty activation of the insulin signalling cascade. At the cellular level, this dysfunction might appear as an impairment of neuroplasticity and neurotransmitter release in neurons, or an alteration in

insulin response such as decreased expression of neuronal glucose uptake (GLUT4) and inflammatory responses. Functionally, brain insulin resistance can manifest an impaired ability to regulate metabolism — in either the brain or periphery — or impaired cognition and mood.

Interestingly, metabolic stress and neuroinflammation are key hallmarks in AD pathology [115, 116] and ample number of evidence suggested that the alterations in brain insulin metabolism could be a pivotal responsible for the progression of these neurodegenerative disease. In support of this hypothesis, AD patients have shown reduced brain insulin receptor sensitivity, hyper phosphorylation of insulin receptor and its downstream second messenger IRS1 and attenuated insulin expression [117, 118]. Reduced brain glucose metabolism has been well described in AD and documented as an early even in the disease progression [119, 120]. Moreover, *post mortem* studies have demonstrated striking reductions of genes expression encoding both insulin and insulin receptor in CNS of AD cases compared to aged controls [121].

Interesting, defective insulin signaling accelerates Aβ production in the brain by enhancing the amyloidogenic processing of the APP [122] and also increasing Aβ aggregation through monosialotetrahexosylganglioside (GM1) clustering and membrane signaling [123]. Thus, oligomer-induced insulin resistance may create a vicious cycle in which oligomers upregulate their own production and aggregation by disrupting insulin physiological actions. Such a mechanism could account in part for Aβ build up in AD brains. Multiple toxic effects of Aβ may impair proper brain insulin signaling and trigger a feed-forward cascade that disrupts neuronal functions through increased cellular stress (e.g. aberrant cytosilic calcium, oxidative stress, ER stress). This condition, in turn, appears to

intensify neuronal insulin resistance and Aβ generation. Because defective neuronal IR/IRS1 function appears critical for the onset of AD-related neuronal damage, it seems likely that bolstering insulin sensitivity and actions could provide encouraging results in preventing/rescuing memory decline. Aβ oligomers, from one side, promote the down- regulation of plasma membrane IR [124] whereas, from the other side, lead to the activation of neuronal tumor necrosis factor-alpha (TNF-α) receptor and the aberrant activation of stress-regulated kinases (i.e. Jun N-terminal kinase (JNK), I kappa B kinase (IKK), and protein kinase R (PKR) [125] and endoplasmic reticulum (ER) stress (PKR-mediated phosphorylation of eIF2α-P) [126], which leads to IRS1 inactivation. The above-mentioned proteins are all down-stream effectors shared by a number of signaling pathways (i.e. lipid metabolism and inflammation) and thus not exclusively related to the insulin signaling, although IRS1 is among their substrates [127]. Given that, BIR appears to be an event secondary to the activation of these kinases due to other mechanisms including the elevation of the oxidative/nitrosative stress levels [128], inflammatory processes and ER stress [125, 126].

The onset of BIR in AD is a matter still under debate because the complexity of the mechanisms underlying this phenomenon.

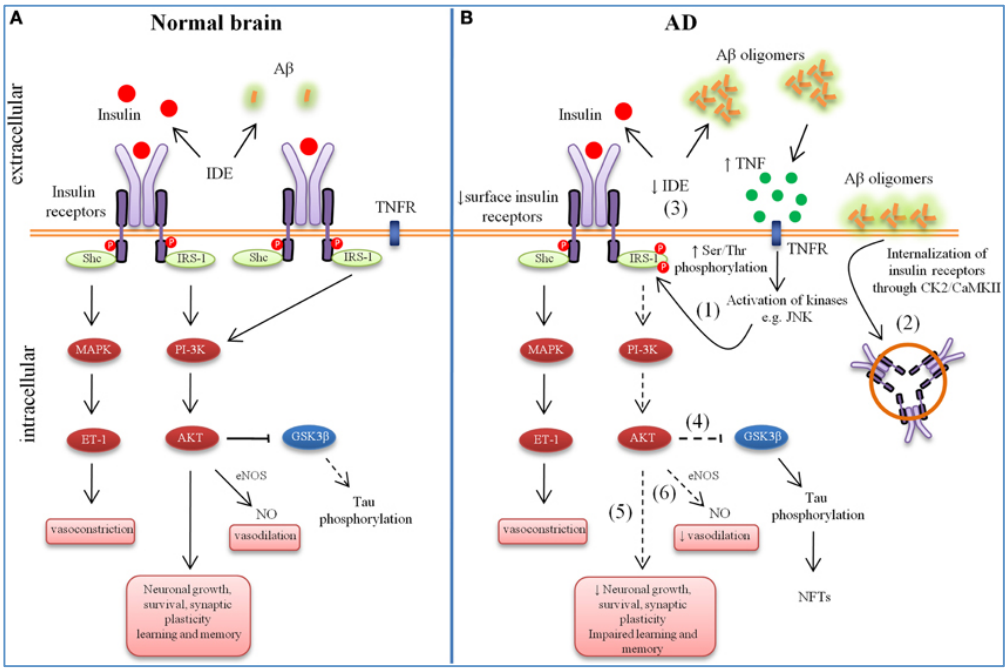

Figure 6. Aberrant brain insulin signaling in AD.

2.2.1 Biliverdin reductase-A

As mentioned previously, insulin signalling contains several regulatory points, which represent critical nodes [129]. Among them Biliverdin reductase-A (BVR-A) has an important role in the modulation of this pathway [130]. BVR-A is one of the two forms of Biliverdin reductase (BVR). BVR is a monomeric protein and consists of two structural domains: an N-terminal dinucleotide-binding domain (Rossmann-fold) and a C-terminal domain, which possesses a six-stranded beta-sheet that is flanked on one face by alpha helices. Both domains take part in the formation of the active site cleft at their interface [131]. The two forms of BVR have a different molecular weight and each of them have two isoforms. BVR-B has been reported to be predominant during fetal development, while BVR-A dominates in adult life.

BVR is evolutionary conserved, soluble protein found in all mammalian cell types analyzed to date, albeit at different levels. Considering mammalian species, the average sequence identity is greater than 80%. In such sequences several conserved key features are found: leucine zipper (bzip) motif, adenine dinucleotide-binding motif, serine/threonine kinase domain, Src homology (SH2) binding domains (YMXM and YSLF), and Zn/metal-binding motif [132, 133]. These features are probably fundamental in the activities of BVR connected with signal transduction pathways.

Both forms generate bilirubin (BR), but only BVR-A reduces biliverdin (BV) into an effective intracellular anti-inflammatory agent, powerful antioxidant and anti-nitrosative molecule called BR-IX- alpha (thereafter BR). BVR-B, instead, prefers the other BV isoforms, such as BV-β, BV-γ and BV-δ. In details, BV is formed when heme is oxidized by the

heme oxygenase (HO) isozymes HO-1 and HO-2, which is reduced by BVR-A to the highly lipophilic BR, [134, 135].

Recent data from Mains et al. suggested that BVR-A, regardless its reductase activity, also has a unique serine/threonine/tyrosine (Ser/Thr/Tyr) kinase activity directly involved in insulin signaling, indeed the tyrosine residues in the two consensus Src homology (SH2)-binding motifs (Tyr198 in YMKM and Tyr228 in YLSF), together with Tyr291, are targets of IR [136]. In particular, IR phosphorylates BVR-A on specific Tyr residues (Tyr198/228/291), resulting in activation of BVR-A kinase activity. Once activated BVR-A is able to phosphorylate IRS1 on Ser residues critical for the insulin signalling activation [136]. Following insulin stimulation, BVR-A is required for the activation and nuclear translocation of the extracellular signal-regulated kinases 1/2 (ERK1/2) [137] as well as for the correct activation of the protein kinase B (PKB/Akt) [138] known to regulate memory processes in the brain [139].

The two activities are differently modulated since of specific Tyr promoted by IR is required for the activation of its kinase activity, whereas the auto-phosphorylation of specific Ser/Thr residues regulates the reductase activity. Interestingly, Ser/Thr auto phosphorylation is independent from Tyr phosphorylation.

An intriguing aspect is that the oxidative stress, reported in AD, induce the impairment of BVR-A in the hippocampus of AD and aMCI subjects due to reduced Tyr phosphorylation and increased 3-NT modifications [140].

In recent studies, my group showed that the dysfunction of BVR-A is one of the earliest events characterizing the development of brain insulin resistance in AD. Indeed, in a longitudinal study conducted with a triple-transgenic murine model of AD (3×Tg-AD), we identified three phases along the progression of AD pathology characterized by: (1) reduced BVR-A protein levels associated with the hyper-activation of IR at 3 months of age; (2) reduced BVR-A levels and activation along with hyper-activation of both IR and IRS1 at 6 months of age; and (3) reduced BVR-A levels and activation associated with the activation of negative feed-back pathways, e.g., mTOR aimed to turn-off IRS1 hyperactivity and thus leading to brain insulin resistance. Furthermore, *in vitro* experiments in neuronal cell lines highlighted that insulin resistance phenomenon was characterized by a consistent impairment of BVR-A, an observation that strengthens the role of this protein as a regulator of the insulin signalling cascade [141].

The involvement of BVR-A in the insulin signaling is fascinating for two main reasons: (i) BVR-A, as IRS1, is a direct target of IR kinase activity and once IR-phosphorylated is able to phosphorylate IRS1 on Ser residues [136, 142]; and (ii) BVR-A contains specific motifs in its sequence through which they possibly modulates IR kinase activity both negatively and positively [142].

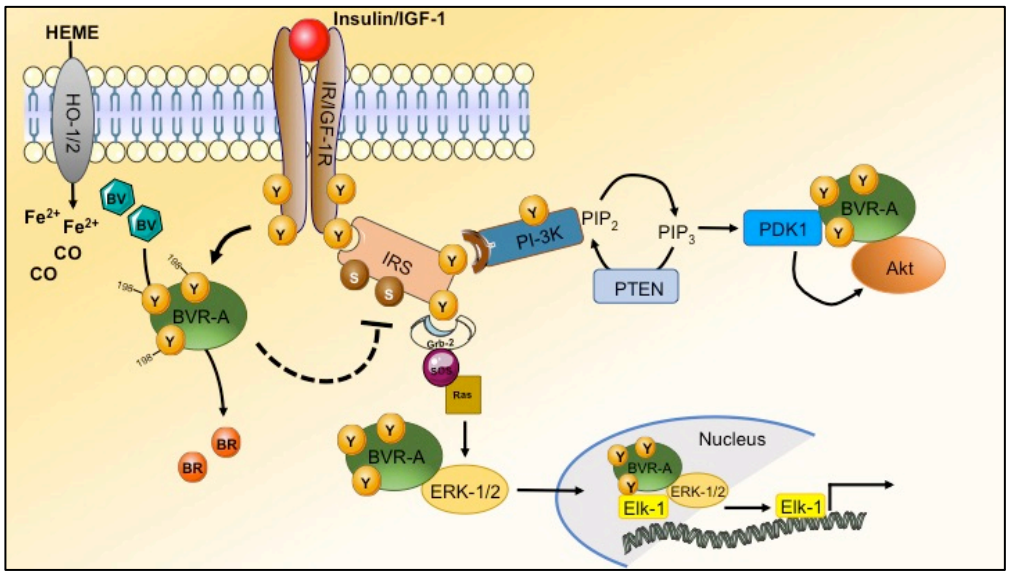

Figure 7. Proposed mechanism leading to BIR in AD. BVR-A, regardless its reductase activity, once IR-phosphorylated is able to phosphorylates IRS1 on Ser inhibitory domains.

2.3 Insulin as a therapy for AD

In recent years, the study of insulin and insulin signaling in neuronal tissues has gained momentum. Proteins involved in transmission of the insulin signal have been detected in many brain regions, including areas involved in Alzheimer's disease (AD), such as the hippocampus and temporal lobes [143]. Whereas insulin signaling is impaired in *post mortem* brain tissue from AD patients [144], and because it is known that insulin positively influences cellular processes such as growth and survival [99], improving insulin action in neurons has emerged as a treatment target able to improve cognitive function. Therefore, restoring insulin to normal levels in the brain by insulin treatment, as showed in laboratory animals, may provide therapeutic benefits in AD subjects.

Interest in insulin as a potential therapy for AD has also stemmed from a number of clinical studies that indicate that individuals with Type 2 diabetes (T2D) have an elevated risk of mild cognitive impairment and AD [145, 146]. In fact, a recent meta-analysis of longitudinal clinical studies found that T2D significantly increased AD risk independently of obesity [147].

Unlike, insulin cannot be administered orally, since it is degraded in the gastrointestinal track by various enzymes. In this frame, the first clinical studies to address the effect of insulin on the brain in the context of cognition were performed with intravenous insulin infusion. Increasing brain insulin levels in AD patients by intravenous administration has been shown to acutely improve performance on hippocampus-dependent memory task [148]. However, high systemic doses would be needed to achieve functionally

effective insulin concentrations in the brain, causing strong peripheral side effects such as hypoglycemia and induction and/or exacerbation of peripheral insulin resistance [149]. Therefore, oral and intravenous route of administration is not viable in clinical setting.

Moreover, infusion of peripheral insulin is not a viable long-term therapy for AD, due to high risks related to hypoglycemia. Recently, direct drug delivery to the CNS has been investigated using intranasal administration. This method of administration provides rapid delivery of insulin to the central nervous system along bulk flow via olfactory and trigeminal perivascular channels, and slower delivery via olfactory bulb axonal transports [150, 151]. Thus, intranasal delivery of insulin is attractive because it is less invasive than intravenous infusion and avoids potential side effects of intravenous insulin infusions, such as hypoglycemia.

Recently, National Institute of Health (NIH) has selected intranasal insulin administration as one of the two therapeutic strategies receiving substantial funding as part of the National Alzheimer's Plan in the US [152]. This plan is a part of the initiatives to find a therapeutic treatment to cure AD by 2025.

Several small-scale clinical trials showed that intranasal insulin (INI) improved memory and attention in healthy participants [153], as well as in patients with mild cognitive impairment and AD [154]. Preclinical studies in different mouse models of aging or AD confirmed the cognitive improvement obtained by INI [155, 156], and also showed the path by which insulin reaches the brain [49]. However, it is still under debate the mechanism(s) by which INI administration might improve learning and memory and whether the INI treatment stimulates or not cerebral insulin signalling leading to a recovery from brain insulin resistance [157].

2. AIMS OF THIS WORK

Within this scenario we focused on the impairment of brain insulin signalling during the progression of AD neuropathology. Because the dysfunction of BVR-A was found to be among the earliest events characterizing the development of brain insulin resistance in in 3xTg-AD mice, we decided to elucidate the role of this protein as a regulator of the insulin signalling cascade during the progression of AD.

Project 1

Brain insulin resistance is associated with increased Aβ production in AD although the molecular mechanisms underlying this link are still largely unknown. Moreover, it has been previously reported a negative association between BVR-A protein levels/activation with BACE1 protein levels in an animal model of AD, thus suggesting a possible interaction. In this frame, we aimed to demonstrate that BVR-A impairment is a molecular bridge linking brain insulin resistance with increased Aβ production. We evaluated age-associated changes of BVR-A, BACE1, insulin signalling cascade and APP processing in the parietal cortex of beagles at 1, 4, 8-10 and 11-12 years and experiments to confirm the hypothesized mechanism(s) have been performed *in vit*ro in HEK293APPswe cells.

Project 2

Among the strategies to ameliorate the activation of the insulin signalling in the brain, intranasal insulin (INI) administration is under evaluation in an active large trial in the field of AD. However, it is still under debate the mechanism(s) by which INI administration might improve learning and memory and whether the INI treatment stimulates or not cerebral insulin signalling leading to a recovery from brain insulin resistance [158]. The goal of this second project was to evaluate whether the beneficial effects of INI treatment were associated with an improvement of brain insulin signalling activation mediated by the amelioration of BVR-A activation. Hence, we hypothesized that INI administration, by favoring the IR-mediated activation of BVR-A, would prevent the alterations of the insulin signalling in the brain. We tested in both adult (6 months of age) and aged (12 months of age) 3xTg-AD mice the effects of intranasal insulin administration, which represents an effective strategy that allows drugs to bypass the BBB and directly reach the brain, thereby avoiding side effects caused by systemic administration.

3. MATERIALS AND METHODS

3.1 Samples

3.1.1 Animals (PROJECT 1)

Aging dogs spontaneously deposit human-type amyloid β (Aβ) peptide [159] and thus are a natural higher mammalian model of aging that rodents. The canine Aβ precursor protein (APP) is virtually identical to human APP (~98% homology). In parallel with progressive Aβ pathology, aged dogs show decline in measures of learning and memory that are correlated with the extent and location of Aβ. Therefore, dogs represent a good animal model to evaluate the processes leading to Aβ accumulation in AD. Parietal cortex samples form fourteen beagles ranging in age from 0.15 to 12 years were obtained from the Lovelace Respiratory Research Institute (Albuquerque, NM, USA). The parietal cortex was chosen as it shows significant Aβ accumulation with age in beagles [160]. All animals had documented dates of birth, comprehensive medical histories and a veterinary examination ensuring that the animal was in good health. According to previous data showing significant age-dependent decline and changes of Aβ levels in the brain of these dogs, our samples were divided in 4 groups based on their age: 1 years (n=3), 4 years (n=3), 8-10 years (n=4) and 11-12 years (n=4) [160].

3.1.2 Human AD case

Slices used for the immunofluorescence analyses were collected from a human AD frontal cortex brain sample (male, 72 years old) obtained from the University of California-Irvine-ADRC Brain Tissue Repository (UCI ADRC) cohorts.

3.1.3 Mouse colonies (PROJECT 2)

4- and 10- month-old 3×Tg-AD male mice (n=8-10 per group/treatment) and their wild-type (WT) male littermates (n=8-10 per group/treatment) were used in this study. The 3×Tg-AD mice harbour 3 mutant human genes (APP_{Swe}, $PS1_{M146V}$, and tau_{P301L}) and have been genetically engineered by LaFerla and colleagues at the Department of Neurobiology and Behaviour, University of California, Irvine [161-163]. Colonies of homozygous 3×Tg-AD and WT mice were established at the vivarium of Puglia and Basilicata Experimental Zooprophylactic Institute (Foggia, Italy). The 3×Tg-AD mice background strain is C57BL6/129SvJ hybrid and genotypes were confirmed by PCR on tail biopsies [161]. The housing conditions were controlled (temperature 22°C, light from 07:00 – 19:00, humidity 50%–60%), and fresh food and water were freely available.

3.2 INI Treatment

Animals received intranasal insulin (Humulin®R, Ely-Lilly, Inadianapolis, IN, USA) administration every other day (2UI total, 4 μL/nostril) or vehicle (saline) during 2 months. All the experiments were performed in strict compliance with the Italian National Laws (DL 116/92), the European Communities Council Directives (86/609/EEC). All efforts were made to minimize the number of animals used in the study and their suffering. Animals were sacrificed at the selected age and the hippocampus and frontal cortex were extracted, flash-frozen, and stored at −80 °C until total protein extraction and further analyses were performed.

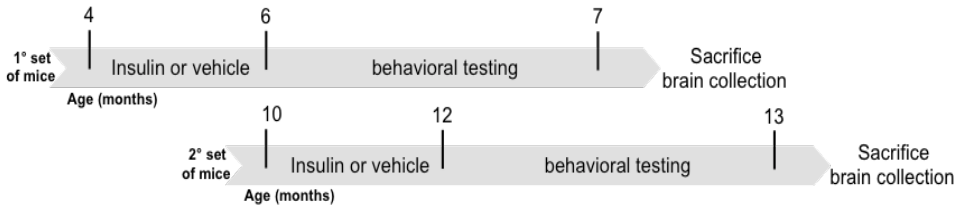

Figure 8. Schematic treatment of INI treatment in 3×Tg-AD mice. 4- and 10- month-old 3×Tg-AD mice and Wild Type (WT) were administered with intranasal Insulin (Humulin®R, Ely-Lilly) and Vehicle (Veh; saline) for 2 months until 6- and 12 months age respectively.

3.3 Behavioral test

We used a serial behavioral testing procedure that has been validated and compared with single testing procedures in our laboratory, and by other investigators [164-167].

The NOR test and the MWM test were used to explore the cognitive behaviours, whereas the tail suspension test (TST) and the Porsolt forced swim test (FST) for antidepressant/depression-like coping behaviors. The experimental procedures were administered to the animals in this sequence, starting with those considered to be least stressful. The minimum interval between two consecutives procedures was 2 days. All tests were performed between 8:00 a.m. and 3:00 p.m., in a dimly lit condition. On the day of testing, the mice were acclimated for about 60 min in the behavioral room before the procedures were initiated. The apparatus was cleaned with 70% alcohol and water after each run. The behaviors were recorded with infrared lighting-sensitive CCD cameras, stored, and analysed as MPEG files. Experimental subjects were weighed every day during the entire period of the experiment.

3.3.1 Novel object recognition test (NOR)

The object recognition task is based on the spontaneous tendency of rodents to explore a novel object longer than a familiar one. Each mouse was habituated to an empty Plexiglas arena (45 × 25 × 20 cm) for 3 consecutive days. On training session (T1) (day 4), mice were exposed for 5 min to two identical objects (A+A) placed at opposite ends of the arena. 30 min and 24 h

later, the animals were subjected to a 5 min testing session where they were exposed to one object familiar (A) and to a novel object B (after 30 min) and object C (after 24 h). Exploration was considered as pointing the head toward an object at a distance of < 2.5 cm from the object, with its neck extended and vibrissae moving. Turning around, chewing, and sitting on the objects were not considered exploratory behaviors. The time of exploration was recorded, and an object recognition index (ORI) were calculated, such that ORI = (TN - TF) / (TN + TF), where TN and TF represent times of exploring the familiar and novel object, respectively [166, 167]. Mice that did not explore both objects during training were discarded from further analysis. Objects used in this task were carefully selected to prevent preference or phobic behaviors. To avoid olfactory cues, the objects were thoroughly cleaned with 70% ethanol and the sawdust was stirred after each trial.

3.3.2 Morris water maze (MWM)

The test was conducted in a circular tank of 1.2 meters in diameter, locates in a room with several extra maze cues as previously described [166]. Briefly, mice were trained to swim to a 14-cm-diameter circular Plexiglas platform submerged 1.5 cm beneath the surface of the water and invisible to the mouse while swimming. The water temperature was kept at 25°C throughout the duration of the testing. The platform was fixed in place, equidistant from the center of the tank and its walls. Mice were subjected to 4 training trials per day and were alternated among 4 random starting points for 5 consecutive days. Mice were allowed to find and escape onto the submerged platform. If the mice failed to find the platform within 60 sec,

they were manually guided to the platform and were allowed to remain on it for 10 sec. After this, each mouse was placed into a holding cage under a warming lamp for 25 sec until the start of the next trial. Retention of the spatial training (the probe trial) was assessed 1.5 and 24 h after the last training session and consisted of a 60-sec trial without the platform. Mice were monitored by a camera mounted in the ceiling directly above the pool, and all trials were stored on videotape for subsequent analysis. The parameters measured during the probe trial included (1) initial latency to cross the platform location and (2) time spent in the target quadrant (Scuderi et al., Transl Psychiatry 2018). Performance was monitored using the EthoVision XT version 7 video tracking software system (Noldus Information Technology Inc., Leesburg, VA).

3.3.3 Forced swim test (FST)

The FST examines the dynamics of transition from an active (swimming) to a passive (immobility) mode of coping in an inescapable water-filled pool. Enhancement of immobility normally ensues after exposure, a phenomenon argued to reflect learned behavioral despair [164-167] and prevented by antidepressant treatment. The FST was performed as previously described [164-167]. Briefly, mice were placed individually into Plexiglas cylindrical bins (20 cm diameter, 50 cm high) filled with water (25–27°C water temperature) to a depth of 20 cm. This depth did not allow the tail and hindpaws to touch the floor of the bin. The mice were allowed to swim for 6 min. After recording, the mice were rescued using a plastic grid and caged near a heat source (lamp). The behavioral tracking system was

calibrated so that a mouse was considered immobile when making only those movements necessary to keep its head above water. The total duration of activity was determined during the last 4 min.

3.3.4 Tail suspension test (TST)

This procedure, which is also used to assess antidepressant-like activity, involved suspending the mouse by the tail from a lever in a white box (30 x 30 x 30 cm). The test has duration of 6 min and is calculated by the immobility time (sec) in the last 4 min of recording. These experimental conditions were similar to those previously described [164-167]. Antidepressant treatment reduces the total time the mouse remains immobile [165].

3.4 Sample preparation for western blot

Total protein extracts were prepared in RIPA buffer (pH 7.4) containing Tris-HCl (50mM, pH 7.4), NaCl (150mM), 1% NP-40, 0.25% sodium deoxycholate, EDTA (1mM), 0.1% SDS, supplemented with proteases inhibitors [phenylmethylsulfonyl fluoride (PMSF, 1mM), sodium fluoride (NaF, 1mM) and sodium orthovanadate (Na_3VO_4, 1mM)]. Brain tissues were homogenized by 20 passes with a Wheaton tissue homogenizer. Both brain tissues homogenates and collected cells were clarified by centrifugation for 1 hr at 16,000 × g, 4°C. The supernatant was then extracted to determine the total protein concentration by the Bradford assay (Pierce, Rockford, IL).

3.5 Slot blot analysis

To evaluate total (i) protein-bound 4-hydroxy-2-nonenals (HNE) and (ii) 3-nitrotyrosine (3-NT) levels, brain samples (5 µl), 12% SDS (5 µl), and 5 µl modified Laemmli buffer containing 0.125 M Tris base, pH 6.8, 4% (v/v) SDS, and 20% (v/v) glycerol were incubated for 20 min at room temperature and then loaded onto nitrocellulose membrane as described below.

Proteins (250 ng) were loaded in each well on a nitrocellulose membrane under vacuum using a slot blot apparatus. The membrane was blocked in blocking buffer (3% bovine serum albumin) in PBS 0.01% (w/v) sodium azide and 0.2% (v/v) Tween 20 for 1 h and incubated with an anti-2,4-dinitrophenylhydrazone (DNP) adducts polyclonal antibody (1:100, EMD Millipore, Billerica, MA, USA, #MAB2223) or HNE polyclonal antibody (1:2000, Novus Biologicals, Abingdon, United Kingdom, #NB100-63093) or an anti 3-NT polyclonal antibody (1:1000, Santa Cruz, Santa Cruz, CA, USA, #sc-32757) in PBS containing 0.01% (w/v) sodium azide and 0.2% (v/v) Tween 20 for 90 min. The membrane was washed in PBS following primary antibody incubation three times at intervals of 5 min each. The membrane was incubated after washing with an anti-rabbit IgG alkaline phosphatase secondary antibody (1:5000, Sigma–Aldrich, St Louis, MO, USA) for 1 h. The membrane was washed three times in PBS for 5 min each and developed with Sigma fast tablets (5-bromo-4-chloro-3-indolyl phosphate/nitroblue tetrazolium substrate [BCIP/NBT substrate]). Blots were dried, acquired with Chemi-Doc MP (Bio-Rad, Hercules, CA, USA) and analyzed using Image Lab software (Bio-Rad, Hercules, CA, USA). No non-specific binding of antibody to the membrane was observed.

3.6 Western blot analysis

For western blots, 30 µg of proteins were resolved on Criterion TGX Stain-Free 4-15% 18-well gel (Bio-Rad Laboratories, #5678084) in a Criterion large format electrophoresis cell (Bio-Rad Laboratories, #1656001) in TGS Running Buffer (Bio-Rad Laboratories, #1610772). Immediately after electrophoresis, the gel was then placed on a Chemi/UV/Stain-Free tray and then placed into a ChemiDoc MP imaging System (Bio-Rad Laboratories, #17001402) and UV-activated based on the appropriate settings with Image Lab Software (Bio-Rad Laboratories) to collect total protein load image. Following electrophoresis and gel imaging, the proteins were transferred via the TransBlot Turbo semi-dry blotting apparatus (Bio-Rad Laboratories, #1704150) onto nitrocellulose membranes (Bio-Rad, Hercules, CA, USA, #162-0115) and membranes were blocked with 3% bovine serum albumin in 0.5% Tween-20/Tris-buffered saline (TTBS) and incubated overnight at 4 °C with the following primary antibodies.

- PROJECT 1 PRIMARY ANTIBODIES: All the primary antibodies used and equivalent diluition are summarized in the Table 1

Antibodies	**Brands**	**Dilution**
BVR-A	Sigma Aldrich	1:1000
BACE1	Cell Signaling	1:1000
BACE1	Santa Cruz	1:1000
Amyloid Precursor Protein, C-Terminal	Sigma Aldrich	1:5000
casein kinase I α	Santa Cruz	1:1000
β-Amyloid (6E10)	BioLegend	1:1000
IRβ	Cell Signaling	1:1000
phospho(Tyr1158/1162/1163)-IRβ	GeneTex	1:1000
akt	Cell Signaling	1:1000
phospho(Ser473)-akt	Cell Signaling	1:1000
mTOR	Cell Signaling	1:1000
phospho(Ser2448)-mTOR	Santa Cruz	1:500
GSK-3β	Santa Cruz	1:500
phospho(Ser9)-GSK-3β	Santa Cruz	1:500
phospho(Try216)-GSK-3β	Santa Cruz	1:500
phospho-Tyrosine	Cell Signaling	1:1000
3NT	Santa Cruz	1:500
phospho-serine	Abcam	1:500

Table 1. List of primary antibody used for Western Blot analysis to developing project 1

- PROJECT 2 PRIMARY ANTIBODIES: All the primary antibodies used and equivalent diluition are summarized in the Table 2

Antibodies	Brands	Dilution
BVR-A	Sigma Aldrich	1:1000
BVR-A	Abcam	1:5000
IRβ	Cell Signaling	1:1000
phospho(Tyr1158/1162/1163)-IRβ	GeneTex	1:1000
IRS1	Cell Signaling	1:1000
phospho(Ser307)-IRS1	Cell Signaling	1:500
phospho(Ser636)-IRS1	Santa Cruz	1:500
akt	Bio-Rad	1:1000
phospho(Ser473)-akt	Cell Signaling	1:1000
ERK1/2	Cell Signaling	1:1000
phospho(Thr202/Tyr204)-ERK1/2	Cell Signaling	1:1000
mTOR	Bio-Rad	1:1000
phospho(Ser2448)-mTOR	Santa Cruz	1:500
phospho-Tyrosine	Cell Signaling	1:2000
IDE	Santa Cruz	1:1000
β-Amyloid (6E10)	BioLegend	1:1000
Tau	Santa Cruz	1:1000
phospho(Ser202, Thr205)-Tau (AT8)	Thermo Scientific	1:1000

Table 2. List of primary antibody used for Western Blot analysis to developing project 2

After 3 washes with TTBS the membranes were incubated for 60 min at room temperature with anti-rabbit/mouse/goat IgG secondary antibody conjugated with horseradish peroxidase (1:5000; Sigma–Aldrich, St Louis, MO, USA). Membranes were developed with Clarity ECL substrate (Bio-Rad Laboratories, #1705061) and then acquired with Chemi-Doc MP (Bio-Rad, Hercules, CA, USA) and analyzed using Image Lab software (Bio-Rad, Hercules, CA, USA) that permits the normalization of a specific protein signal with the β-actin signal in the same lane or total proteins loaded.

3.7 Immunoprecipitation

The immunoprecipitation procedure was performed as previously described [168], with minor modifications. Briefly, 150 μg of proteins extracts were dissolved in 500μl of RIPA buffer (10mMTris, pH 7.6; 140mM NaCl; 0.5% NP-40) supplemented with protease and phosphatase inhibitors and incubated with 1μg of BVR-A or BACE1 primary antibody at 4 °C overnight. Immunocomplexes were collected using protein A/G beads (Sigma–Aldrich, St Louis, MO, USA) for 2h at 4 °C and then washed 5 times with immunoprecipitation buffer. Immunoprecipitated proteins were recovered by resuspending the pellets in reducing SDS buffers and subjected to electrophoresis on 12% and 4%-15% gels followed by western blot analysis. Total BVR-A or BACE1 were used as a loading control as previously described [169-172].

3.8 Cell culture and treatments

The HEK cells were grown in Dulbecco's modified Eagle's medium (DMEM) supplemented with 10% fetal bovine serum (FBS), 2 mM L-glutamine, penicillin (20 units/ml) and streptomycin (20 mg/ml), (GIBCO, Gaithersburg, MD, U.S.A.). Cells were maintained at 37°C in a saturated humidity atmosphere containing 95% air and 5% CO_2. Cells were seeded at density of $40x10^3/cm^2$ in 6 wells culture dishes for the subsequent treatments aimed to (i) induce the activation the insulin signalling cascade, (ii) induce insulin resistance and (iii) recovery cells from insulin resistance. In a first set of experiments HEK cells were treated with insulin (humulin®R, Ely-Lilly, Inadianapolis, IN, USA) 100 nM for different times (2-6-12-24 h) to select the best time-to-treatment to be used in the other experiments. Then, to mimic insulin over-exposure known to promote insulin resistance [173], at the selected time, cells were treated with an additional dose of insulin (100 nM) for other 2 h. Thereafter, medium was discarded, cells were washed twice with PBS, and rechallenged with DMEM with 10% FBS containing insulin (100 nM-500 nM-1 uM) for additional two hours to mimic the effect of INI treatment aimed to recover insulin signalling cascade activation. In parallel, to test the effects produced by the silencing of BVR-A on insulin signalling activation, HEK cells were seeded at density of $40x10^3/cm^2$ in 6 wells culture dishes. After 24 h medium has been replaced with DMEM with 10% FBS, without antibiotics. Following, cells have been transfected with 10 pmol of a small-interfering RNA (siRNA) for BVR-A (Ambion, Life Technologies, LuBioScience GmbH, Lucerne, Switzerland, #4392420) using Lipofectamine® RNAiMAX reagent (Invitrogen, Life Technologies, LuBioScience GmbH, Lucerne, Switzerland, #13778-030) according to the

manufacturer's protocol, and then treated with insulin as described above. At the end of each treatment, cells were washed twice with PBS, collected and proteins were extracted as described below. In parallel, collected medium (mixed with protease and phosphatase inhibitors) was treated with trichloroacetic acid to precipitate soluble proteins pools to be used for the analysis of extracellular Aβ levels.

3.9 Peptide treatments

HEK cells were plated as described above and then treated with the myristoilated peptide (myr-KYCCSRK) (Biomatik, Wilmington, Delaware, USA) at the dose of 10 and 20 μM [174, 175] in combination with insulin (100 or 500 nM) for 2 h.

3.10 Whole-cell LTP in organotypic hippocampal slices

Hippocampal organotypic slice cultures were prepared from postnatal day 4–7 rats through a McIllwain tissue chopper as previously described in Spinelli et al. 2017. Slices (350 μm) were placed on semiporous membranes (Millipore) fed by tissue medium (for 1 liter: 788 ml 1xMEM (GIBCO, #11575-032, 7.16 g HEPES, 0.49 g $NaHCO_3$, 4.8 g D-glucose, 50 μl 25% ascorbic acid, 50 μl (10 mg/ml) insulin, 200 ml horse serum, 2 ml 1 M $MgSO_4$, 1 ml 1 M $CaCl_2$). Slices were incubated at 35 °C in 5% CO_2 and after 5–7 days CA1 pyramidal neurons were transfected with ballistic gene transfer (Gene-Gun, Bio-Rad, CA, USA). shRNAs were transfected together

with a plasmid enconding enhanced green fluorescent protein (EGFP) to identify the transfected neurons. LTP experiments were performed 2 days after transfection after stimulating the Schaffer collateral fibers by means of a bipolar tungsten electrode (FHC, Neural microTargeting Worldwide) as previously described [176, 177]. Slices were incubated in artificial cerebrospinal fluid (ACSF) containing (in mM): 119 NaCl, 2.5 KCl, 4 $CaCl_2$, 4 $MgCl_2$, 1 NaH_2PO_4, 26 $NaHCO_3$, 11 D-glucose, and 0.005 2-chloroadenosine, gassed with 95% O_2/5% CO_2. Whole-cell recording pipettes (3–4 MΩ) were filled with a solution containing (in mM): 135 $CsMeSO_3$, 8 NaCl, 10 HEPES, 0.25 EGTA, 2 Mg_2ATP, 0.3 Na_3GTP, 0.1 spermine, 7 phosphocreatine, and 5 QX-314, pH 7.25–7.30 (osmolarity 300). Data were collected with a MultiClamp 700B amplifier (Molecular Devices), digitized at 10 kHz using the Digidata 1440A data acquisition system (Molecular Devices) and analysed using Clampfit software (Molecular Devices). LTP was induced by pairing 200 stimuli at 2 Hz with a holding potential of 0 mV. To avoid "wash-out" of LTP, the induction protocol was applied within 5–7 min of achieving whole-cell configuration, The magnitude of LTP was calculated on basis of the averaged EPSC values during the last 5 min of recordings (from min 25 to min 30). LTP magnitude was expressed as the percentage change in the mean EPSC peak amplitude normalized to baseline values 100% (i.e., mean values of recording before LTP induction).

3.11 Immunohistochemistry

Free-floating 50 μm-thick sections were used for immunohistochemical studies. Briefly, for single labeling, all sections were washed with 0.1 M Tris-buffered saline (TBS), pH 7.4, and then pretreated with 3% hydrogen peroxide in 10% methanol to block endogenous peroxidase activity. Sections were subsequently washed in TBS with 0.1% Triton X-100 and then blocked for thirty minutes in TBS-A with 3% bovine serum albumin (TBS-B). Sections were further incubated overnight at room temperature with the primary antibody: BVR-A (anti-rabbit, 1:2000) and BACE1 (anti-rabbit, 1:500) for PROJECT 1. Following two washes with TBS-A and a wash in TBS-B, sections were incubated in anti-rabbit biotinylated anti-IgG (1 hour) and then in avidin biotin complex (1 hour) (ABC, Elite Immunoperoxidase, Vector Laboratories, Burlingame, CA, USA). The primary antibody was visualized using brown DAB substrate (Vector Laboratories). For double labeling experiments where both antibodies were raised in the same species intervening formaldehyde treatment was used between the first and second immunolabel. Primary antibody labeling was detected using the brown DAB substrate (Vector Labs), while the second label was visualized using the Blue SG substrate (Vector Labs).

3.12 Confocal microscopy

Brain sections were incubated overnight at room temperature with the same primary antibody used for the immunohistochemistry. Alexa Fluor secondary antibody 488 (1:200, Molecular Probes, Eugene, OR) was used to visualize the first label and Alexa Fluor secondary antibody 568 (1:200, Molecular Probes, Eugene, OR) was used to visualize the second label. Sections were allowed to dry on slides prior to coverslipping with VectaShield mounting media with DAPI (Vector Laboratories, Burlingame, CA, USA). Confocal images were taken with a Nikon confocal microscope system A1+ and NIS-Elements C's software (Carl Zeiss, Inc., Thornwood, NY). Single plane images were acquired with a 40x Plan Fluor immersion objective (NA 1.3) with emission long pass of 505 nm for the detection of BACE1 antibody (green channel, Alexa Fluor 488) and 550-600 nm for the detection of BVR-A (red channel, Alexa Fluor 568).

3.13 Statistical analyses

All data are presented as means ± SEM of n independent samples per group. Behavioral and biochemical data were analysed by two-way analyses of variance (ANOVA) with genotype (3×Tg-AD *vs* WT) and treatment (Insulin *vs* vehicle) as between-subject factors. Tukey's honestly significant difference (HSD) test or Bonferroni's test were used for multiple *post-hoc* comparisons when required. Student t-test was used to evaluate differences observed in aging dogs study and cellular experiments. $p<0.05$ was considered significantly different from the reference value. All statistical analysis was performed using GraphPad Prism 5.0 software.

PROJECT 1

4. RESULTS

4.1 Early Impairment of insulin signalling cascade in the parietal cortex of beagles

We first characterized the activation state of the insulin signalling cascade by evaluating age-associated changes of IR, Akt, GSK-3β and mTOR protein levels and phosphorylation in the parietal cortex (Fig. 9A). We were not able to evaluate changes of IRS1 because none of the antibodies we tested to evaluate protein levels or Ser307/Ser636 phosphorylation of IRS1 recognized canine IRS1. We found that IR protein levels were significantly increased at 4 years (+ 70%, p= 0.02) with respect to 1 year-old dogs and become reduced in older dogs both at 8-10 years (-20%, p=0.02) and 11-12 years (-35% , p= 0.04), with respect to 4 years-old dogs. When we evaluated the active form of IR with respect to total protein levels (activation index) in each group, we found that the $pIR^{Tyr1158/1162/1163}$/IR ratio was significantly reduced at 4 years (-80%, p=0.05), at 8 years (-60%, p=0.05) and at 11-12 years (-70%, p=0.03) with respect to younger dogs (Fig. 9B). These data therefore suggest that an early impairment of the IR activation characterizes the parietal cortex of these dogs along the course of their life. In agreement with reduced IR activation, we also observed a significant reduction of the Akt activation index ($pAkt^{Ser473}$/Akt ratio) starting at 4 years (-20%, p=0.03) and still evident at 12 years (–20%, p=0.02) (Fig. 9C). Two of the main targets of Akt activity are GSK-3β and the mTOR. GSK-3β is a

constitutively activated protein inhibited following Akt activation, while mTOR is activated by Akt [178, 179]. No changes of mTOR protein levels were observed, while we found a significant decrease of mTOR activation index (pmTOR^{Ser2448}/mTOR: 8-10 year, –25%, p=0.04; 11-12 years, –40%, p=0.04) (Fig. 9D). While reduced mTOR activation parallels reduced Akt activation, similar changes did not characterize GSK-3β. Although we found no changes of GSK-3β protein levels, GSK-3β activatory (Tyr216) and inhibitory (Ser9) phosphorylation revealed that the GSK-3β activation index (p^{Tyr216}GSK-3β/GSK-3β) was significantly reduced only in aged beagles at 11-12 years (-40%, p=0.01), while the inactivation index (p^{Ser9}GSK-3β/GSK-3β) was significantly increased quite early, starting at 4 years of age (+50%, p=0.02) (Fig. 9E). Interestingly, the GSK-3β inactivation/activation indexes ratio resulted in a significant increased GSK-3β inactivation (4 years, +80%, p=0.01; 8-10 years, +70, p=0.05; and 11-12 years, +140%, p=0.02), thus indicating that GSK-3β is mainly inactivated in the parietal cortex with age (Fig. 9F).

These results suggest that beagles develop alterations of insulin signaling in the parietal cortex, underlying a condition of brain insulin resistance similar to those observed in AD [180-183].

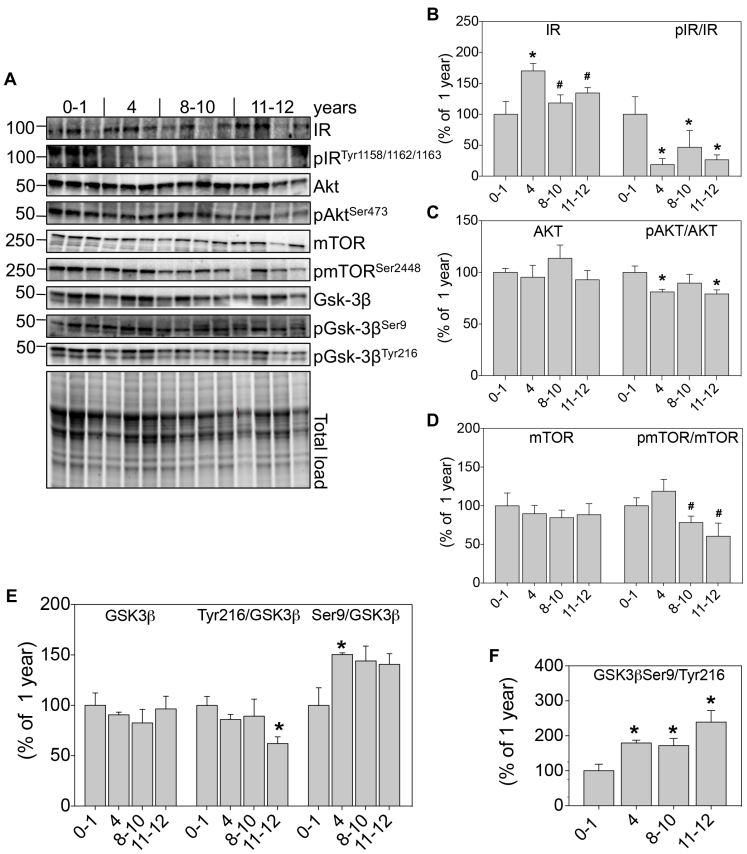

Figure 9. Early impairment of insulin signalling in the parietal cortex of beagles. Proteins associated with insulin signalling including IR protein levels, IR activation [pIR$^{(Tyr1162/1163)}$], AKT protein levels, AKT activation [pAKT$^{(Ser473)}$], mTOR protein levels, mTOR activation [mTOR$^{(Ser2558)}$], GSK3β protein levels, GSK-3β inactivation [GSK-3β$^{(Ser9)}$] and activation [GSK-3β$^{(Tyr216)}$] were measured by Western Blot in the parietal cortex of beagles at 0-1 (n=3), 4 (n=3), 8-10 (n=4) and 11-12 (n=4) years. Panel A: western blot analyses. Representative bands are shown. Panels B-C-D-E-F: densitometric analyses of western blot protein bands. Protein levels were normalized per total protein load. IR, AKT, mTOR and GSK-3β-associated phosphorylation were normalized by taking into account the respective protein levels and are expressed as the ratio between the phosphorylated form and the total protein levels: pIR$^{(Tyr1162/1163)}$/IR, pAKT$^{(Ser473)/}$AKT, pGSK-3β$^{(Ser9)}$/GSK-3β and pGSK-3β$^{(Tyr216)}$/GSK-3β and pmTOR$^{(SER2448)}$/mTOR. Densitometric values shown are given as percentage of 1 year set as 100%. Mean ± SEM, *$p < 0.05$ vs 0-1years and $^{\#}p < 0.05$ vs 4 years (Student's *t*-test).

4.2 Reduced BVR-A activation in the parietal cortex of aged beagles

We previously reported reduced BVR-A phosphorylation along with an increase of 3-nitrotyrosine (3-NT) on BVR-A, which negatively affected BVR kinase activity in post-mortem hippocampus from AD and amnestic mild cognitive impairment (MCI) subjects [171, 172, 184]. Furthermore, in a longitudinal study conducted in 3xTg-AD mice we demonstrated that reduced BVR-A Tyr phosphorylation (observed at 6 months) precedes the increase of 3-NT modifications (observed at 12 months) on BVR-A in the hippocampus [141]. Together these alterations may contribute to a persistent impairment of BVR-A kinase activity, which triggers the alterations of brain insulin signaling in parallel with the progression of AD pathology [141].

Based on this premise, we evaluated changes of BVR-A protein levels, activatory phosphorylation (pBVR-A^{Tyr}) and oxidative stress-induced post-translational modifications (3NT-BVR-A) in the parietal cortex of beagles with age (Fig. 10A&C). No significant changes for BVR-A protein levels were observed (Fig. 10B). With regard to the BVR-A activation index (pBVR-A^{Tyr}/BVR-A), we found a significant decrease at 4 years (-35%, p=0.01), at 8-10 years (-40%, p=0.001) and at 11-12 years (-20%, p=0.01) (Fig. 10D). 3-NT levels on BVR-A were significantly increased only in the oldest dogs (+40%, p=0.04) (Fig.10E). Keeping in mind that phosphorylation and nitration processes share the same targets – i.e., Tyr residues – and are mutually exclusive events [185] the evaluation of 3-NT/pTyr levels on BVR-A show a significant increase of this ratio starting at 4 years and persisting until 11-12 years (4 years, +60%, p=0.03; 8-10 years, +60, p=0.009; and 11-

12 years, +70%, p=0.04) (Fig. 10F). This observation may suggest that reduced BVR-A phosphorylation could leave BVR-A Tyr residues available for oxidative stress-induced modifications. Indeed, total 3-NT modifications start to accumulate at 4 years becoming significant at 8-10 years (+40%, p=0.01) and remaining elevated also at 11-12 years in the parietal cortex (Fig. 10G).

Overall these results further demonstrate that the impairment of BVR-A – primarily driven by reduced Tyr phosphorylation – is an early event during the aging process and is associated with a dysfunction of the insulin signaling cascade in the brain.

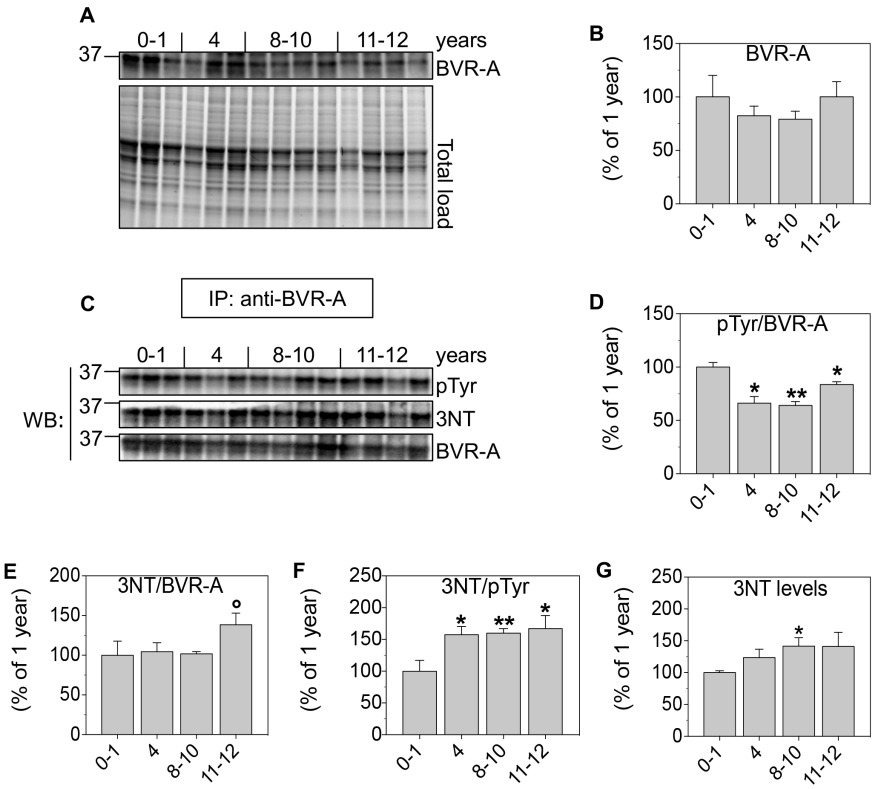

Figure 10. BVR-A activation in the parietal cortex of beagles. BVR-A protein levels, Tyr phosphorylation (pTyr) and 3-nitrotyrosine (3-NT) modifications on BVR-A were measured by immunoprecipitation/Western Blot in the parietal cortex of beagles at 0-1 (n=3), 4 (n=3), 8-10 (n=4) and 11-12 (n=4) years. Panels A-C: western blot analyses. Representative bands are shown. Panels B-D-E-F-G: densitometric analyses of western blot protein bands. BVR-A protein levels were normalized per total protein load. pTyr levels and 3-NTmodifications on BVR-A were normalized by using total BVR-A as loading control. Densitometric values shown are given as percentage of 1 year set as 100%. Mean ± SEM, *$p < 0.05$ vs 0-1 years and °$p < 0.05$ vs 8-10 years (Student's *t*-test).

4.3 Reduced BVR-A activation is associated with an increased CKI-mediated phosphorylation of BACE1 in the parietal cortex

The negative association between BVR-A activation and BACE1 levels found in our previous work [186] likely indicated the possibility of an interaction between these two proteins. BVR-A possess a Ser/Thr/Tyr kinase activity [187] and previous studies reported that Ser phosphorylation of BACE1 regulates BACE1 trafficking from the endosomes to the plasma membrane [188, 189]. For that reason, we first hypothesized that BVR-A could phosphorylate BACE1 as BVR-A does with other proteins [187, 190]. That said, we tested the hypothesis that BVR-A and BACE1 can form a complex. We first evaluated total BACE1 protein levels, that were significantly decreased at 8-10 years (-20%, p=0.01) with respect to younger dogs, and also reduced at 11-12 years (Fig. 11B). Then, we looked at the possible interaction between BVR-A and BACE1 through the immunoprecipitation of BACE1 followed by the evaluation of the levels of total BVR-A as well as its active form (pBVR-A^{Tyr}) bound to BACE1 (Fig. 11C). Our data demonstrated that BVR-A immunoprecipitates with BACE1 and that a significant decrease of their interaction occurs only in aged dogs at 11-12 years (-20%, p=0.01) with respect to younger dogs (Fig. 11D). Interestingly, the evaluation of the pBVR-A^{Tyr} /BACE1 complex showed a significant reduction of the active form of BVR-A bound to BACE1 both at 8-10 years (-30%, p=0.03) and 11-12 years (- 40%, p=0.05) compared to younger dogs (Fig. 11E).

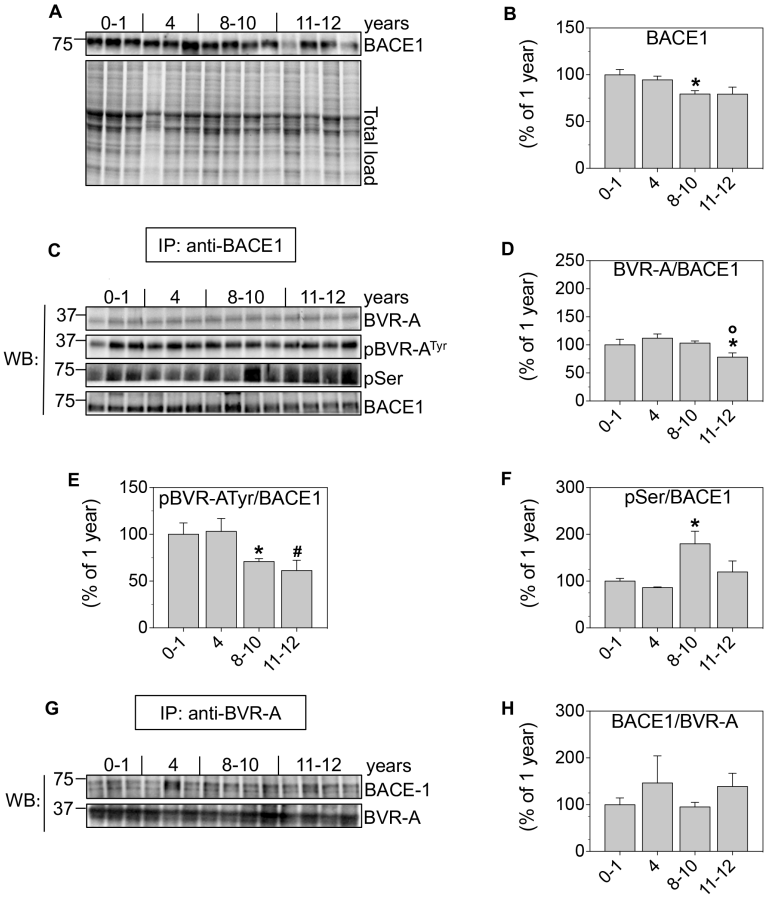

Figure 11. Reduced BVR-A activation is associated with increased Ser phosphorylation of BACE1 in the parietal cortex of beagles. BACE1 protein levels, BVR-A levels, pBVR-A^{Tyr} levels and BACE1 Ser phosphorylation levels were measured by immunoprecipitation/ Western Blot in the parietal cortex of beagles at 0-1 (n=3), 4 (n=3), 8-10 (n=4) and 11-12 (n=4) years. Panels A-C-G: western blot analyses. Representative bands are shown. Panels B-D-E-F-H: densitometric analyses of western blot protein bands. BACE1 protein levels were normalized per total protein load. BVR-A levels and BACE1 Ser phosphorylation levels on BACE1 were normalized by using total BACE1 as loading control. pBVR-A^{Tyr} levels on BACE1 has been calculated by normalizing first pBVR-A^{Tyr} for total BVR-A and then by normalizing the obtained value for total BACE1 used as loading control. BACE1 levels on BVR-A were normalized using total BVR-A as loading control. Densitometric values shown are given as percentage of 1 year set as 100%. Mean ± SEM, *$p < 0.05$ vs 0-1 years, $^{\#}p < 0.05$ vs 4 years and $^{\circ}p < 0.05$ vs 8-10 years (Student's *t*-test)

These data agree with the observed impairment of BVR-A in the parietal cortex, which is also reflected on the interaction with BACE1. To further prove that BVR-A effectively interacts with BACE1, we immunoprecipitated BVR-A and then we looked for BACE1. As showed in Fig. 3H, we found that BACE1 immunopreciptated together with BVR-A, although no significant changes occur with age. We also evaluated the expression of these proteins in the brain by immunohistochemistry and immunofluorescence analyses that confirmed the neuronal co-localization of BVR-A and BACE1 in the brain of beagles at (8-10 years) (Fig. 12). Furthermore, co-localization was also observed in a human AD case (Fig. 12).

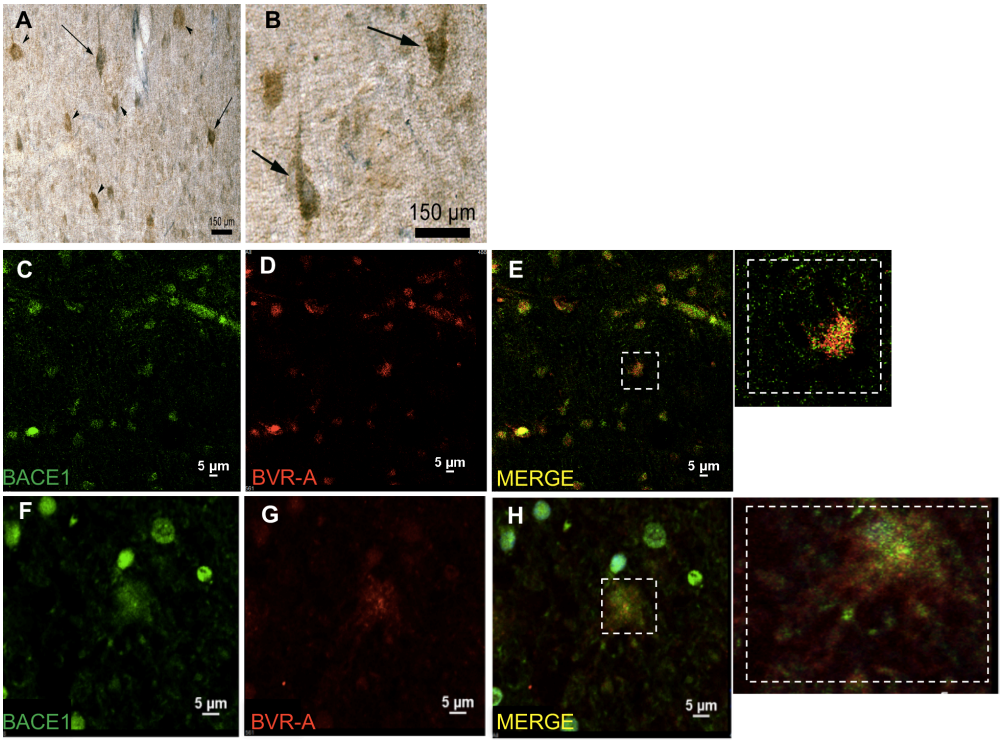

Figure 12. BVR-A and BACE1 co-localization in neurons. Double-staining immunohistochemistry with anti-BACE1 antibody (brown) and anti-BVR-A antibody (blue) in the parietal cortex of beagles at 8-10 years. Some neurons show positive co-localization (arrows) and show positive signal for BACE1 (arrowhead) (Panel A&B). Representative confocal immunofluorescence double labeling in the parietal cortex of beagles at 8-10 years utilizing BACE1 (green, Panel C) and BVR-A (red, Panel D) revealed co-localization of the two antibodies within neurons (Panel E). Representative confocal immunofluorescence double labeling in the frontal cortex of a human AD brain (Panel F-G-H).

To test our hypothesis about a possible BVR-A-mediated phosphorylation of BACE1, we looked at BACE1 Ser phosphorylation levels. Our results reveal that BACE1 is significantly phosphorylated on Ser residues at 8-10 years (+70%, p=0.05) with respect to 1 year (Fig. 11F). This finding, however, was not consistent with our hypothesis because increased BACE1 Ser phosphorylation was associated with reduced pBVR-A^{Tyr}. For that reason, we suggest the existence of a third player, which mediates the phosphorylation of BACE1 and that could be normally inhibited by BVR-A. Among the proteins known to phosphorylate BACE1, CKI was previously reported to have a role in AD [191-194], since it can phosphorylate mature BACE1 at the serine residue 498 in the C-terminal domain to regulate BACE1 recycling from the endosomes to the plasma membrane [188, 189]. We therefore evaluated the age-associated changes of CKIα protein total levels and its association with BACE1 in the parietal cortex (Fig. 13A). We found that CKIα protein levels were significantly increased in all the aged groups relative to 1 year old animals (4 years, +50%, p=0.007; 8-10 years, +60%, p=0.01; and 11-12 years, +60%, p=0.01) (Fig. 13B). Furthermore, a significant increase of CKIα bound to BACE1 (CKIα/BACE1) at 8-10 years (+30%, p=0.03) was observed, compared to the younger group of animals (Fig. 13D).

These results are in agreement both with increased BACE1 Ser phosphorylation and reduced BVR-A activation observed at 8-10 years, thus supporting our hypothesis that under normal conditions, BVR-A could prevent the CKI-mediated phosphorylation of BACE1, while the disruption of BVR-A kinase activity allows such phosphorylation.

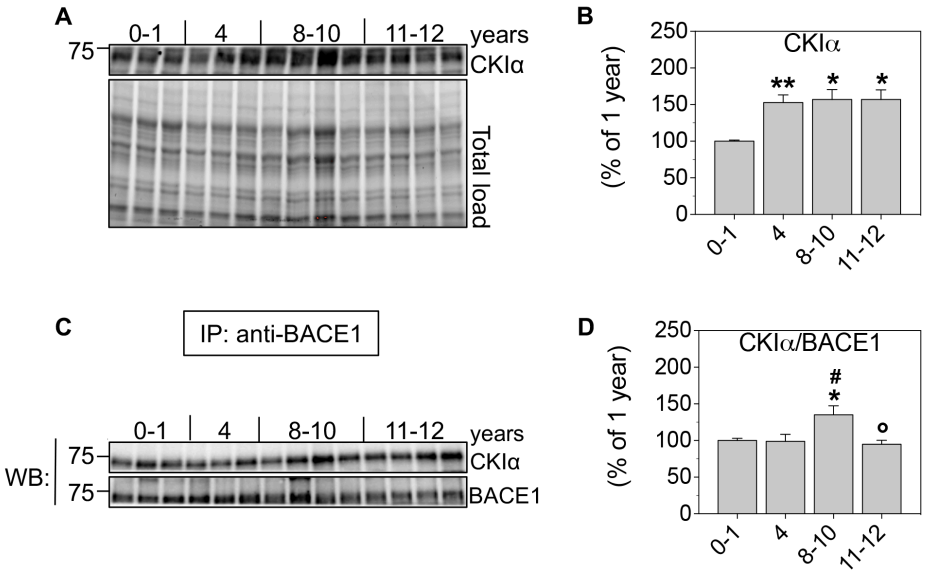

Figure 13. Increased CKIα levels and CKIα association with BACE1 in parietal cortex of beagles. CKIα protein levels and CKIα levels with BACE1 were measured by immunoprecipitation/ Western Blot in the parietal cortex of beagles at 0-1 (n=3), 4 (n=3), 8-10 (n=4) and 11-12 (n=4) years. Panels A-C: western blot analyses. Representative bands are shown. Panels B-D: densitometric analyses of western blot protein bands. CKIα protein levels were normalized per total protein load. CKIα with BACE1 levels were normalized by using total BACE1 as loading control. BACE1 levels on BVR-A were normalized using total BVR-A as loading control. Densitometric values shown are given as percentage of 1 year set as 100%. Mean ± SEM, *$p < 0.05$ vs 0-1 years, **$p < 0.01$ vs 0-1 years, $^{\#}p < 0.05$ vs 4 years and $^{\circ}p < 0.05$ vs 8-10 years (Student's *t*-test).

4.4 Increased BACE1 Ser phosphorylation is associated with increased Aβ levels in the parietal cortex

Phosphorylation favours the recycling of BACE1 from the early endosome to the trans-Golgi network (TGN) and subsequent re-delivery to the plasma membrane [195]. Furthermore, phosphorylated BACE1 colocalized with its protein substrate βAPP and the over-expression of constitutive phosphorylated BACE1 protein is associated with increased Aβ production *in vitro* [188]. To test whether increased BACE1 Ser phosphorylation was associated with an increase of Aβ levels, we evaluated age-associated changes of APP and its cleavage products (Fig. 14A).

Our data demonstrate a decrease of APP protein levels with age, which becomes significant at 11-12 years (-20%, p=0.003) (Fig. 14B). In parallel, we found an age-dependent increase of the BACE1-dependent APP cleavage product (APP CTFβ) without changes of the α-secretase mediated APP cleavage products (APP CTFα). Increased CTFβ levels becomes significant at 8-10 years (+ 100%, p=0.02) with respect to 1 year old dogs (Fig. 14D&E). Furthermore, the evaluation of the CTFβ / CTFα ratio show a significant increase at the same age (+130%, p= 0.02) (Fig. 14F). Along with these changes, we found a significant increase of Aβ dodecamer (Aβ*56, + 300%, p=0.04) at 8-10 years (Fig. 14C), that, together with the observed increase of APP CTFβ at the same age, suggest an increase of the amyloidogenic pathway.

These observations therefore suggest that increased CKI-mediated BACE1 Ser phosphorylation favors the amyloidogenic cleavage of APP, resulting in increased Aβ levels in the brain.

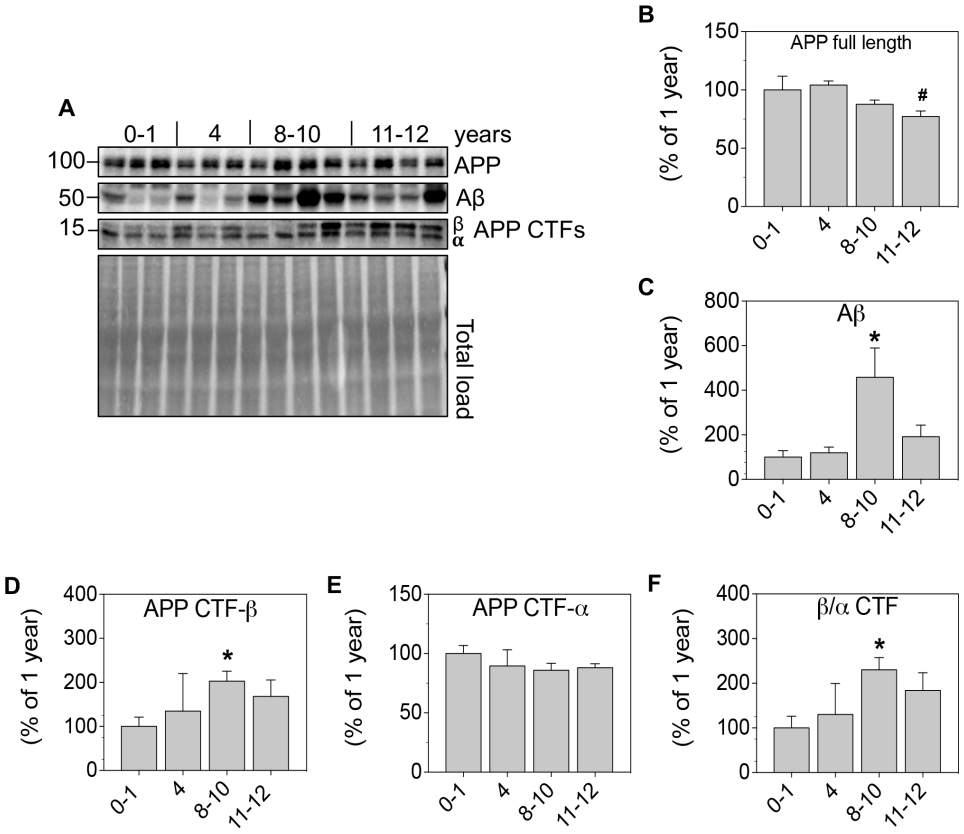

Figure 14. Aβ oligomers and APP production in parietal cortex of beagles. APP, sAPPα, sAPPβ and Aβ protein levels were measured by Western Blot in the parietal cortex of beagles at 0-1 (n=3), 4 (n=3), 8-10 (n=4) and 11-12 (n=4) years. Panel A: western blot analyses. Representative bands are shown. Panels B-C-D-E-F: densitometric analyses of western blot protein bands. APP, sAPPα, sAPPβ and Aβ levels were normalized per total protein load. Densitometric values shown are given as percentage of 1 year set as 100%. Mean ± SEM, *$p < 0.05$ vs 0-1 years and $^{\#}p < 0.05$ vs 4 years (Student's *t*-test).

4.5 Insulin resistance-associated BVR-A impairment promotes the increase of Aβ production by favoring the CKI-mediated Ser phosphorylation of BACE1

In order to demonstrate that decreased BVR-A activation favors CKI-mediated phosphorylation of BACE1 under insulin resistance conditions, we took advantage of a previously published protocol designed to induce insulin resistance *in vitro*. Indeed, we reported that loss of BVR-A obtained through a specific siRNA triggers the development of insulin resistance when cells are treated with a physiological dose of insulin [141].

We found that insulin treatment (100 nM, for 2h) led to a significant increase of BVR-A (+20%, p=0.01) and BACE1 (+80%, p=0.01) protein levels, without alterations of CKIα levels, in control cells (Fig. 15B,C&D, column 2). These changes were not associated with increased Aβ production (Fig. 15H, column 2). Indeed, a consistent reduction of Aβ*56 release in the medium (-40%, p=0.01) was observed. Insulin treatment led to an increased association of CKIα to BACE1 (+200%, p=0.01) (Fig. 15M, column 2). However, CKIα does not affect BACE1 Ser phosphorylation, which was found to be significantly reduced (-80%, p=0.03) (Fig. 15L, column 2). Overall, it seems that despite an increased association between CKIα and BACE1 following insulin treatment, CKIα is unable to mediate the phosphorylation of BACE1, thus resulting in a lower Aβ*56 production.

To demonstrate that BVR-A has a role in this mechanism, we silenced BVR-A and we looked at the effect of insulin. Insulin led to a significant increase of CKIα protein levels (+20%, p=0.01) in siRNA-treated cells, without significant changes of BACE1 (Fig. 15C&D, column 5). Further, we observed a significant increase of extracellular Aβ*56 content (+30,

p=0.0004) in siRNA-treated cells exposed to insulin, with respect to siRNA-treated cells (Fig. 15H, column 4 *vs* column 5). In agreement with our hypothesis, we found that silencing BVR-A did not promote changes of CKIα-bound to BACE1 (Fig. 15M, column 4), but led to a significant increase in phosphorylation of BACE1 (+250%, p=0.01) (Fig. 15L, column 4 vs column 5). Insulin treatment in siRNA-treated cells increased the association of CKIα with BACE1 (+300%, p=0.01) (Fig. 15M, column 4 *vs* column 5) and further increased the phosphorylation of BACE1 (+150%, p=0.01) with respect to siRNA-treated cells not exposed to insulin (Fig. 15L, column 4 *vs* column 5). When we compared the effect of insulin in siRNA-treated cells to control cells, we found that insulin promotes a significant increase of both intracellular (+50, p=0.05) and extracellular Aβ levels (+70%, p=0.03) (Fig. 15G&H, column 2 *vs* column 5) along with an increase of BACE1 phosphorylation (+400%, p=0.01) (Fig. 15L, column 3 *vs* column 5), despite no changes in the association between CKI and BACE1 (Fig. 15M, column 2 vs column 5).

Overall, these results are consistent with the notion that BVR-A plays a role in controlling the trafficking of BACE1 and that loss of BVR-A function is associated with an increased recycling of BACE1, leading to increased Aβ production.

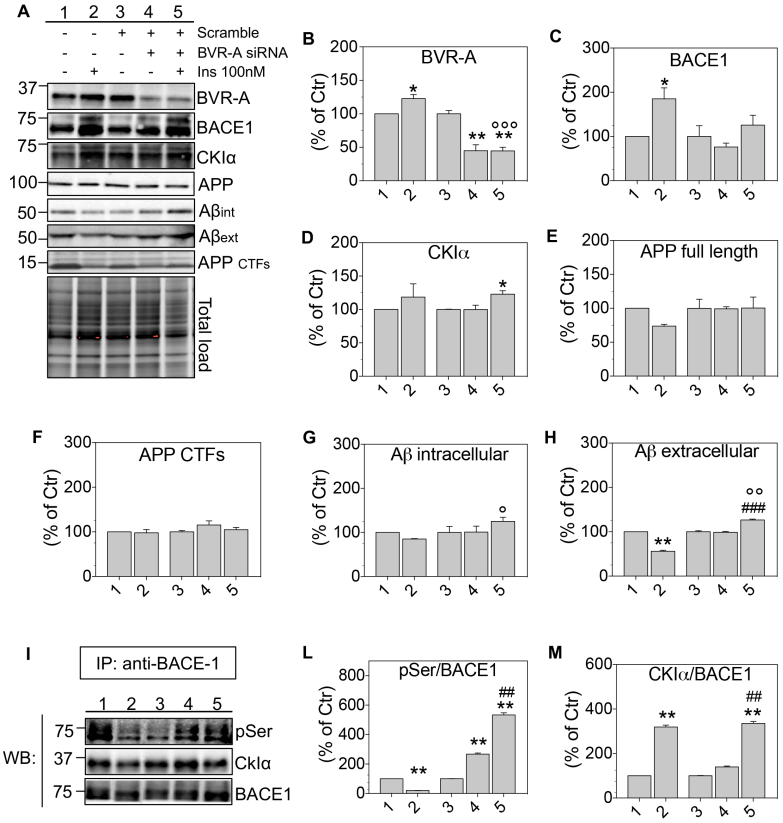

Figure 15. Insulin resistance-associated BVR-A impairment promotes the increase of Aβ production by favoring the CKIα-mediated Ser phosphorylation of BACE1. Western blot analysis of BVR-A, BACE1, CKIα, APP, Aβ intracellular, Aβ extracellular, APP CTFs protein levels in HEK293APPsw cells treated with BVR-A siRNA and insulin (100nM). Panel A: Western blot analyses. Representative bands are shown. Panels B-C-D-E-F-G-H: densitometric analyses of western blot protein bands. BVR-A, BACE1, CKIα, APP, Aβ intracellular, Aβ extracellular, APP CTFs protein levels were normalized per total protein load. Densitometric values shown are given as percentage of Ctr cells set as 100% (n=3 independent cultures/group). Mean ± SEM, *$p < 0.05$ and **$p < 0.01$ vs Ctr cells; $^{\#\#}p < 0.01$ and $^{\#\#\#}p < 0.001$ siRNA-treated cells; $^{\circ}p < 0.05$, $^{\circ\circ}p < 0.01$ and $^{\circ\circ\circ}p < 0.001$ vs insulin-treated cells (Student's *t*-test). Panel I: BACE1 Ser phosphorylation levels and CKIα levels on BACE1 were measured by immunoprecipitation/ Western Blot in HEK293APPsw cells treated with BVR-A siRNA and insulin (100 nM). Western blot analyses. Representative bands are shown. Panels L-M: Densitometric analyses of western blot protein bands. BACE1 Ser phosphorylation levels and CKIα levels on BACE1 were normalized by using total BACE1 as loading control. Densitometric values shown are given as percentage of Ctr set as 100% (n=3 independent cultures/group). Mean ± SEM, **$p < 0.01$ vs Ctr cells, $^{\#\#}p < 0.01$ vs siRNA-treated cells (Student's *t*-test)

5. DISCUSSION

Several studies highlight that brain insulin resistance is directly associated with increased Aβ production [207, 208] or reduced Aβ clearance [209-211] in AD. Furthermore, brain insulin resistance may also exacerbate pre-existing AD pathology [181, 212]. While the role of Aβ in promoting brain insulin resistance – mainly by reducing the membrane-bound fraction of IR available for binding with insulin [213-217] – is known, the molecular mechanisms through which brain insulin resistance favors the production of β-amyloid peptides are still largely unknown.

In this context, we describe a potential mechanism through which the impairment of BVR-A (known to trigger the development of brain insulin resistance [141]) promotes BACE1-mediated cleavage of APP and increases Aβ levels in the brain (Fig. 18). In the hypothesized pathway, an interaction among BVR-A/BACE1/CKIα occurs. BACE1 immunoprecipitates with both BVR-A and CKIα. Our data also suggest that BVR-A exerts a regulatory role on CKIα, thus preventing CKIα-mediated Ser phosphorylation of BACE1 and consequent recycling of BACE1 to plasma membranes [195]. The early impairment of BVR-A kinase activity would trigger BACE1 recycling at the plasma membrane along with alterations of insulin signalling during the progression of AD pathology in the parietal cortex, thus representing a molecular link between brain insulin resistance and Aβ production.

The ability of BVR-A to interact with other proteins has precedents in the literature. Indeed, several sequence motifs within the BVR-A structure were identified as possible protein–protein interaction sites: the cysteine-containing ^{275}KKRILHC and ^{290}KYCCSRK in the C-terminal α-helix, and the two SH2-binding motifs (^{198}YMKM and ^{228}YLSF) [175]. BVR-A

influences cellular signaling pathways by different mechanisms (reviewed in [187]) among which: (i) kinase-kinase activity for the transfer of phosphate groups to the kinase substrate (i.e., BVR-A/IRS1 and BVR-A/IPKC-ζ); (ii) binding to and inducing change in the conformation of the kinase substrate (i.e., BVR-A/Akt and BVR-A/PKC-βII); (iii) translocating signaling effector molecules through the nuclear pore complexes (i.e., BVR-A/ERK1/2); and (iv) being a scaffold protein for the formation of tertiary signaling modules involving its C- and D-boxes in the cytoplasm and in the nucleus (i.e., BVR-A/MEK/ERK and BVR-A/PKCσ/ERK2).

Our data demonstrate that BVR-A physically interacts with BACE1, since they have been co-immunoprecipitated from parietal cortex samples. Furthermore, they have been found to co-localize in neurons both in dogs and AD. However, the simple binding of BVR-A seems to not affect BACE1 Ser phosphorylation. Rather, since the levels of pTyr-BVR-A (active) bound to BACE1 are significantly reduced at 8 years of age when increased BACE1 Ser phosphorylation and increased Aβ levels are observed, we think that BVR-A influences BACE1 mainly through a kinase-kinase mechanism involving CKIα. CK1 proteins are characterized by multiple serine sites whose phosphorylation inhibits their activity [218]. Therefore BVR-A Ser kinase activity could be implicated in this process. Indeed, the association between BACE1 and CKIα occurs independently from the presence of BVR-A, thus excluding the possibility that BVR-A normally limits the interaction between BACE1 and CKIα. Conversely, either the reduced BVR-A activation or the silencing of BVR-A are associated with increased BACE1 Ser phosphorylation in parietal cortex and HEK293APPsw cells, respectively. The BVR-A-mediated inhibition of CKIα is further strengthen by our data showing that insulin treatment (known to induce BVR-A

activation [141, 199]) is associated with reduced BACE1 Ser phosphorylation levels in HEK293APPsw cells, while the opposite occurs in cells lacking BVR-A. Considering that BACE1 Ser phosphorylation has been demonstrated to be specifically mediated by CKIα [188, 189], the suggested inhibitory role for BVR-A on CKIα could represent a conceivable mechanism.

These results, in agreement with the proposed role for the CKI protein family in human AD [191-194, 219], further strengthen the validity of beagles as a spontaneous mammalian model to study Aβ-associated pathology in aging and AD. In particular, CKIα, CKIδ and CKIε were elevated in human AD hippocampus [219]. Furthermore, CKI isoforms accumulate in AD lesions but the pattern varies with isoform. CKIα strongly co-localizes with NFTs, whereas Ck1δ immunostaining is far more intense in granulovacuolar degeneration than in NFTs [220]. Considering that the studies that demonstrated CKI-mediated phosphorylation of BACE1 did not discriminate among the different CKI isoforms [188, 189, 195], we selected CKIα as our target because among the antibodies tested only those against this isoform recognized the canine protein. Although the different isoforms differ in length or in the C-terminal (24–200 amino acids) non-catalytic domain, they show a high homology in their catalytic domain [218].

The impairment of BVR-A kinase activity not only favours CKIα-mediated phosphorylation of BACE1 but is also associated with molecular alterations of the insulin signalling cascade in the parietal cortex. This is of interest in light of the fact that insulin signalling (i) regulates synaptic plasticity in the brain thus affecting cognitive functions [196, 200, 221-224] and (ii) is disrupted in AD (reviewed in [180, 225]).

Mechanistically, insulin resistance phenomenon is characterized by an

inadequate response to insulin by target cells [226] due to reduced IR levels/activation and/or increased levels of inhibitory phosphorylation of IRS1 [181, 207, 227].

Due to the similarities in the molecular processes underlying the development insulin resistance in type 2 diabetes (T2DM), AD has been also defined as type 3 diabetes [228-230]. In this context, T2DM has been proposed as a risk factor for AD principally because the high levels of circulating insulin observed in the first phase of T2DM, may elevate brain and cerebrospinal fluid insulin levels, which in turn down-regulates IR at the blood brain barrier and reduces insulin transport and insulin signalling activation into the brain [231-234].

However, brain insulin resistance can also develop independently from systemic insulin resistance. Most of studies conducted so far – in particular those coming from De Felice group – clearly demonstrated that increased Aβ oligomers production lead to the activation of neuronal TNF-α receptor and the aberrant activation of stress-regulated kinases [i.e. Jun N-terminal kinase (JNK), I kappa B kinase (IKK), and protein kinase R (PKR)] [216, 235] and endoplasmic reticulum (ER) stress (PKR-mediated phosphorylation of eIF2α-P) [235], which leads to IRS1 inhibition. This implies a role for Aβ-mediated neuroinflammation in the development of brain insulin resistance independently from a systemic insulin resistant state.

Our previous results collected in the hippocampus of 3xTg-AD mice further support the idea that alterations of insulin signalling cascade can develop independently from peripheral insulin resistance. We identified the reduced activation of BVR-A as an early molecular event favoring the development of brain insulin resistance since it occurs before a significant inhibition of IRS1 [141]. In particular, in a longitudinal study conducted in

3xTg-AD mice we identified an early phase characterized by reduced BVR-A activation and IRS1 hyper-activation (at 6 months of age) and a late phase in which the persistent reduction of BVR-A activity was associated with a significant inhibition of IRS1 and thus brain insulin resistance (at 12-18 months of age) [141]. Changes of BVR-A and insulin signalling in the brain precede significant alterations of glucose tolerance in 3xTg-AD [236, 237]. Furthermore, we also found that reduced BVR-A activation was evident before a consistent rise in Aβ levels and a significant elevation of TNF-α [141] in the hippocampus, thus representing an early event.

All together these evidences support the role of brain insulin resistance in the progression of AD neuropathology, although the mechanisms through which brain insulin resistance develops or is sustained, could be different.

Interestingly, also in this study, we found that the impairment of the insulin signalling cascade – which is characterized by the typical signs of brain insulin resistance observed in human AD (i.e., reduced IR and Akt activation and increased GSK-3β inhibition [180-183]) – occurs earlier than either (i) Aβ accumulation in the parietal cortex (for additional studies in dogs see also [160, 238]) or (ii) significant manifestations of cognitive decline in beagles [239], thus representing an antecedent event. Moreover, alterations of insulin signalling occur even before a consistent elevation of pro-inflammatory processes in the brain, which has been demonstrated to develop mainly after 8 years of age in beagles [240-245].

We are aware that one limitation of our study is the lack of any metabolic information (i.e. fasting glucose or insulin levels) about the animals used. Indeed, we cannot completely exclude that an altered metabolic profile in these dogs could impact on the molecular changes observed in the

brain. However, as previously reported in 2 longitudinal studies [246, 247], beagles show significant alterations of serum chemistry values possibly referring to an altered metabolic profile (i.e., fasting glucose, triglycerides, ALT, AST) only after 9 years of age. These evidences, therefore, could support our idea about the development of brain insulin resistance independently from peripheral metabolic changes since the first alterations we have found are evident already at 4 years in the parietal cortex.

The observed dysfunction of BVR-A most probably favours these alterations since it occurs in parallel with the reduction of IR and Akt activation, in agreement with our and others previous results. Indeed, BVR-A regulates both IR and Akt activation *in vitro* [174, 198]. Loss of BVR-A triggers the development of both brain [141] and systemic [248, 249] insulin resistance in mice. BVR-A kinase activity is also disrupted in human post-mortem hippocampus of both MCI and AD cases [171, 172] and is reduced in plasma collected from MCI and AD patients [184]. Furthermore, we demonstrated that insulin treatment (100 nM) promote the inhibition of IRS1 instead of the activation of the insulin signalling cascade in neuronal cells lacking BVR-A [141]. Similarly, we found a consistent reduction of BVR-A activation in cells in which we induced insulin resistance [141].

Reduced BVR-A activation in the parietal cortex in dogs, appears to be mainly driven by a reduction of Tyr residue phosphorylation as observed in young 3xTg-AD mice [141], whereas a significant oxidative/nitrosative stress-induced increase of 3-NT on BVR-A occurs at a late stage as we observed in human AD [171]. This observation, highlight the role of oxidative/nitrosative stress as a factor contributing to the alterations of the insulin signalling in the brain. While at the beginning low/mild levels of nitrosative stress contribute to BVR-A dysfunction, the consequent impairment of insulin signalling cascade can even favor the significant

increase of total 3-NT levels as observed in our samples with age. Indeed, insulin signalling plays a pivotal role in the maintenance of mitochondrial functions normally deputed to energy production [250-252]. Therefore, the development of brain insulin resistance would promote mitochondrial dysfunctions responsible for reduced energy production, in turn associated with an increase of reactive oxygen/nitrogen species formation, finally leading to the oxidative/nitrosative damage of mitochondria as well as other cellular components [253].

Of note, the impairment of BVR-A not only alters the physiological activation of the insulin signalling but also precedes the accumulation of β-amyloid peptide in the parietal cortex, thus further strengthening our hypothesis that the role of this protein is to serve as a molecular link bridging brain insulin resistance and Aβ production. Results collected *in vitro* support this mechanism since HEK293APPsw cells silenced for BVR-A show increased Aβ production when stimulated with a physiological dose of insulin. Moreover, data from beagles are in agreement with data collected in 3xTg-AD mice where the impairment of BVR-A was observed before a significant Aβ accumulation in the hippocampus was observed [141].

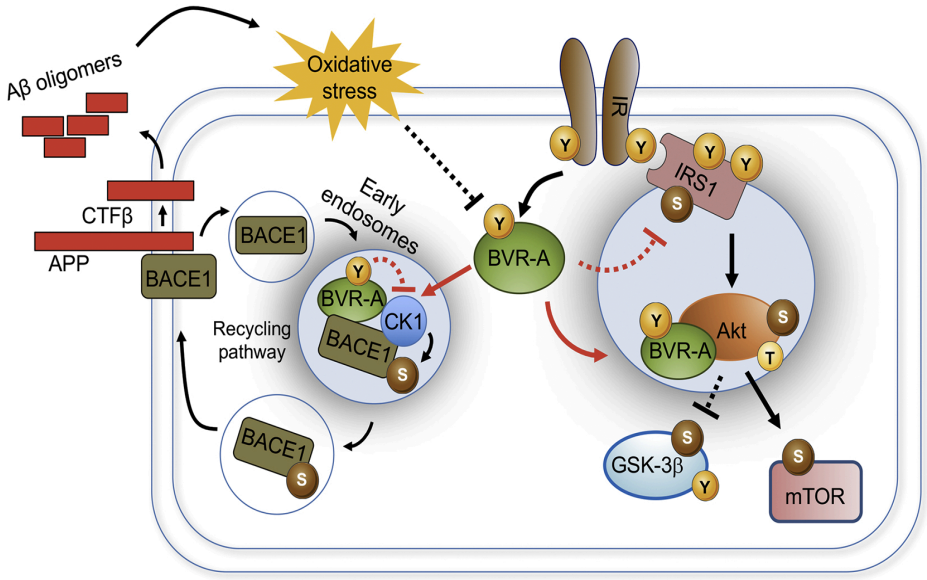

Figure 16. Hypothesized mechanism through which impairment of BVR-A links brain insulin resistance with increased Aβ production in AD. Under physiological conditions insulin receptor (IR) phosphorylates biliverdin reductase-A (BVR-A) on tyrosine (Y) residues promoting BVR-A kinase activity [187]. Through this kinase activity BVR-A regulates the activation of insulin receptor substrate-1 (IRS1) by phosphorylating IRS1 on Ser (S) residues, which normally inhibit IRS1 activation. In this way, BVR-A prevents IRS1 hyper-activation. In parallel, BVR-A favors the activation of protein kinase B (Akt), which inhibits the activation of glycogen synthase kinase-3β (GSK-3β) while promotes the activation of mammalian target of rapamycin (mTOR). Here, we suggest that BVR-A activation plays a critical role also in the regulation of beta secretase 1 (BACE1) recycling to the plasma membrane. The proposed path probably occurs at the level of the early endosomes where casein kinase 1(CK1)-mediated Ser phosphorylation of BACE1 favors BACE1 recycling to plasma membrane [188, 189]. We suggest that during the progression of Alzheimer disease (AD) pathology the early dysfunction of BVR-A (1) impairs the activation of the insulin signalling cascade and in parallel (2) promotes CK1-mediated BACE1 recycling at the plasma membrane, where BACE1 cleaves amyloid precursor protein (APP), leading to increased beta amyloid (Aβ) production. In turn, in a vicious cycle, increased Aβ oligomers trigger the elevation of oxidative and nitrosative stress levels, which further impair BVR-A. Arrows, activation; dotted lines, inhibition. Red arrows/lines, BVR-A functions impaired in AD.

PROJECT 2

6. RESULTS

6.1. Intranasal insulin administration improves short-term learning and memory in 6- and 12-month-old 3×Tg-AD mice.

We tested the effects of insulin treatment on both short- and long-term memory in both 6- and 12-month-old 3×Tg-AD mice and age-matched WT littermates, performing hippocampal- and cortical-dependent tasks as measured by morris water maze (MWM) and novel object recognition (NOR) tests. Spatial learning and memory were measured by MWM, in which mice received 4 training trials/day for 5 consecutive days to locate the hidden platform. Statistics demonstrated no difference in spatial memory during 5 days of training (acquisition) among all experimental groups at 6 and 12 months of age, indicating there is no difference in motivation or ability to perform the task (Fig. 17B). To determine the effects of insulin on memory, the platform was removed from the maze, and tests were conducted 1.5 or 24 h following the last training trial to independently assess both short- and long-term memory, respectively. Insulin significantly rescued the short-term (1.5 h) spatial memory deficits present in both 6- and 12-month-old 3×Tg-AD mice, as indicated by a significantly decreased latency to cross the platform location and increased time spent in target quadrant of the 3×Tg-AD mice treated with insulin compared to vehicle-treated 3×Tg-AD (Figures 17C and D). Moreover, insulin had no significant effects on learning or memory retention in WT mice. When a probe session was performed at 24 hours

(long-term memory) after the last training session, at 6 months of age, insulin induced only a trend toward a decrease (-32%) in the 3×Tg-AD compared to vehicle-treated 3×Tg-AD mice (Fig. 17C); conversely, the latency to cross platform location was significantly decreased (-58%) at 12 months of age in insulin-treated 3×Tg-AD mice compared to age-matched vehicle-treated 3×Tg-AD mice (Fig. 17C). Regarding the time spent in the target quadrant at 24 h after the last training session, insulin induced only a trend toward an increase in the 3×Tg-AD compared to vehicle-treated 3×Tg-AD mice (+35% and +52%, respectively, at 6 and 12 months of age) (Fig. 17D). Finally, multiple *post-hoc* comparisons showed that 3×Tg-AD mice treated with insulin performed similarly to the WT mice in all probe trials and at both time-points.

The NOR test exploits the natural tendency of mice to explore objects perceived as novel. As previously described, the retention session was performed at two different time points (30 min or 24 h) after the exploration session in order to assess both short- and long-term memory, respectively. Two-way ANOVA for the object recognition index (ORI) at a time-point of 30 min (short-term memory) either in 6- and 12-month-old mice revealed a significant main effect of genotype and treatment, while no significant genotype-by-treatment interaction effect was found. Multiple *post-hoc* comparisons showed a significant higher ORI in insulin-treated 3×Tg-AD with respect to vehicle-treated 3×Tg-AD mice, indicating that insulin significantly improves the short-term recognition memory in the 3×Tg-AD mice (Fig. 19E). When the probe trial was performed 24 h after the exploration session (long-term memory), we observed only a significant main effect of genotype among the four groups (Fig. 17E). Although insulin-treated 3×Tg-AD mice performed better than vehicle-treated 3×Tg-AD mice, multiple *post-hoc* comparisons did not reach any significant difference

(+26% and +21%, respectively, at 6 and 12 months of age). Finally, at both time points, the *post-hoc* analysis indicated that insulin had no effect on the performance of WT mice.

Overall, these data indicate that insulin significantly both prevents and rescues the impairment of the short-term memory in either 6- and 12-month-old 3×Tg-AD mice, respectively with no significant effects on long-term memory. Moreover, insulin apparently exerts no significant effects on learning or memory in both adult and aged WT mice.

6.2 Intranasal insulin administration ameliorates the depressive-like behaviour in 3×Tg-AD mice.

Depressive-like behaviours were measured by the tail suspension test (TST) and forced swim test (FST). Statistical details are reported in Table 1. At 6 and 12 months of age, significant main effects of treatment, genotype, and genotype-by-treatment interactions were observed, except for the interaction in the older group of animals. As previously demonstrated [165, 166], *post-hoc* comparisons revealed that the immobility time in both tests was higher in vehicle-treated 3×Tg-AD than in vehicle-treated WT mice (Fig. 17F&G). Moreover, insulin significantly decreased the immobility time in the 3×Tg-AD mice for both tests, either at 6 and 12 months of age (Fig. 17F&G).

Taken together, these results confirm that 3×Tg-AD mice show a depressive-like phenotype, which is reversed by insulin treatment at 6 and 12 months of age. Moreover, insulin has no significant effect on WT mice.

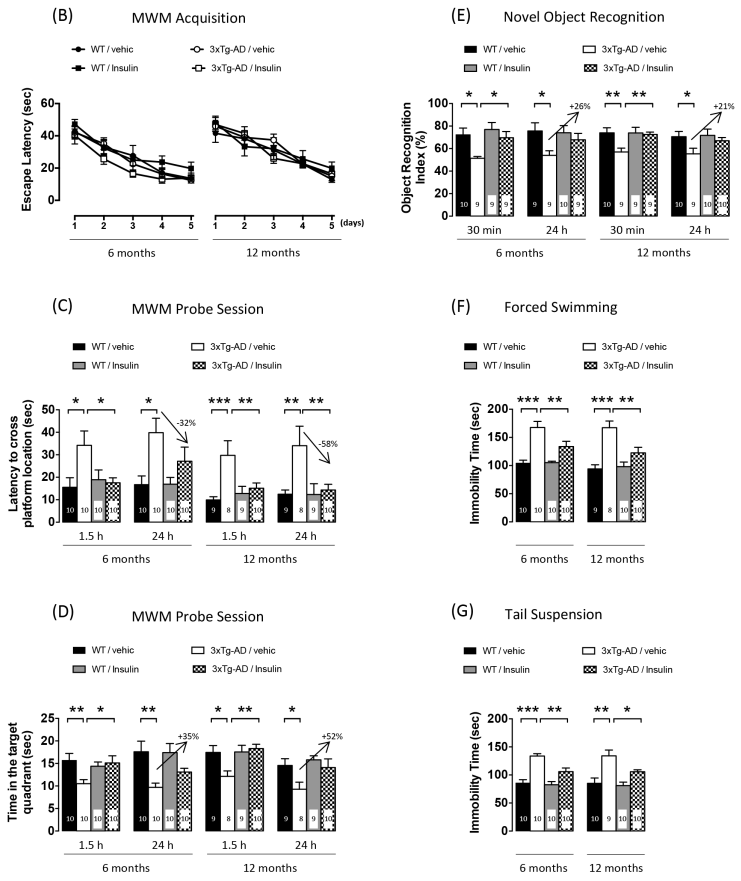

Figure 17. Insulin rescues short-term memory deficits and ameliorates the depressive-like phenotype in the 3×Tg-AD mice. (A) Schematic representation of the experimental design. Evaluation of the cognitive (B-E) and emotional phenotype (F and G) of 6- and 12-month-old 3×Tg-AD and age-matched Non-Tg mice chronically treated with vehicle or insulin. Short- and long-term memory of mice was evaluated (B-D) by Morris water maze (MWM) and (E) novel object recognition (NOR) test (NORT). Moreover, the emotional phenotype of mice was evaluated by (F) forced swimming test (FST) and (G) tail suspension test (TST). Sample size is indicated in the bars. Data are presented as means ± SEM. Statistical analysis was performed by two-way ANOVA followed by Tukey's multiple comparison test (*$p < 0.05$; **$p < 0.01$; ***$p < 0.001$).

6.3 Intranasal insulin administration prevents the impairment of BVR-A and the early dysfunction of the insulin signalling cascade in adult 3×Tg-AD mice at 6 months of age.

According to our hypothesis, the impairment of BVR-A is associated with the dysfunction of the insulin signalling cascade, which contributes to the cognitive impairment observed in AD [181, 196]. However, no data exist about the role of BVR-A in the hippocampal synaptic plasticity. To investigate this aspect, we studied long-term potentiation (LTP) at CA3–CA1 synapses in hippocampal organotypic slices biolistically transfected with shRNA for BVR-A together with a plasmid enconding enhanced green fluorescent protein (EGFP) to identify the transfected neurons (Fig. 18A). Silencing of BVR-A significantly reduced the LTP magnitude at CA3-CA1 synapses compared with LTP observed in neurons transfected with a scrambled shRNA (shLuc=261+/-92.4% *versus* shBVR-A=176.9 +/-66.8%, $p = 0.049$; Fig. 20B).

These data demonstrate for the first time that BVR-A has a role in the hippocampal synaptic plasticity and therefore its impairment in AD could be crucial to mediate cognitive and learning dysfunctions.

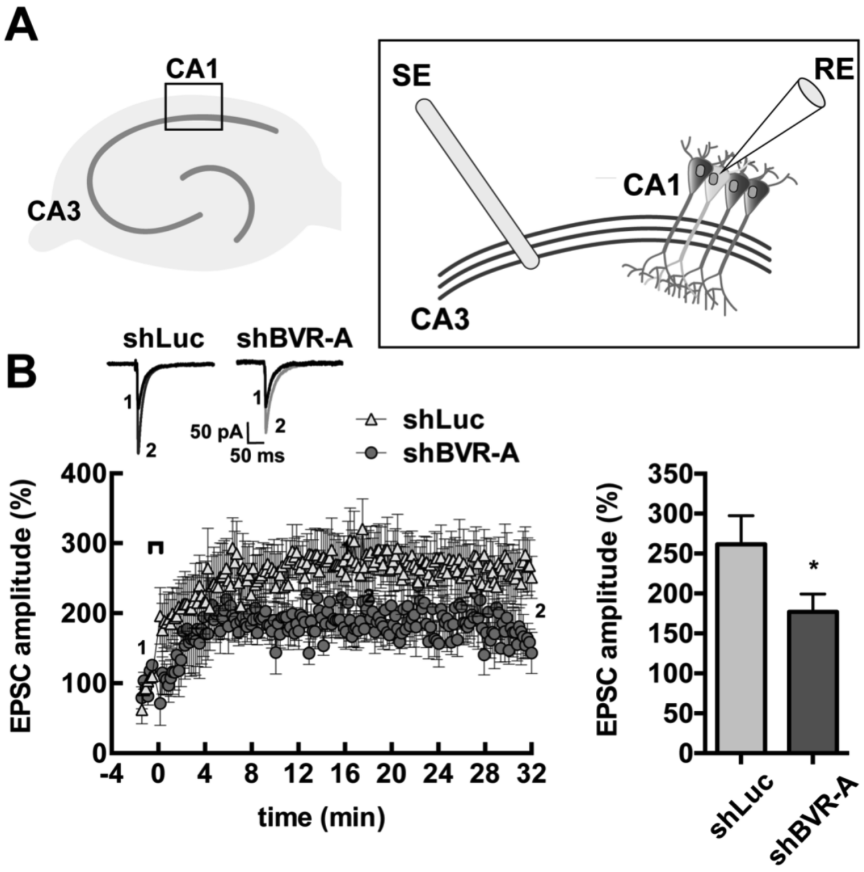

Figure 18. Hippocampal LTP was inhibited in organotypic brain slices in which BVR-A was silenced. (A) Schematic representation of whole-cell recording from CA1 hippocampal pyramidal neuron in organotypic hippocampal slice (see methods for details). (B) Time course of LTP at CA3-CA1 synapses in hippocampal organotypic slices transfected with BVR-A shRNA or scrambled shRNA. Results are expressed as percentages of baseline EPSC amplitude (=100%). Insets (top) show representative EPSC at baseline (1) and during the last 5 min of LTP recording (2). C) Mean LTP values during the last 5 min ($n = 7$-8/group). Data are expressed as mean ± SEM *$p < 0.05$.

To determine whether INI administration was effective in preventing the impairment of BVR-A and the early alterations of the insulin signalling cascade observed in 3×Tg-AD mice at 6 months of age [141], here we evaluated changes of (i) BVR-A protein levels and Tyr phosphorylation together with (ii) the levels and activation of some main components of the insulin signalling cascade in the hippocampus and cortex of 3×Tg-AD mice and their littermate WT controls, treated with vehicle or insulin for 2 months (from 4 to 6 months of age). First, we confirmed our previous results showing reduced BVR-A levels and activation in the hippocampus of 6-month-old vehicle-treated 3×Tg-AD mice compared to vehicle-treated WT mice (Fig. 19A-C). INI treatment did not affect BVR-A protein levels (Fig. 19A&C), while INI was effective in preventing the observed impairment of BVR-A activation in 3×Tg-AD mice (Fig. 19B&C). No significant changes were observed between INI-treated and vehicle-treated WT mice (Fig. 19A-C).

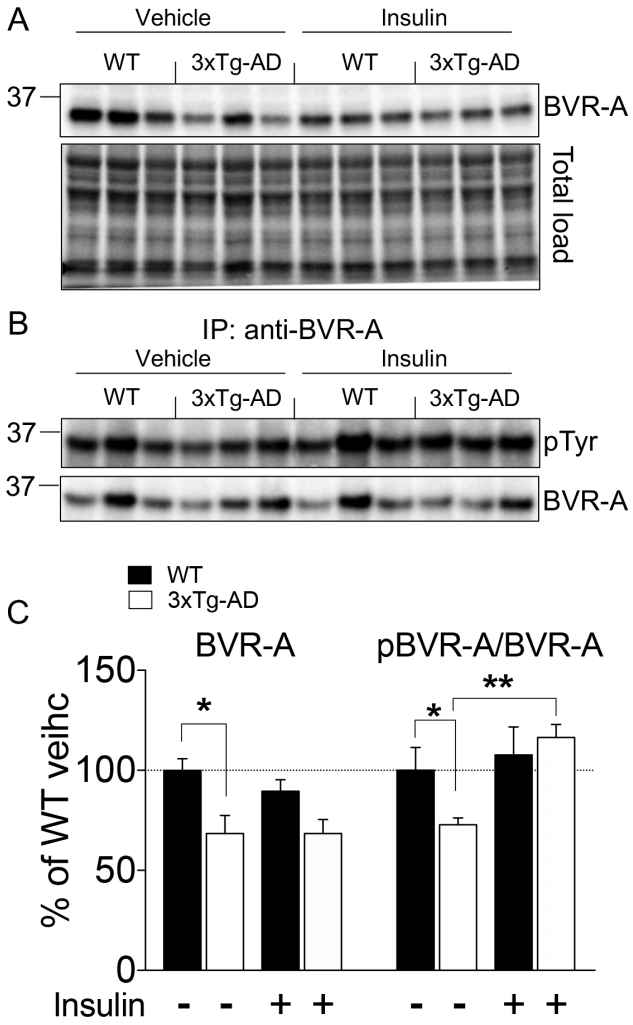

Figure 19. Intranasal insulin prevents the early impairment of BVR-A in the hippocampus of 3×Tg-AD mice at 6 months of age. (A-B) Immunoblot analysis and (C) densitometric evaluation of changes of BVR-A protein levels and Tyr-phosphorylation (pTyr) observed in the hippocampus of 3×Tg-AD mice and WT littermate controls treated with vehicle (vehic) or insulin from 4 to 6 months of age. Densitometric values shown are given as percentage of WT vehic mice set as 100%. BVR-A protein levels were normalized per total protein load. pTyr levels on BVR-A were normalized by using total BVR-A as loading control following immunoprecipitation [169, 170]. Data are presented as means ± SEM (n=6 mice/group). Statistical analysis was performed by Two-way ANOVA followed by Bonferroni's multiple comparison test (*$p < 0.05$).

Consistent with our hypothesis, the activation of BVR-A, induced by INI treatment, resulted in a significant improvement of the insulin signalling cascade in the hippocampus of 3×Tg-AD mice (Fig. 20). In particular, we found that INI further stimulated IR activation ($pIR^{Tyr1158/1161/1162}$/IR) in adult 3×Tg-AD mice compared to age-matched vehicle-treated 3×Tg-AD mice, leaving unchanged the IR protein levels (Fig. 20B&C). Moreover, we evaluated the activation of IRS1 by analysing the levels of two of the best characterized sites known to promote IRS1 inhibition and thus insulin resistance even in AD brain: Ser307 and Ser636 [181, 197]. INI did not induce changes of IRS1 levels, while INI prevented the pathological hyper-activation of IRS1 in 3×Tg-AD mice, as demonstrated by the extent of IRS1 inhibition (mostly $pIRS1^{Ser636}$/IRS1), which returns close to those observed for WT mice (Fig. 20B&D). Rescue of the BVR-A/IRS1 axis activation was reflected by the activation of the downstream targets. Here, we extended our previous findings [141] by showing that ERK1/2 levels did not change across all the experimental groups, while their activation was significantly increased in the hippocampus of vehicle-treated 3×Tg-AD mice and it was partially reduced (~70%, p=0.07) following INI administration (Fig. 20B&E). Further, we found that Akt protein levels in the hippocampus of 3×Tg-AD mice were significantly increased compared to vehicle-treated WT mice, and were not affected by INI treatment (Fig. 20B&F); conversely, Akt activation was strongly stimulated following insulin administration in 3×Tg-AD mice compared to vehicle-treated group ($pAkt^{Ser473}$/Akt, Fig. 20B&F). The improvement of Akt activation was associated with the amelioration of mTOR activation, whose reduction was prevented in INI-treated 3×Tg-AD mice ($p\text{-}mTOR^{Ser2448}$/mTOR, Fig. 20B&G). Keeping in mind the role of BVR-A in regulating insulin signalling at different levels [187, 198, 199],

these observations further support our hypothesis that the impairment of BVR-A is associated upstream with the hyper-activation of the IR/IRS1 axis, while downstream with an aberrant activation of MAPK and Akt/mTOR axes. Instead, INI treatment prevents the alterations of BVR-A and ameliorates the entire activation of the insulin signalling in the hippocampus of adult 3×Tg-AD mice.

In WT mice, INI treatment led to a significant increase of the IR activation (Fig. 20C) – indicating the stimulatory effect of administered insulin – which, was associated with a reduction of IRS1 Ser636 phosphorylation (~40%, p=0.06, Fig. 20D), along with a significant increase of ERK1/2 activation (Fig. 20E). No changes of the Akt/mTOR pathway were observed in the hippocampus of INI-treated WT mice with respect to vehicle-treated WT mice (Fig. 20F&G). This is in agreement with the well-known possibility that the two main harms of the insulin signalling cascade, i.e., the MAPK and the Akt pathways, are not stimulated simultaneously [200, 201].

Taken together, these lines of evidence suggest that the impairment of BVR-A occurs early along the progression of AD pathology in 3×Tg-AD mice and is associated with a dysfunction of the insulin signalling cascade mainly in the hippocampus, which can be significantly prevented by INI administration.

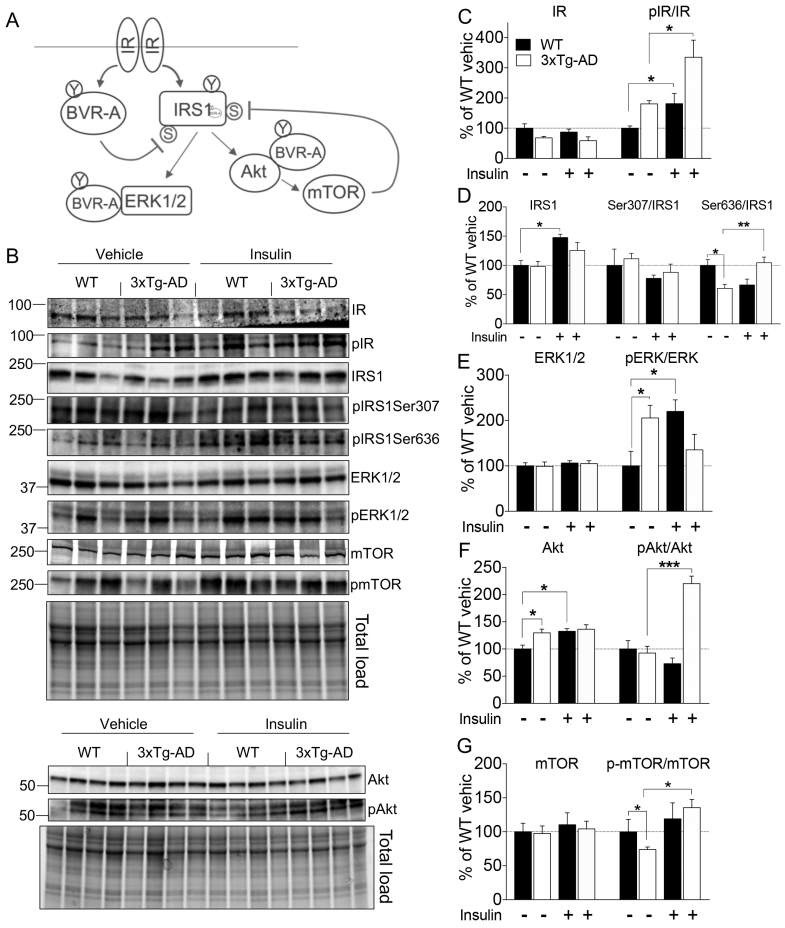

Figure 20. Intranasal insulin promotes IR activation and prevents the early impairment of the insulin signalling cascade in the hippocampus of 3×Tg-AD at 6 months of age. (A) Schematic representation of the insulin signalling cascade. Blue arrows: activation; red line: inhibition; Y: tyrosine residues; S: serine residues. (B) Immunoblot analysis and (C-G) densitometric evaluation of IR, IRS1, ERK1/2, Akt and mTOR protein levels and phosphorylation measured in the hippocampus of 3×Tg-AD mice and in WT littermate controls treated with vehicle (vehic) or insulin from 4 to 6 months of age. Densitometric values shown are given as percentage of WT vehic mice set as 100%. Protein levels were normalized per total protein load. Proteins' phosphorylation was normalized by taking into account the respective protein levels and are expressed as the ratio between the phosphorylated form and the total protein levels: pIR$^{(Tyr1158/1162/1163)}$/IR, pIRS1$^{(Ser307\ or\ Ser636)}$/IRS1, pERK1/2$^{(Thr202/Tyr204)}$/ERK1/2, pAkt$^{(Ser243)}$/Akt, pmTOR$^{(Ser2448)}$/mTOR. Data are presented as means ± SEM (n=6 mice/group). Statistical analysis was performed by Two-way ANOVA followed by Bonferroni's multiple comparison test (*$p < 0.05$, **$p < 0.01$).

6.4 Intranasal insulin administration recovers BVR-A activation and prevents the onset of brain insulin resistance in aged 3×Tg-AD mice at 12 months of age.

To further characterize the molecular mechanisms underlying the beneficial effects of INI, we evaluated whether insulin treatment (from 10 to 12 months) was effective in recovering the activation of BVR-A and thus preventing the onset of brain insulin resistance in aged (12 months) 3×Tg-AD mice [141].

In agreement with what we observed with adult (6 months) 3×Tg-AD mice, INI administration to aged 3×Tg-AD mice did not promote changes of brain BVR-A protein levels, which remained reduced even after the treatment, whereas INI significantly recovered the activation of BVR-A in the hippocampus of aged 3×Tg-AD mice (Fig. 21C). Unexpectedly, INI treatment promoted a significant reduction of BVR-A activation in the hippocampus of WT mice compared to the vehicle-treated WT mice (Fig. 21C).

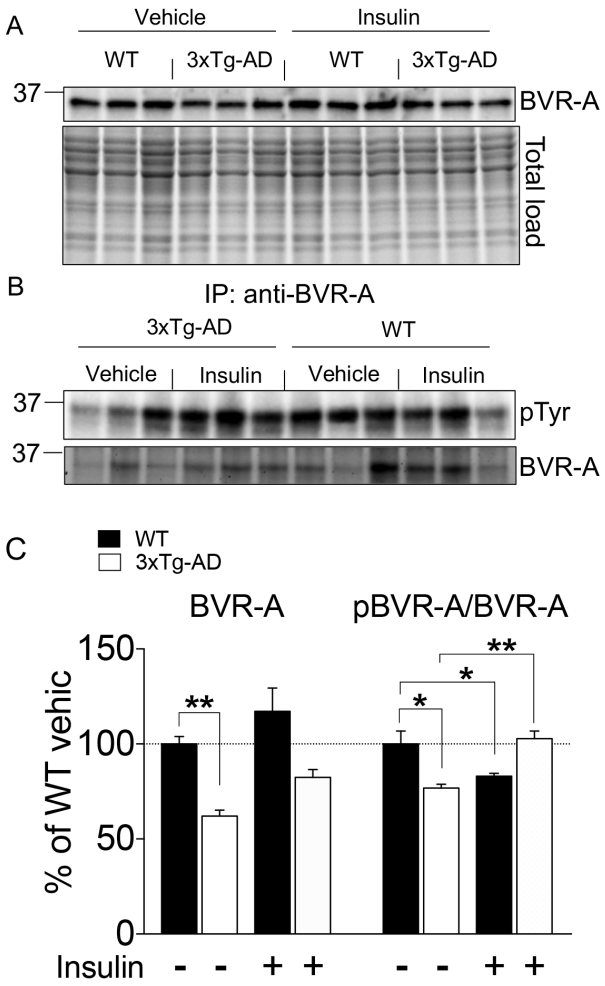

Figure 21. Intranasal insulin recovers BVR-A activation in the hippocampus of 3×Tg-AD mice at 12 months of age. (A-B) Immunoblot analysis and (C) densitometric evaluation of changes of BVR-A protein levels and Tyr-phosphorylation (pTyr) observed in the hippocampus of 3×Tg-AD mice and WT littermate controls treated with vehicle (vehic) or insulin from 10 to 12 months of age. Densitometric values shown are given as percentage of WT vehic mice set as 100%. BVR-A protein levels were normalized per total protein load. pTyr levels on BVR-A were normalized by using total BVR-A as loading control following immunoprecipitation [169, 170]. Data are presented as means ± SEM (n=6 mice/group). Statistical analysis was performed by One-way ANOVA followed by Bonferroni's multiple comparison test (*$p < 0.05$; **$p < 0.01$).

The evaluation of the insulin signalling cascade revealed that INI administration did not promote an increase of IR protein levels (Fig. 22A&B), while INI led to a consistent activation of the IR in the hippocampus of aged 3×Tg-AD mice compared to vehicle-treated 3×Tg-AD mice (Fig. 22A&B). With regard to IRS1 activation, here we strengthened our previous findings [141] by also showing a significant elevation of IRS1 Ser636 phosphorylation (Fig. 22A&C), which, together the observed impairment of the IR, are indicative of a condition of brain insulin resistance. INI significantly reduced the levels of IRS1 Ser636 phosphorylation in 3×Tg-AD mice, which were reported close to those of vehicle-treated WT mice (Fig. 22A&C). Downstream from IR, the amelioration of the BVR-A/IRS1 axis positively did impact on both ERK1/2 and Akt pathways in the hippocampus of aged 3×Tg-AD mice. Although we did not find changes for ERK1/2 or Akt protein levels (Fig. 22D&E), we found significant differences in terms of their activation. Indeed, the insulin resistance phenomenon was associated with no changes of ERK1/2 activation (Fig. 22D), but a consistent impairment of Akt activation in the hippocampus of vehicle-treated 3×Tg-AD mice was found (Fig. 22E). Strikingly, INI was effective in promoting the activation of both ERK1/2 (Fig. 22A&D) and Akt (Fig. 22A&E) proteins, thus indicating an improved insulin signalling activation. Downstream from Akt, we did not observe changes for mTOR protein levels and activation in aged 3×Tg-AD mice following INI treatment (Fig. 22F). However, by considering that IRS1 Ser636 is a direct target of mTOR when aberrantly activated [197], it seems that INI administration ameliorates the regulation of the Akt/mTOR axis finally resulting in a reduction of IRS1 Ser636 phosphorylation.

In WT mice, insulin administration promoted the activation of the IR without significant changes of the downstream targets, except for Akt whose activation was significantly reduced (Fig. 22A&E). Other than Akt, we also noticed an augmentation mTOR activation (~78%, p=0.08, Fig. 22A&F), which, together with reduced BVR-A activation, could be representative of an impairment of the insulin signalling cascade. These results, therefore, possibly suggest that insulin, if administered for long time to an adult brain that is not compromised, could favour/accelerate the impairment of insulin signalling [as shown by [202-204].

Overall, these results suggest that INI administration improves the activation of BVR-A and prevents the onset of brain insulin resistance in the brain of aged 3×Tg-AD mice.

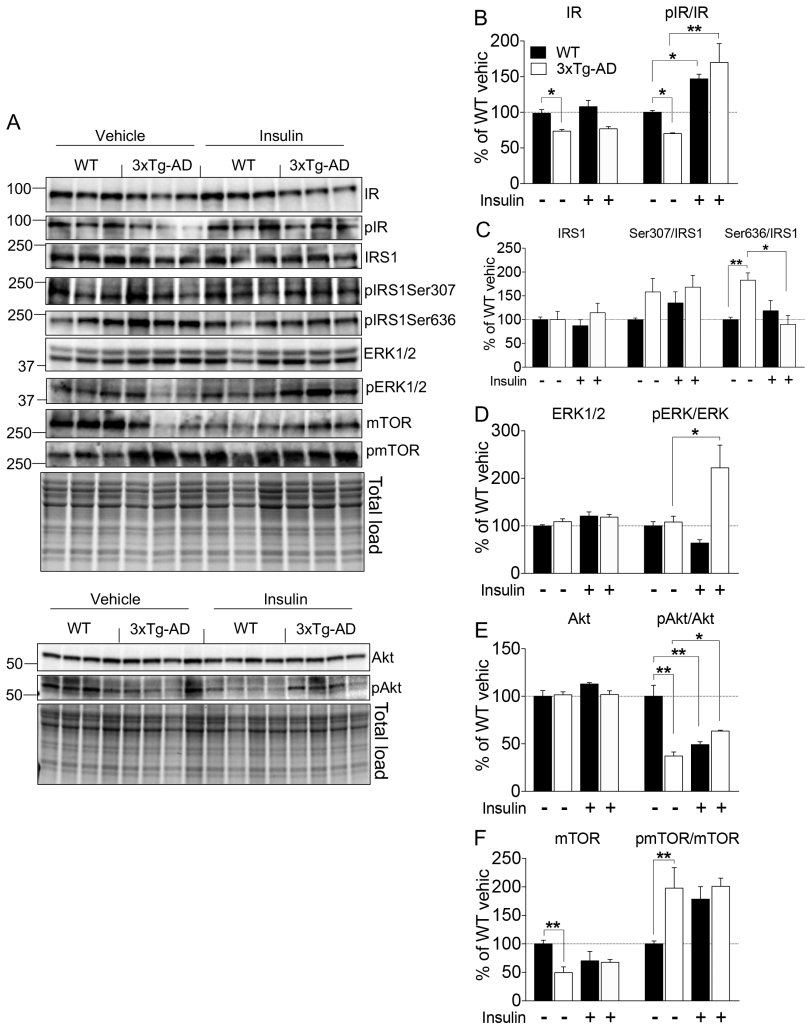

Figure 22. Intranasal insulin promotes IR activation and prevents the onset of brain insulin resistance in the hippocampus of 3×Tg-AD at 12 months of age. (A) Immunoblot analysis and (B-F) densitometric evaluation of IR, IRS1, ERK1/2, Akt and mTOR protein levels and phosphorylation measured in the hippocampus of 3×Tg-AD mice and in WT littermate controls treated with vehicle (vehic) or insulin from 10 to 12 months of age. Densitometric values shown are given as percentage of WT vehic mice set as 100%. Protein levels were normalized per total protein load. Proteins' phosphorylation were normalized by taking into account the respective protein levels and are expressed as the ratio between the phosphorylated form and the total protein levels: pIR$^{(Tyr1158/1162/1163)}$/IR, pIRS1$^{(Ser307\ or\ Ser636)}$/IRS1, pERK1/2$^{(Thr202/Tyr204)}$/ERK1/2, pAkt$^{(Ser243)}$/Akt, pmTOR$^{(Ser2448)}$/mTOR. Data are presented as means ± SEM (n=6 mice/group). Statistical analysis was performed by Two-way ANOVA followed by Bonferroni's multiple comparison test (*$p < 0.05$, **$p < 0.01$).

6.5 BVR-A is required for the correct transduction of the insulin signalling cascade *in vitro*.

To investigate whether BVR-A activation is essential to mediate the beneficial effects of the INI administration in 3×Tg-AD mice, we performed several *in vitro* experiments aimed to demonstrate that insulin's ability to recover cells from insulin resistance requires BVR-A. First, we tested whether insulin (100 nM) at different times (2-6-12-24 h) promotes the activation of its downstream targets in controls cells and in cells in which BVR-A had been silenced (to mimic a condition in which BVR-A does not work). We found that insulin leads to the activation of ERK1/2 and Akt only in control cells (Fig. 23F&H, respectively). In siRNA-treated cells insulin failed to promote its downstream effects. Rather, insulin treatment favours the inhibitory phosphorylation of IRS1 along with suppression of ERK1/2 and Akt activation (Fig. 23F&H, respectively). These results, therefore, indicate that BVR-A is required to mediate the correct transduction of the insulin signalling cascade, which otherwise would be shifted toward a condition of insulin resistance.

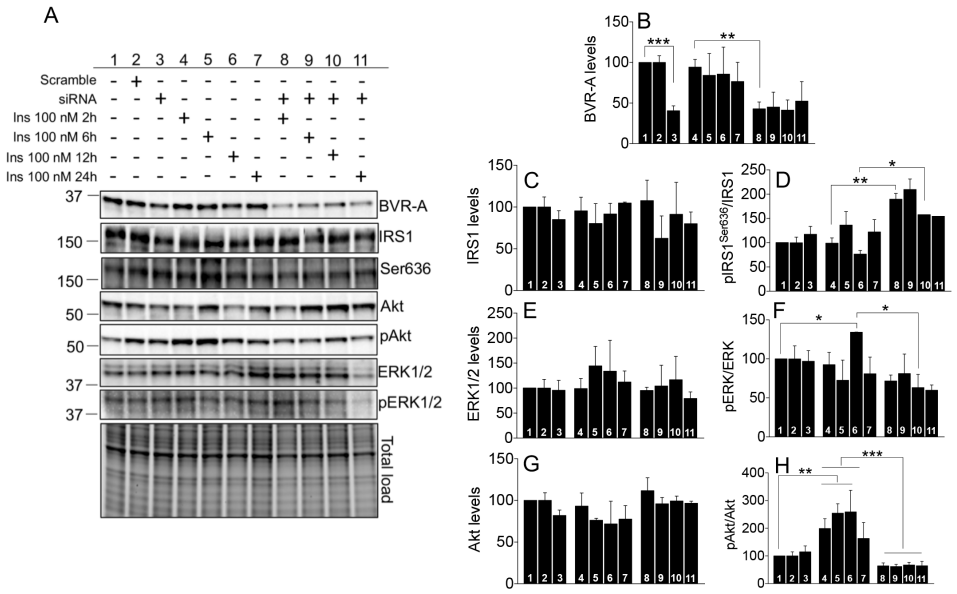

Figure 23. BVR-A is required to mediate the correct activation of the IS cascade *in vitro*. (A) Immunoblot analysis and (C-G) densitometric evaluation of BVR-A, IRS1, ERK1/2 and Akt protein levels along with their activation evaluated in HEK cells following insulin treatment at different times. Numbers in panel (B) and those indicated in each column of the densitometric analysis are matched. Densitometric values shown are given as percentage of control cells (column 1) set as 100%. Protein levels were normalized per total protein load. Proteins' phosphorylation were normalized by taking into account the respective protein levels and are expressed as the ratio between the phosphorylated form and the total protein levels: pIRS1$^{(Ser636)}$/IRS1, pERK1/2$^{(Thr202/Tyr204)}$/ERK1/2 and pAkt$^{(Ser243)}$/Akt. Data are presented as means ± SEM (n=3 independent cultures/group). *$p < 0.05$ (Student t-test).

Based on these data and due to the fact that Akt was the main target modulated by the INI administration in 3×Tg-AD mice, we selected 2 h as time for treatment to use in the subsequent experiments. As shown in Fig. 24A, we set up a protocol in which, first we induced insulin resistance and then we tried to recovery insulin signalling activation both in control and siRNA-treated cells, by re-challenging these cells with increasing doses of insulin (to mimic the effect of the INI administration).

Indeed, we found that insulin (100 nM, for 2h) promoted the activation of IR, Akt and mTOR in control cells (Fig. 24C-G, column 4), whereas a significant increase of IRS1 inhibition (Fig. 24D, column 5), a reduction of Akt activation (Fig. 24F, column 5) and a sustained activation of mTOR (Fig. 24G, column 5) were observed when we induced insulin resistance by over-exposing these cells to additional insulin (100 nM, for additional 2h). Similar changes were found in siRNA-treated cells where insulin treatment (100 nM, 2 h) directly promoted insulin resistance (Fig. 24C-G, column 9). At this point, both control and siRNA-treated cells were re-challenged with fresh medium containing increasing doses of insulin (100 nM-500 nM-1 μM, for 2 h) to test whether insulin was able to recover the activation of the insulin signalling cascade. We found that insulin, at all the concentrations tested, further increased the activation of IR both in control (Fig. 24C, columns 6-8) and siRNA-treated cells (Fig. 24C, columns 10-12). Notwithstanding this result, we observed a difference in terms of activation of the downstream targets. In control cells, among the tested doses, insulin at 500 nM was able to partially recover the activation of Akt (Fig. 24F, column 7), thus possibly indicating an amelioration of the insulin signalling cascade. Conversely, neither of the tested doses was effective in promoting Akt activation in siRNA-treated cells (Fig. 24F, columns 10-12). Increased Akt

activation was also associated with a reduction of mTOR activation in control cells (Fig. 24G, column 7). Instead, a persistent mTOR activation even further elevated at the highest dose of insulin (1 μM) was observed in cells in which BVR-A was silenced (Fig. 24G, columns 10-12).

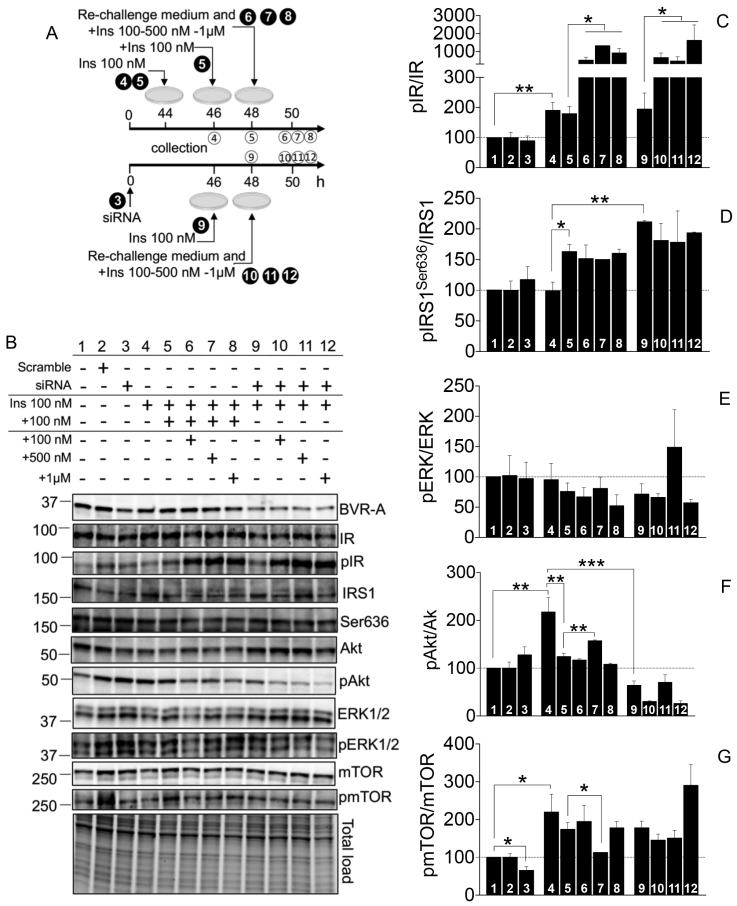

Figure 24. BVR-A is required recovery insulin signalling activation *in vitro*. (A) Scheme of the protocol used to induce the activation of the insulin signalling as well as insulin resistance in HEK cells (for details see Material and Methods). For each condition, numbers in plain circle indicate the treatment while those in empty circle are relative the collection time. (B) Immunoblot analysis and (C-G) densitometric evaluation of BVR-A, IR, IRS1, ERK1/2, Akt and mTOR activation evaluated following different insulin treatments in control HEK cells or in cells in which BVR-A was silenced through a specific siRNA. Numbers in panel (B) and those indicated in each column of the densitometric analysis are matched and are indicative of the treatment performed as also indicated in (A). Densitometric values shown are given as percentage of control cells (column 1) set as 100%. Protein levels were normalized per total protein load. Proteins' phosphorylation were normalized by taking into account the respective protein levels and are expressed as the ratio between the phosphorylated form and the total protein levels: $pIR^{(Tyr1158/1162/1163)}$/IR, $pIRS1^{(Ser636)}$/IRS1, $pERK1/2^{(Thr202/Tyr204)}$/ERK1/2, $pAkt^{(Ser243)}$/Akt, $pmTOR^{(Ser2448)}$/mTOR. Data are presented as means ± SEM (n=3 independent cultures/group). *$p < 0.05$ (Student t-test).

To further confirm the pivotal role of BVR-A, we took advantage of the use of the BVR-A- mimetic peptide ^{290}KYCCSRK, which has been previously demonstrated to mimic the kinase activity of BVR-A toward the IR/IRS1 axis thus favoring the activation of the insulin signalling cascade [174, 205]. Strikingly, we found that insulin (100 nM, for 2h) did not induce insulin resistance if administered together with the peptide (10 and 20 μM) in siRNA-treated cells (Fig. 27, columns 5-7). The treatment with the peptide at both the tested doses favors the activation of the insulin signalling cascade as demonstrated by the significant reduction of IRS1 inhibition (Fig. 25D, columns 6-7), the increase of both ERK1/2 (Fig. 25E, coulmns 6-7) and Akt activation (Fig. 25F, columns 6-7) and the reduction of mTOR activation (Fig. 25G, columns 6-7). Furthermore, the peptide allows recovery of siRNA-treated cells from insulin resistance (Fig. 25, columns 8-10). Indeed, while insulin alone is not able to recover insulin signalling activation, insulin does if administered together with the peptide, which leads to a significant reduction of IRS1 inhibition (Fig. 25D, columns 8-10) along with a significant activation of Akt (Fig. 25F, columns 8-10) and a reduction of mTOR activation (Fig. 25G, columns 8-10).

Overall these findings demonstrate the central role that BVR-A plays in the regulation of the insulin signalling cascade and also strengthen the notion of the role played by BVR-A in the molecular mechanisms underlying the beneficial effects of the INI administration.

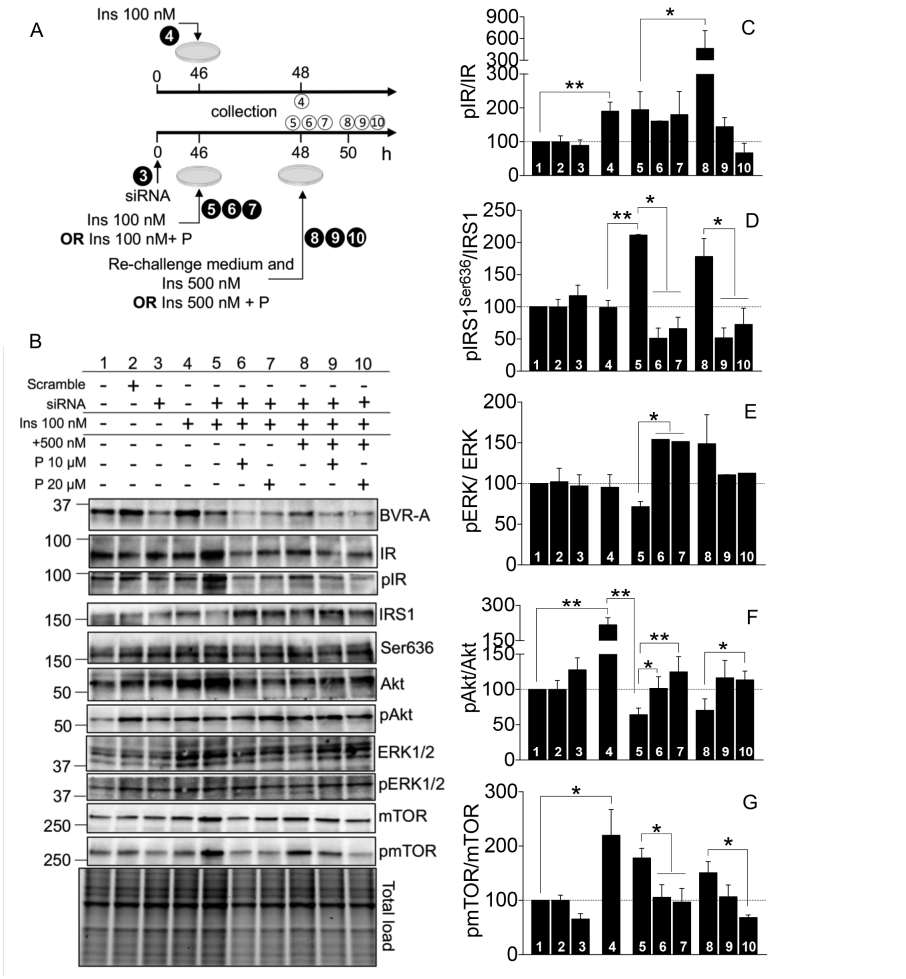

Figure 25. The BVR-A mimetic peptide ^{290}KYCCSRK recovers the correct activation of the insulin signalling cascade in cells lacking BVR-A. (A) Scheme of the protocol used to treat cells (for details see Material and Methods). For each condition, numbers in plain circle indicate the treatment while those in empty circle are relative the collection time. (B) Immunoblot analysis and (C-G) densitometric evaluation of BVR-A, IR, IRS1, ERK1/2, Akt and mTOR activation evaluated in control cells or in cells silenced for BVR-A and treated with insulin alone or in combination with the ^{290}KYCCSRK peptide (P). Numbers in panel (B) and those indicated in each column of the densitometric analysis are matched and are indicative of the treatment performed as also indicated in (A). Densitometric values shown are given as percentage of control cells (column 1) set as 100%. Protein levels were normalized per total protein load. Proteins' phosphorylation were normalized by taking into account the respective protein levels and are expressed as the ratio between the phosphorylated form and the total protein levels: pIR$^{(Tyr1158/1162/1163)}$/IR, pIRS1$^{(Ser636)}$/IRS1, pERK1/2$^{(Thr202/Tyr204)}$/ERK1/2, pAkt$^{(Ser243)}$/Akt, pmTOR$^{(Ser2448)}$/mTOR. Data are presented as means ± SEM (n=3 independent cultures/group). *$p < 0.05$ and **$p < 0.01$ (Student t-test).

6.6 Amelioration of insulin signalling activation is associated with reduced oxidative stress levels and AD neuropathological markers in the hippocampus and cortex of INI-treated 3×Tg-AD mice.

We previously reported that the dysregulation of the insulin signalling cascade in the hippocampus of 3×Tg-AD mice was associated with increased oxidative/nitrosative stress levels as well as a worsening of AD-like neuropathology [141]. To further explore whether the improved functionality of the insulin signalling cascade following INI administration might affect the above-mentioned pathological features of AD brain, we evaluated changes of oxidative/nitrosative stress markers, Aβ oligomers and Tau levels, and phosphorylation in the hippocampus and cortex of WT and 3×Tg-AD mice both at 6 and 12 months of age.

We found that INI treatment significantly reduced 3-NT levels in the hippocampus both in adult (Fig. 26A) and aged (Fig. 26D) 3×Tg-AD mice.

In parallel, western blot analysis revealed that INI treatment did not significantly modify the expression of full-length APP and Aβ dodecamer (Aβ*56) either in the hippocampus of 6-month-old insulin-treated 3×Tg-AD mice (Fig. 26B&C). Rather, we observed a significant reduction of Aβ oligomers in hippocampus (Fig. 26E&F) of 12-month-old 3×Tg-AD. To better understand the mechanisms responsible for the observed reduction of Aβ in the hippocampus of 3×Tg-AD mice following INI administration, we analysed the expression levels of the insulin-degrading enzyme (IDE), known to be involved in the degradation of Aβ [206]. Regardless of the age of the mice, we observed no significant changes in the expression levels of IDE either in the hippocampus of 3×Tg-AD mice after INI administration (Fig.

26B&F) thus suggesting that probably other degradative or clearance mechanisms are responsible for the observed reduction of Aβ oligomers.

Finally, we found that INI administration was able to ameliorate Tau pathology both in hippocampus and frontal cortex of 3×Tg-AD mice. In particular, we observed reduced phosphorylation levels of tau protein on Ser202/Thr205 residues in the hippocampus of adult (Fig. 26B&C) and aged (Fig. 26E&F) 3×Tg-AD mice.

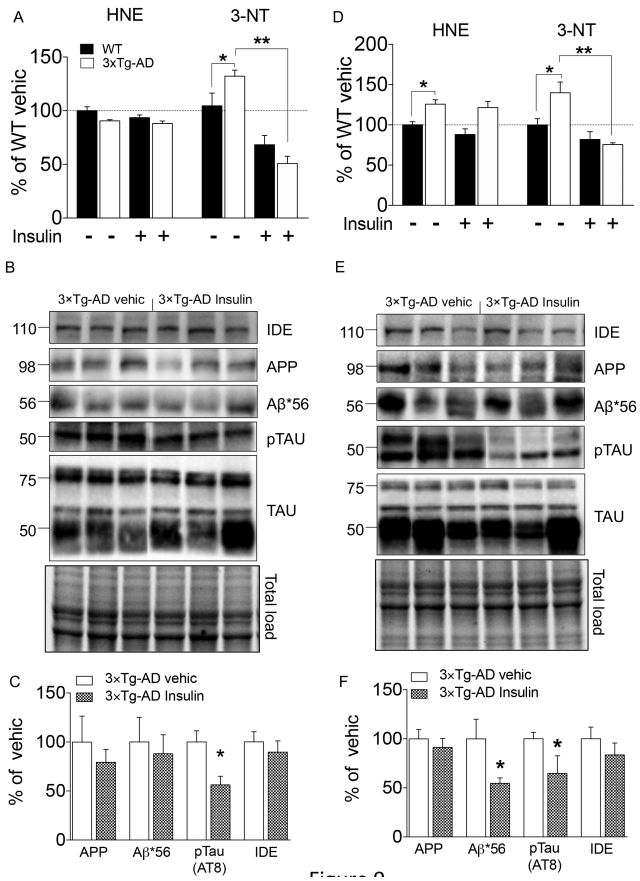

Figure 26. Improvement of insulin signalling cascade activation following insulin administration is associated with reduced nitrosative stress levels and an improvement of AD neuropathology in the hippocampus of 3×Tg-AD mice. Changes of oxidative (HNE) and nitrosative (3-NT) stress levels evaluated in the hippocampus of 3×Tg-AD mice and WT littermate controls treated with vehicle (vehic) or insulin from 4 to 6 months (A) and from 10 to 12 months (D) of age. Data are presented as means ± SEM (n=6 mice/group). Statistical analysis was performed by Two-way ANOVA followed by Bonferroni's multiple comparison test (*$p < 0.05$, **$p < 0.01$). (B and E) Immunoblot analysis and (C and F) densitometric evaluation of changes of full-length APP, Aβ dodecamer (Aβ*56), Tau phosphorylation and IDE measured in the hippocampus of 3×Tg-AD treated with vehicle or insulin from 4 to 6 months (B and C) and from 10 to 12 months (E and F) of age. For oxidative/nitrosative stress markers values shown are given as percentage of WT vehic mice set as 100%. Densitometric values shown are given as percentage of 3×Tg-AD vehic mice set as 100%. Protein levels were normalized per total protein load. Tau phosphorylation was normalized by taking into account the respective protein levels and are expressed as the ratio between the phosphorylated form and the total protein levels: $pTau^{(Ser202/Thr205)}$/Tau. Data are presented as means ± SEM (n=6 mice/group) *$p < 0.05$ (Student t-test)

7. Discussion

With a long prodromal period of 10 to 20 years, AD and related dementias are becoming a priority for many governments, considering that 1% of global gross domestic product is spent on dementia care [254]. Brain insulin resistance greatly contributes to this preclinical period during which only subtle behavioral symptoms are evident [158], and no reliable biomarkers indicative of any potential risks are available [255]. Therefore, the comprehension of the initiating molecular events leading to brain insulin resistance is fundamental to strengthen the set-up of new prevention strategies aimed to reduce both the risks and the dramatic outcomes of metabolic dysfunctions in the brain.

To better characterize the molecular mechanisms underlying the alterations of brain insulin signalling, we focused on the protein BVR-A [187], whose impairment was demonstrated to precede the canonical molecular alterations associated with the insulin resistance phenomenon, i.e., reduced IR or increased IRS1 inhibition [181, 200, 216, 253] in 3xTg-AD mice [141]. Hence, we hypothesized that INI administration, by favoring the IR-mediated activation of BVR-A, would prevent the alterations of the insulin signalling in the brain. Indeed, despite the reported beneficial effects of INI administration in humans [256-260], the molecular mechanisms that underlie the effects of insulin are still poor understood. In particular, it is not clear whether or not intranasal insulin overcomes insulin resistance by promoting the activation of the insulin signalling cascade [158, 261].

Here, we provided some answers to this point by demonstrating that INI treatment promoted the activation of the IR and its downstream targets in the brain of both adult and aged 3×Tg-AD mice. Remarkably, improvement

of insulin signalling activation occurs along with an improvement of BVR-A activation both in the hippocampus.

In agreement with our hypothesis, INI administration prevented the early impairment of BVR-A activation in 3×Tg-AD mice (Fig. 19). Indeed, an improved BVR-A activation seems to be useful to dampen IRS-1 hyper-activation (as indexed by decreased Ser636 phosphorylation) (Fig. 20D), and it is also associated with an improvement of Akt phosphorylation (Fig. 20F) [198], which also prevents the failure of mTOR activation (Fig. 20G), in the hippocampus of 3×Tg-AD mice at 6 months of age.

As previously reported, other than the brain insulin resistance phenomenon, also this non-physiological hyper-activation phase could produce deleterious effects in terms of learning and memory functions [262-266]. Interestingly, by preventing the early alterations of the insulin signalling cascade in the 6-month-old 3×Tg-AD mice, INI also significantly ameliorated the short-term spatial learning in MWM, as well as the short-term working memory in the NOR task (Fig. 17). Differently, the long-term memory (spatial and working) was not significantly affected by INI treatment, although we observed a trend toward an improvement of cognitive dysfunctions compared to vehicle-treated 3×Tg-AD mice. Other authors found that INI treatment was able to positively affect the long-term memory in C57BL/6 mice [267]. The discrepancy may be attributed to the differences in the experimental contexts and animals (transgenic *versus* non-transgenic mice, adult/aged *versus* very young), and mostly due to the use of different dosage of insulin and scheme of treatment (80 μg/every other day for 2 months *versus* 900μg/day for 7 days), which may have affected the assessment of the cognitive phenotype in our experiments versus those reported by other authors.

Also of interest, to our knowledge this is the first study showing that INI treatment ameliorates depressive-like behaviour in the 6-month-old 3×Tg-AD mice performing two different tests (Fig. 17). It is prudent, in fact, to test parallel depressive paradigms to strongly confirm phenotype. We therefore decided to perform two subsequent tests that are indicators of depressive behavior: forced swimming and tail suspension. We previously demonstrated that 3×Tg-AD mice show a depressive-like phenotype [165, 166] that is completely reversed by INI treatment.

Collectively, these observations agree with the well-known role of insulin in modulating synaptic plasticity [that is, LTP and long-term depression (LTD)] via Akt [200, 221]. Furthermore, insulin has a crucial role in the development and maintenance of excitatory synapses [200, 222] and has been shown to promote dendritic spine formation and excitatory synapse development through activation of the Akt/mTOR axis [200, 223]. In this picture, our results showing that silencing of BVR-A is sufficient to promote a dysfunction of LTP in rat brain slices (Fig. 18) represent an intriguing novelty, that, together with the observed impairment of the insulin signalling, further supports a role for BVR-A in the molecular mechanisms regulating cognitive functions (Fig. 17).

The effectiveness of INI administration is evident also in aged (12 months of age) 3×Tg-AD mice used to test the hypothesis that INI, by rescuing BVR-A impairment, prevents the onset of brain insulin resistance. Indeed, at 12 months of age these mice show a reduction of BVR-A activation along with clearly signs of insulin resistance including: (i) reduced IR levels and activation (Fig. 22B); (ii) increased IRS1 Ser636 phosphorylation (Fig. 24C); (iii) uncoupling of Akt/mTOR signalling (Figures 22E&F). Interestingly, we found that INI treatment was able to recover the activation of BVR-A (Fig. 21) and to prevent the increased IRS1

inhibition (Fig. 22C), which results in a downstream improvement of both Akt (Fig. 22E) and ERK1/2 activation (Fig. 22D) finally leading to a significant recovery in terms of cognitive functions (Fig. 22F) [196, 200, 224, 268]. In fact, at the behavioural level, 12-month-old 3×Tg-AD mice confirm the phenotype of younger 3×Tg-AD mice. In particular, INI treatment significantly enhances short-term spatial and working memory, as well as evokes depressive-like behavior in 3×Tg-AD mice (Fig. 17). As far as the long-term memory, INI treatment significantly decreases (-58%) the latency to cross platform location in the MWM and, although not significant, also ameliorates other behavioral endpoints of spatial and working memory in the 3×Tg-AD mice compared to age-matched, vehicle-treated 3×Tg-AD mice.

Surprisingly, we did not see a decrease of mTOR activation – which is among the kinases whose aberrant activity is known to mediate IRS1 inhibition [197, 269] also in AD [179, 182, 270-273] – in aged 3×Tg-AD mice following insulin treatment. However, we believe that the improvement of Akt activation together with the observed decrease of IRS1 phosphorylation on a site known to be target of mTOR kinase activity [Ser636 [197], are indicative of an improved regulation of the Akt/mTOR axis.

All these lines of evidence suggest that changes of BVR-A are strongly associated with alterations of the insulin signalling cascade in the brain. However, whether BVR-A is directly involved in the beneficial effects of INI both in adult and aged mice remained to be investigated. For that reason, we performed several *in vitro* experiments by using cells in which BVR-A was silenced to clarify the role of BVR-A in the mechanisms associated with insulin resistance (Figures 24&25). First, our results demonstrated that cells lacking BVR-A and treated with insulin develop insulin resistance rather than a physiological activation of the insulin

signalling (Fig.23 and Fig. 24). Indeed, an increase of IRS1 Ser636 phosphorylation (Fig. 24D, column 5), a decrease of Akt activation (Fig. 24F, column 5) along with a persistent activation of mTOR (Fig. 24G, column 5) was observed. Interestingly, these results agree with the molecular changes observed in 3×Tg-AD mice at 12 months of age (Fig. 22). At that age, we showed that BVR-A is required to recover cells from insulin resistance (Fig. 24), since the above-cited alterations were retrieved only in control cells but not in cells lacking BVR-A, following the exposure to high dose insulin (500 nM) (Fig. 24). These data, therefore, strongly support the mechanism hypothesized for INI-treated mice. The essential role for BVR-A is strengthened by the results collected in cells lacking BVR-A and treated with a BVR-A-mimetic peptide (Fig. 25). As mentioned before, several sequence motifs within BVR-A structure were identified as possible protein–protein interaction sites [175]. Among these peptides, ^{290}KYCCSRK was found to stimulate IR-mediated phosphorylation/activation of BVR-A finally leading to an increase glucose up-take in HEK cells [174, 205]. However, these observations were limited to the evaluation of basal glucose up-take. Thus, we tested whether the ^{290}KYCCSRK peptide could rescue cells from insulin resistance, and we demonstrated that in cells lacking BVR-A insulin promotes the activation of the insulin signalling cascade, and thus recoveries cells from insulin resistance, only if administered together with the peptide (Fig. 25). Indeed, decreased IRS1 inhibition, increased ERK1/2 and Akt activation, and decreased mTOR hyper-activity were observed (Fig. 25).

The recovery of insulin signalling physiological activation in 3×Tg-AD mice had beneficial effects also on Aβ and Tau pathology and is able to reduce the accumulation of oxidative damage both in adult and aged 3×Tg-AD mice (Fig. 26). Accordingly, previous data demonstrated that insulin

deficiency leads to increased Tau phosphorylation, which was reversed by insulin administration directly in the brain [274-277], and that higher brain insulin concentrations may reduce amyloid oligomerization and toxicity [214], increase synaptogenesis [278], or modulate long-term potentiation and depression in the hippocampus, thus improving learning and memory [279].

8. CONCLUSIONS

Brain insulin resistance (BIR) could be a pivotal responsible for the progression of AD. Mechanistically, this condition is defined as an alteration on insulin response that could be caused by a reduction of brain insulin receptor sensitivity. Interesting, insulin signaling is impaired in *post mortem* brain tissue from AD patients [144], and as long as the role of insulin in cells growth and survival [99] is known, improving insulin action in neurons has emerged as an intriguing strategy to improve cognitive functions. Therefore, restoring insulin signalling activation in the brain by insulin treatment may provide therapeutic benefits in AD subjects.

Among the regulatory points of this signaling, BVR-A was found to be impaired quite early during the progression of AD as demonstrated by several data collected by our group including this thesis work. Indeed, results showed here provide additional observations strengthen the hypothesis that the impairment of BVR-A is an early event in the progression of AD pathology and that it occurs before insulin signalling impairment and Aβ deposition. Interestingly, we demonstrate that recovering BVR-A activity allows to rescue early alterations of the insulin signalling cascade and to prevent the onset of brain insulin resistance. These changes are associated with a reduction of nitrosative stress, Tau phosphorylation and Aβ oligomers in brain, along with improved cognitive functions.

In addition, we show for the first time that BVR-A impairment might favor an increased Aβ production in the brain through the regulation of BACE1 recycling, thus representing a possible molecular link between BIR and AD pathology. In this contest, BVR-A represents a molecular target to be

further investigated in AD. Indeed, the modulation of BVR-A activity could delay the onset of brain insulin resistance along with an improved regulation of the APP cleavage, which would result in reduced Aβ levels in the brain.

Strikingly, our results represent a step forward for the comprehension of the very early mechanisms responsible for the alteration of the insulin signalling cascade, finally resulting in brain insulin resistance, along the progression of AD neuropathology. The comprehension of the initiating molecular events is fundamental to develop new prevention strategies and to improve therapeutic strategies for the treatment of this disease.

Within this scenario our data suggest the key role of BVR-A in the progression of AD neuropathology supporting the importance of this protein as a potential therapeutic target to prevent brain insulin resistance in AD and to stop or delay the neurodegenerative process.

9. REFERENCES

1. A. Alzheimer, R.A.S., H.N. Schnitzlein, F.R. Murtagh, 8(6) (1995) 429-31., *An English translation of Alzheimer's 1907 paper, "Uber eine eigenartige Erkankung der Hirnrinde".* Clin. Anat., 1995. **8**(6): p. 429-31.

2. M. Goedert, M.G.S., , Science 314(5800) (2006) 777-781., *A Century of Alzheimer's Disease.* Science, 2006. **314**(5800): p. 777-781.

3. Duthey, B., *Alzheimer disease and other dementias.* Priority Medicines for Europe and the World. " A public Health Approach to Innovation" 2004. **6**(11): p. 1-74.

4. Liesi E. Hebert, J.W., Paul A. Scherr, Denis A. Evans, *Alzheimer disease in the United States (2010–2050) estimated using the 2010 census.* neurology, 2013. **80**(19): p. 1768-1773.

5. Lendon CL, A.F., Goate AM., *Exploring the etiology of Alzheimer disease using molecular genetics. .* JAMA, 1997: p. 825-831.

6. S.C. Janicki, N.S., *Hormonal Influences on Cognition and Risk for Alzheimer Disease,.* Curr Neurol Neurosci Rep, 2010. **10**(5): p. 359-366.

7. Gendron, T.F. and L. Petrucelli, *The role of tau in neurodegeneration.* Mol Neurodegener, 2009. **4**: p. 13.

8. Selkoe, D.J., *The cell biology of beta-amyloid precursor protein and presenilin in Alzheimer's disease.* Trends Cell Biol, 1998. **8**(11): p. 447-53.

9. F.K. Wiseman, T.A.-J., J. Hardy, A. Karmiloff-Smith, D. Nizetic, V.L. Tybulewicz, E.M. Fisher, and A. Strydom, *A genetic cause of Alzheimer disease: mechanistic insights from Down syndrome, .* Nature Reviews Neuroscience, 2015.

10. Masters, C.L., et al., *Alzheimer's disease.* Nat Rev Dis Primers, 2015. **1**: p. 15056.

11. Goate, A., et al., *Segregation of a missense mutation in the amyloid precursor protein gene with familial Alzheimer's disease.* Nature, 1991. **349**(6311): p. 704-6.

12. Barber, R.C., *The genetics of Alzheimer's disease,.* Scientifica (Cairo), 2012. **246210**.

13. Geldmacher, D.S. and P.J. Whitehouse, Jr., *Differential diagnosis of Alzheimer's disease.* Neurology, 1997. **48**(5 Suppl 6): p. S2-9.

14. McKhann, G.M., et al., *The diagnosis of dementia due to Alzheimer's disease: recommendations from the National Institute on Aging-Alzheimer's Association workgroups on diagnostic guidelines for Alzheimer's disease.* Alzheimers Dement, 2011. **7**(3): p. 263-9.

15. Sperling RA, A.P., Beckett LA, Bennett DA, Craft S, Fagan AM, Iwatsubo T, Jack CR Jr, Kaye J, Montine TJ, Park DC, Reiman EM, Rowe CC, Siemers E, Stern Y, Yaffe K, Carrillo MC, Thies B, Morrison-Bogorad M, Wagster MV, Phelps CH, *Toward defining the preclinical stages of Alzheimer's disease: recommendations from the National Institute on Aging-Alzheimer's Association workgroups on diagnostic guidelines for Alzheimer's disease.* Alzheimers Dement. , 2011. **7**(3): p. 280-92.

16. RC, P., *Mild cognitive impairment: transition between aging and Alzheimer's disease.* neurologia, 2000. **15**(3): p. 93-101.

17. Bayer TA1, C.R., Masters CL, Beyreuther K, Multhaup G., *It all sticks together--the APP-related family of proteins and Alzheimer's disease.* molecular psychiatry, 1999. **4**(6): p. 524-8.

18. Priller C, B.T., Mitteregger G, Krebs B, Kretzschmar HA, Herms J *Synapse formation and function is modulated by the amyloid precursor protein.* The Journal of Neuroscience, Jul 2006. **26**(27): p. 7212-21.

19. Zheng H, K.E., *The amyloid precursor protein: beyond amyloid.* Molecular Neurodegeneration, 2006. **1**(1): p. 5.

20. Yoshikai S, S.H., Doh-ura K, Furuya H, Sakaki Y (Mar 1990). "". Gene. 87 (2): 257–63, *Genomic organization of the human amyloid beta-protein precursor gene.* gene, 1990. **87**(2): p. 257-63.

21. Goate, A., *Segregation of a missense mutation in the amyloid beta-protein precursor gene with familial Alzheimer's disease.* J Alzheimers Dis, 2006. **9**(3 Suppl): p. 341-7.

22. Rohan de Silva, H.A., et al., *Cell-specific expression of beta-amyloid precursor protein isoform mRNAs and proteins in neurons and astrocytes.* Brain Res Mol Brain Res, 1997. **47**(1-2): p. 147-56.

23. Park SA, S.G., Bredesen DE, Koo EH, *Mechanism of cytotoxicity mediated by the C31 fragment of the amyloid precursor protein.* Biochem Biophys Res Commun., 2009. **388**(2): p. 450-5.

24. Gervais FG, X.D., Robertson GS, Vaillancourt JP, Zhu Y, Huang J, LeBlanc A, Smith D, Rigby M, Shearman MS, Clarke EE, Zheng H, Van Der Ploeg LH, Ruffolo SC, Thornberry NA, Xanthoudakis S, Zamboni RJ, Roy S, Nicholson DW., *Involvement of caspases in proteolytic cleavage of Alzheimer's amyloid-beta precursor protein and amyloidogenic A beta peptide formation.* CELL, 1999. **97**(3): p. 395-406.

25. Kojro E1, F.F., *The non-amyloidogenic pathway: structure and function of alpha-secretases.* Subcell Biochem. , 2005. **38**: p. 105-27.

26. Haass C, S.D., *Soluble protein oligomers in neurodegeneration: lessons from the Alzheimer's amyloid beta-peptide.* Nat Rev Mol Cell Biol. , 2007. **8**(2): p. 101-12.

27. nikolaev A, M.T., O'Leary DD, Tessier Lavigne M, *APP binds DR6 to trigger axon pruning and neuron death via distinct caspases.* nature, 2009. **475**: p. 981-989.

28. Yankner BA, D.L., Fisher S, Villa-Komaroff L, Oster-Granite ML, Neve RL., *Neurotoxicity of a fragment of the amyloid precursor associated with Alzheimer's disease.* science, 1989. **245**(4916): p. 417-20.

29. Hussain I, P.D., Howlett DR, Tew DG, Meek TD, Chapman C, Gloger IS, Murphy KE, Southan CD, Ryan DM, Smith TS, Simmons DL, Walsh FS, Dingwall C, Christie G., *Identification of a novel aspartic protease (Asp 2) as beta-secretase.* Mol Cell Neurosci., 1999. **14**(6): p. 419-27.

30. Bennett BD, D.P., Haniu M, Teplow DB, Kahn S, Louis JC, Citron M, Vassar R., *A furin-like convertase mediates propeptide cleavage of BACE, the Alzheimer's beta -secretase.* J Biol Chem., 2000. **275**(48): p. 37712-7.

31. Sinha S1 Anderson JP, B.R., Basi GS, Caccavello R, Davis D, Doan M, Dovey HF, Frigon N, Hong J, Jacobson-Croak K, Jewett N, Keim P, Knops J, Lieberburg I, Power M, Tan H, Tatsuno G, Tung J, Schenk D, Seubert P, Suomensaari SM, Wang S, Walker D, Zhao J, McConlogue L, John V, *Purification and cloning of amyloid precursor protein beta-secretase from human brain.* nature, 1999. **402**(6761): p. 537-540.

32. Vassar R, B.B., Babu-Khan S, Kahn S, Mendiaz EA, Denis P, Teplow DB, Ross S, Amarante P, Loeloff R, Luo Y, Fisher S, Fuller J, Edenson S, Lile J, Jarosinski MA, Biere AL, Curran E, Burgess T, Louis JC, Collins F, Treanor J, Rogers G, Citron M., *Beta-secretase cleavage of Alzheimer's amyloid precursor protein by the transmembrane aspartic protease BACE.* Science, 1999. **286**(5440): p. 735-41.

33. Creemers JW, I.D.D., Plets E, Serneels L, Taylor NA, Multhaup G, Craessaerts K, Annaert W, De Strooper B., *Processing of beta-secretase by furin and other members of the proprotein convertase family.* JOURNAL OF BIOLOGICAL CHEMISTRY, 2001. **276**(6): p. 4211-7.

34. Lin X, K.G., Wu S, Downs D, Dashti A, Tang J., *Human aspartic protease memapsin 2 cleaves the beta-secretase site of beta-amyloid precursor protein.* Proc Natl Acad Sci U S A., 2000. **6097**(4): p. 1456-60.

35. Haass C, S.M., Hung AY, Vigo-Pelfrey C, Mellon A, Ostaszewski BL, Lieberburg I, Koo EH, Schenk D, Teplow DB, et al., *Amyloid beta-peptide is produced by cultured cells during normal metabolism.* Nature, 1992. **359**(6393): p. 322-5.

36. Koo EH, S.S., Selkoe DJ, Koo CH., *Trafficking of cell-surface amyloid beta-protein precursor. I. Secretion, endocytosis and recycling as detected by labeled monoclonal antibody.* J Cell Sci., 1996. **109**(Pt 5): p. 991-8.

37. Huse JT, P.D., Leslie GJ, Lee VM, Doms RW., *Maturation and endosomal targeting of beta-site amyloid precursor protein-cleaving enzyme. The Alzheimer's disease beta-secretase.* J Biol Chem, 2000. **275**(43): p. 33729-37.

38. Walter J, F.R., Hartung B, Willem M, Kaether C, Capell A, Lammich S, Multhaup G, Haass C, *Phosphorylation regulates intracellular trafficking of beta-secretase.* J Biol Chem, 2001. **276**(18): p. 14634-41.

39. Vancura A, S.A., Leichus B, Kuret J., *A prenylation motif is required for plasma membrane localization and biochemical function of casein kinase I in budding yeast.* J Biol Chem., 1994. **269**(30): p. 19271-8.

40. Babu P, B.J., Panek HR, Jordan SL, Forbrich BM, Kelley SC, Colvin RT, Robinson LC., *Plasma membrane localization of the Yck2p yeast casein kinase 1 isoform requires the C-terminal extension and secretory pathway function.* J Cell Sci., 2002. **115**(Pt24): p. 4957-6.

41. Davidson G, W.W., Shen J, Bilic J, Fenger U, Stannek P, Glinka A, Niehrs C., *Casein kinase 1 gamma couples Wnt receptor activation to cytoplasmic signal transduction.* Nature., 2005. **8**(438): p. 867-72.

42. Amit S, H.A., Birman Y, Andersen JS, Ben-Shushan E, Mann M, Ben-Neriah Y, Alkalay I., *Axin-mediated CKI phosphorylation of beta-catenin at Ser 45: a molecular switch for the Wnt pathway.* Genes Dev. , 2002. **16**(9): p. 1066-76.

43. Marc Flajolet, G.H., Myriam Heiman, Angie Lin, Angus C. Nairn and Paul Greengard, *Regulation of Alzheimer's disease amyloid-β formation by casein kinase I.* Proc Natl Acad Sci U S A., 2007 **104**(10): p. 4159-4164.

44. D. Puzzo and O. Arancio, 33, S111–S120., *Amyloid-β Peptide: Dr. Jekyll or Mr. Hyde?* J. Alzheimer's Dis, 2013. **33**: p. S111-S120.

45. Pearson HA, P.C., *Physiological roles for amyloid beta peptides.* J Physiol., 2006. **15**(575): p. 5-10.

46. Kayed, R., et al., *Common structure of soluble amyloid oligomers implies common mechanism of pathogenesis.* Science, 2003. **300**(5618): p. 486-9.

47. Selkoe, D.J., *The molecular pathology of Alzheimer's disease.* neuron, 1991. **6**(4): p. 487-98.

48. J.A. Hardy, G.A.H., *Alzheimer's disease: the amyloid cascade hypothesis.* science, 1992. **256**(5054): p. 184.

49. Lochhead JJ, T.R., *Intranasal delivery of biologics to the central nervous system. .* Adv Drug Deliv Rev, 2012. **64**(7): p. 614-628.

50. G. Forloni, V.A., P. La Vitola, C. Balducci, *Oligomeropathies and pathogenesis of Alzheimer and Parkinson's diseases.* Movement Disorders 2016.

51. A. Deshpande, E.M., C. Glabe, J. Busciglio, *Different conformations of amyloid β induce neurotoxicity by distinct mechanisms in human*

cortical neurons. The Journal of neuroscience 2006. **26**(22): p. 6011-6018.

52. C.J. Hensley K, M.M., Aksenova M, Harris M, Wu JF, Floyd RA and Butterfield DA, *A model for b-amyloid aggregation and neurotoxicity based on free radical generation by the peptide: relevance to Alzheimer disease.* Proc. Natl. Acad. Sci., 1994. **91**: p. 3270–3274.

53. X. Wang, W.W., L. Li, G. Perry, H.G. Lee, X. Zhu, , *Oxidative stress and mitochondrial dysfunction in Alzheimer's disease,.* Biochim Biophys Acta, 2014. **1842**: p. 1240-1247.

54. Kozlowski H, J.-K.A., Brasun J, Gaggelli E, Valensin D, Valensin G. , *Copper, iron, and zinc ions homeostasis and their role in neurodegenerative disorders (metal uptake, transport, distribution and regulation).* Coord Chem Rev. , 2009. **253**: p. 2665-2685.

55. Miura T, S.K., Kohata N, Takeuchi H, *Metal binding modes of Alzheimer's amyloid β-peptide in insoluble aggregates and soluble complexes.* Biochemistry, 2000. **39**(7024-7031).

56. Kim, T.S., et al., *Decreased plasma antioxidants in patients with Alzheimer's disease.* Int J Geriatr Psychiatry,, 2006. **21**(4): p. 344-8.

57. Dean, R.T., et al., 1997. 324 (Pt 1): p. 1-18., *Biochemistry and pathology of radical-mediated*
protein oxidation. Biochem J,, 1997. **324**((Pt 1)): p. 1-18.

58. Levine, R.L., et al., 1994. 233: p. 346-57., *Carbonyl assays for determination of oxidatively*

modified proteins. . Methods Enzymol, 1994. **233**: p. 346-57.

59. Beckman, J.S., *Protein tyrosine nitration and peroxynitrite.* FASEB J, 2002. **16**(9): p. 1144.

60. Butterfield, D.A.a.J.K., *Brain protein oxidation in age-related neurodegenerative disorders that are associated with aggregated proteins.* Mech Ageing Dev, 2001. **122**(9): p. 945-62.

61. Egea PF, S.R., Walter P. , *Targeting proteins to membranes: structure of the signal recognition particle. .* Curr Opin Struct Biol., 2005. **15**(2): p. 213-20.

62. Patzelt C, L.A., Duguid JR, Carroll RJ, Keim PS, Heinrikson RL, Steiner DF., *Detection and kinetic behavior of preproinsulin in pancreatic islets. .* Proc Natl Acad Sci U S A. , 1978. **75**(3): p. 1260–4.

63. Steiner DFKW, C.J., Oyer PE, Rubenstein A. In: Steiner DF, Freinkel N, editors. . , *The biosynthesis of insulin.* Handbook of physiology—Section 7 Endocrinology I. Williams & Wilkins; , Baltimore: 1972: p. 175–198.

64. Nishi M, S.T., Nagamatsu S, Bell GI, Steiner DF., *Islet amyloid polypeptide. A new beta cell secretory product related to islet amyloid deposits.* J Biol Chem. , 1990. **265**(8): p. 4173–6.

65. Havrankova J., R.J., Brownstein M. , *Insulin receptors are widely distributed in the central nervous system of the rat.* nature, 1978. **272**: p. 827-829.

66. Havrankova J, R.J., Brownstein MJ, *Concentrations of insulin and insulin receptors in the brain are independent of peripheral insulin levels. Studies of obese and streptozotocin-treated rodents.* J Clin Invest, 1979. **64**(2): p. 636-42.

67. Genders A. J., F.V., Abramson S. R., Barrett E. J. , *Endothelial cells actively concentrate insulin during its transendothelial transport.* Microcirculation 2013. **20**: p. 434-439.

68. Woods SC, P.D.J., *Relationship between plasma and cerebrospinal fluid Insulin levels of dogs.* Am J Physiol, 1977. **233**(4): p. E331-4.

69. Baura GD, F.D., Porte D Jr, Kahn SE, Bergman RN, Cobelli C, et al. and 92(4):1824–30., *Saturable transport of insulin from plasma into the central nervous system of dogs in vivo. A mechanism for regulated insulin delivery to the brain. .* J Clin Invest, 1993. **92**(4): p. 1824-30.

70. Banks WA, K.A., *Differential permeability of the blood-brain barrier to two pancreatic peptides: insulin and amylin.* Peptides, 1998. **19**(5): p. 883-9.

71. Kaiyala KJ, P.R., Kahn SE,Woods SC, Schwartz MW. , *Obesity induced by a high-fat diet is associated with reduced brain insulin transport in dogs.* Diabetes 2000. **49**(9): p. 1525-33.

72. Heidenreich K. A., G.P.R., *Structural and functional characteristics of insulin receptors in rat neuroblastoma cells.* J. Neurochem. , 1985. **45**: p. 1642–1648.

73. Marks J. L., K.M.G., Baskin D. G. , *Localization of insulin and type 1 IGF receptors in rat brain by in vitro autoradiography and in situ hybridization.* Adv. Exp. Med. Biol. , 1991. **293**: p. 459–470.

74. De Felice F. G., L.M.V., Ferreira S. T. , *How does brain insulin resistance develop in Alzheimer's disease?* Alzheimers Dement. , 2014. **10**: p. S26–S32. .

75. McNay E. C., R.A.K., *Brain insulin signaling: a key component of cognitive processes and a potential basis for cognitive impairment in type 2 diabetes.* Neurobiol. Learn. Mem., 2011. **96**: p. 432–442.

76. Unger J, M.T., Moxley RT, White M, Moss A, Livingston JN., *Distribution of insulin receptor-like immunoreactivity in the rat forebrain.* Neuroscience. , 1989. **31**: p. 143-157.

77. Choi J, K.J., Racz B, Burette A, Lee JR, Kim S, Na M, Lee HW, Kim K, Weinberg RJ, Kim E. , *Regulation of dendritic spine morphogenesis by insulin receptor substrate 53, a downstream effector of Rac1 and Cdc42 small GTPases.* J Neurosci., 2005. **25**: p. 869-879.

78. Govind S, K.R., Monfries C, Lim L, Ahmed S. , *Cdc42Hs facilitates cytoskeletal reorganization and neurite outgrowth by localizing the 58-kD insulin receptor substrate to filamentous actin.* J Cell Biol, 2001. **152**: p. 579-594.

79. Schulingkamp RJ, P.T., Hung D, Raffa RB. , *Insulin receptors and insulin action in the brain: review and clinical implications. .* Neurosci Biobehav Rev, 2000. **24**(8): p. 855-72.

80. Moller DE, Y.A., Caro JF, Flier JS., *Tissue-specific expression of two alternatively spliced insulin receptor mRNAs in man. .* Mol Endocrinol 1989. **3**(8): p. 1263-9.

81. Vienberg SG, B.S., Sorensen H, Stidsen CE, Kjeldsen T, Glendorf T, et al. , *Receptor-isoform-selective insulin analogues give tissue-preferential effects. .* Biochem J, 2011. **440**(3): p. 301-8.

82. Unger JW, M.A., Livingston JN., *Immunohistochemical localization of insulin receptors and phosphotyrosine in the brainstem of the adult rat.* neuscience, 1991. **42**(3): p. 853-61.

83. Eastman, J.L.M.J.M.C.J., *Subcellular Localization of Rat Brain Insulin Binding Sites.* journal of neurochemistry, 1988. **50**(3).

84. MF., W., *Insulin signaling in health and disease. .* science, 2003. **302**: p. 1710-1711.

85. DJ., W., *Insulin receptor substrate proteins and neuroendocrine function.* Biochem Soc Trans., 2001. **29**: p. 525-529.

86. Saltiel AR, P.J., *Insulin signaling pathways in time and space. .* TRENDS CELL BIOL 2002. **12**(2): p. 65-71.

87. Pilch PF, S.M., Benson RJ, Fine RE., *Coated vesicles participate in the receptor-mediated endocytosis of insulin.* J Cell Biol 1983. **96**(1): p. 133-8.

88. Heffetz D, Z.Y., *Receptor aggregation is necessary for activation of the soluble insulin receptor kinase.* J Biol Chem 1986. **261**(2): p. 889-94.

89. Taguchi A, W.M., *Insulin-like signaling, nutrient homeostasis, and life span.* Annu Rev Physiol 2008. **70**: p. 191-212.

90. Saltiel AR, K.C., *Insulin signalling and the regulation of glucose and lipid metabolism. .* nature, 2001. **414**: p. 799-806.

91. Schulingkamp RJ, P.T., Hung D, Raffa RB. , *Insulin receptors and insulin action in the brain: review and clinical implications. .* Neurosci Biobehav Rev., 2000. **24**: p. 855-872.

92. King, G.L., Park, K. & Li, Q. : 2015 . Diabetes 65, 1462–1471 (2016). *Selective insulin resistance and the development of cardiovascular diseases in diabetes.* Edwin Bierman Award lecture - Diabetes, 2016. **65**: p. 1462-1471.

93. Haeusler, R.A., McGraw, T. E. & Accili, D, *Biochemical and cellular properties of insulin receptor signalling.* Nat. Rev. Mol. Cell Biol, 2017.

94. Tanti, J.F.a.J.J., *Cellular mechanisms of insulin resistance: role of stress-regulated serine kinases and insulin receptor substrates (IRS) serine phosphorylation.* Curr Opin Pharmacol, 2009. **9**(6): p. 753-62.

95. Shah, O.J., Z. Wang, and T. Hunter, *nappropriate activation of the TSC/Rheb/mTOR/S6K cassette induces IRS1/2 depletion, insulin resistance, and cell survival deficiencies. .* Curr Biol, 2004. **14**(18): p. 1650-5.

96. C, O.N., *PI3-kinase/Akt/mTOR signaling: impaired on/off switches in aging, cognitive decline and Alzheimer's disease.* Exp Gerontol, , 2013. **48**(7): p. 647-53.

97. Bruss MD, A.E., Lienhard GE, Cartee GD., *Increased phosphorylation of Akt substrate of 160 kDa (AS160) in rat skeletal muscle in response to insulin or contractile activity.* Diabetes, 2005. **54**(1): p. 41-50.

98. **Cole GM, F.S.**, *The role of insulin and neurotrophic factor signaling in brain aging and Alzheimer's Disease.* EXP GERONTOL., 2007. **42**(1-2): p. 10-21.

99. van der Heide LP, R.G., Smidt MP, *Insulin signaling in the central nervous system: learning to survive.* Prog neurobiol., 2006. **79**(4): p. 205-21.

100. A1, E., *An integrated and unifying hypothesis for the metabolic basis of sporadic Alzheimer's disease.* J Alzheimers Dis., 2008. **13**(3): p. 241-53.

101. Zheng WH1, K.S., Quirion R., *Insulin-like growth factor-1-induced phosphorylation of transcription factor FKHRL1 is mediated by phosphatidylinositol 3-kinase/Akt kinase and role of this pathway in insulin-like growth factor-1-induced survival of cultured hippocampal neurons.* Mol Pharmacol., 2002. **62**(2): p. 225-33.

102. Takei, N.a.H.N., *mTOR signaling and its roles in normal and abnormal brain development.* Front Mol Neurosci, 2014. **7**: p. 28.

103. Kim, D., et al., *Regulation and localization of ribosomal protein S6 kinase 1 isoforms. .* Growth Factors, 2009. **27**(1): p. 12-21.

104. Magnuson, B., B. Ekim, and D.C. Fingar, *Regulation and function of ribosomal protein S6 kinase (S6K) within mTOR signalling networks.* Biochem J, 2012. **441**(1): p. 1-21.

105. Khoutorsky, A., et al., , *Translational control of nociception via 4E-binding protein 1.* ELIFE, 2015. **4**.

106. S. Srinivasan, M.O., Z. Liu, S. Fatrai, E. Bernal- Mizrachi, and M. A. Permutt, *Endoplasmic reticulum stress-induced apoptosis is partly mediated by reduced insulin signaling through phosphatidylinositol 3-kinase/Akt and increased glycogen synthase kinase-3β in mouse insulinoma cells.* Diabetes, 2005. **54**(4): p. 968-975.

107. X. Fang, S.X.Y., Y. Lu, R. C. Bast, J. R. Woodgett, and G. B. Mills *Phosphorylation and inactivation of glycogen synthase kinase 3 by protein kinase A.* Procedings of the National Academy of Sciences of the United States of America, 2000. **97**(22): p. 11960-11965.

108. N. Goode, K.H., J. R. Woodgett, and P. J. Parker *Differential regulation of glycogen synthase kinase-3β by protein kinase C isotypes.* Journal of Biological Chemistry, 1992. **267**(24): p. 16878–16882.

109. Z. Sui, A.D.K.c., and S. B. Maggirwar, *Recruitment of active glycogen synthase kinase-3 into neuronal lipid rafts.* Biochemical and Biophysical Research Communications, 2006. **345**(4): p. 1643-1648.

110. Johnson, J.A.H.a.G.V.W., *Transient increases in intracellular calcium result in prolonged site-selective increases in Tau phosphorylation through a glycogen syn- thase kinase 3β-dependent pathway.* Journal of Biological Chemistry,, 1999. **274**(30): p. 21395-21401.

111. M. Lesort, R.S.J., and G. V. W. Johnson, *Insulin transiently increases tau phosphorylation: involvement of glycogen synthase kinase-3β and Fyn tyrosine kinase.* Journal of Neurochemistry, 1999. **72**(2): p. 576-584.

112. Freeman, R.J.C.a.R.S., *Glycogen synthase kinase- 3β activity is critical for neuronal death caused by inhibiting phosphatidylinositol 3-kinase or Akt but not for death caused by nerve growth factor withdrawal.* Journal of Biological Chemistry, 2000. **275**(44): p. 34266-34271.

113. I. G. Onyango, J.P.B., and J. B. Tuttle, *Endogenous oxidative stress in sporadic Alzheimer's disease neuronal cybrids reduces viability by increasing apoptosis through pro-death signaling pathways and is mimicked by oxidant*
exposure of control cybrids. neurobiology of disease, 2005. **19**(1-2): p. 312-322.

114. M. P. Mattson, S.M., and B. Martin, *A neural signaling triumvirate that influences ageing and age- related disease: insulin/IGF-1, BDNF and serotonin.* Ageing Research Reviews, 2004. **3**(4): p. 445–464.

115. Bomfim TR, F.-G.L., Sathler LB, Brito-Moreira J, Houzel JC, Decker H, et al., *An anti-diabetes agent protects the mouse brain from defective insulin signaling caused by Alzheimer's diseaseassociated Ab oligomers.* J Clin Invest 2012. **122**: p. 1339-53.

116. Talbot K, W.H., Kazi H, Han L, Bakshi KP, Stucky A, et al. , *Demonstrated brain insulin resistance in Alzheimer's disease patients is associated with IGF-1 resistance, IRS-1 dysregulation, and cognitive decline.* J Clin Invest, 2012. **122**: p. 1316-38.

117. Watson, G.S., and Craft, S., *The role of insulin resistance in the pathogenesis of Alzheimer's disease: implications for treatment.* cns drugs, 2003. **17**: p. 27-45.

118. Rivera, E.J., Goldin, A., Fulmer, N., Tavares, R., Wands, J. R., and De La Monte, S. M. , *Insulin and insulin-like growth factor expression and function deteriorate with progression of Alzheimer's disease: link to brain reductions in acetylcholine.* J. Alzheimers Dis., 2005. **8**: p. 247-268.

119. de Leon MJ, M.L., Blennow K, et al. Ann N Y . , *Imaging and CSF studies in the preclinical diagnosis of Alzheimer's disease. .* Acad Sci, 2007. **1097**: p. 114-145.

120. L., M., *FDG-PET studies in MCI and AD. Brain glucose metabolism in the early and specific diagnosis of Alzheimer's disease. .* Eur J Nucl Med Mol Imaging, 2005. **32**: p. 486-510.

121. Steen E, T.B., Rivera EJ, et al., *mpaired insulin and insulin-like growth factor expression and signaling mechanisms in Alzheimer's disease-is this type 3 diabetes? .* J Alzheimers Dis, 2005. **7**: p. 63-80.

122. Wang X, Z., Xie J-W,Wang T,Wang S-L, TengW-P, et al., *Insulin deficiency exacerbates cerebral amyloidosis and behavioral deficits in an Alzheimer transgenic mouse model.* Mol Neurodegen 2010. **5**: p. 46.

123. Yamamoto N, M.T., Sobue K, Tanida M, Kasahara R, Naruse K, et al. , *Brain insulin resistance accelerates Ab fibrillogenesis by inducing GM1 ganglioside clustering in the presynaptic membranes.* J Neurochem, 2012. **121**: p. 619-28.

124. F.G. De Felice, M.N.V., T.R. Bomfim, H. Decker, P.T. Velasco, M.P. Lambert, K. L. Viola, W.Q. Zhao, S.T. Ferreira, W.L. Klein, *Protection of synapses against Alzheimer's-linked toxins: insulin signaling prevents the pathogenic binding of Abeta oligomers, .* Proc. Natl. Acad. Sci. United S. Am., 2009. **106**: p. 1971-1976.

125. T.R. Bomfim, L.F.-G., L.B. Sathler, J. Brito-Moreira, J.C. Houzel,, M.A.S. H. Decker, H. Kazi, H.M. Melo, P.L. McClean, C. Holscher, S., and K.T. E. Arnold, W.L. Klein, D.P. Munoz, S.T. Ferreira, F.G. De Felice, *An anti-diabetes agent protects the mouse brain from defective insulin signaling caused by Alzheimer's disease- associated Abeta oligomers.* J. Clin. Investig., 2012. **122**(1339-1353).

126. M.V. Lourenco, J.R.C., R.L. Frozza, T.R. Bomfim, L. Forny-Germano, A., L.B.S. F. Batista, J. Brito-Moreira, O.B. Amaral, C.A. Silva, L. Freitas-Correa, S. Espirito-Santo, P. Campello-Costa, J.C. Houzel, W.L. Klein, C. Holscher, J., and A.M.S. B. Carvalheira, L.A. Velloso, D.P. Munoz, S.T. Ferreira, F.G. De Felice, *TNF-alpha mediates PKR-dependent memory impairment and brain IRS-1 inhibition induced by Alzheimer's beta-amyloid oligomers in mice and mon- keys.* Cell. Metab., 2013. **18**: p. 831-843.

127. K.D. Copps, M.F.W., *Regulation of insulin sensitivity by serine/threonine phosphorylation of insulin receptor substrate proteins IRS1 and IRS2.* DiabeTologia 2012. **55**: p. 2565-2582.

128. D.A. Butterfield, F.D.D., E. Barone, *Elevated risk of type 2 diabetes for development of Alzheimer disease: a key role for oxidative stress in brain, .* Biochim Biophys Acta, 2014. **1842**: p. 1693-1706.

129. Taniguchi CM, E.B., Kahn CR, *Critical nodes in signalling pathways: insights into insulin action.* Nat Rev Mol Cell Biol 2006. **7**(2): p. 85-96.

130. J. Kapitulnik, M.D.M., *Pleiotropic functions of biliverdin reductase: cellular signaling and generation of cytoprotective and cytotoxic bilirubin.* Trends Pharmacol. Sci., 2009. **30**: p. 129-137.

131. Whitby FG, P.J., Hill CP, McCoubrey W, Maines MD. , *Crystal structure of a biliverdin-IX alpha reductase enzyme-cofactor complex.* J Mol Biol, 2002. **319**: p. 1199-1210.

132. Maines MD, P.B., Huang TJ, McCoubrey WK Jr, *Human biliverdin IXalpha reductase is a zinc-metalloprotein. Characterization of purified and Escherichia coli expressed enzymes.* Eur J Biochem., 1996. **235**((1-2)): p. 372-81.

133. MD, M., *New insights into biliverdin reductase functions: linking heme metabolism to cell signaling.* Physiology (Bethesda), 2005. **20**: p. 382-9.

134. Stocker, R., *Antioxidant activities of bile pigments.* Antioxid. Redox Signa, 2004. **6**: p. 841-849.

135. E. Barone, S.T., R. Cassano, A. Sgambato, B. De Paola, E. Di Stasio, and P.P. N. Picci, C. Mancuso, *Characterization of the S-denitrosylating activity of bilirubin.* J. Cell. Mol. Med. , 2009. **13**: p. 2365-2375.

136. N. Lerner-Marmarosh, J.S., M.D. Torno, A. Kravets, Z. Hu, M.D. Maines, 102 (2005) 7109–7114., *Human biliverdin reductase: a member*

of the insulin receptor substrate fa- mily with serine/threonine/tyrosine kinase activity,. Proc. Natl. Acad. Sci. U.S.A. , 2005. **102**: p. 7109-7114.

137. Lerner-Marmarosh N, M.T., Gibbs PE, Maines MD *Human biliverdin reductase is an ERK activator; hBVR is an ERK nuclear transporter and is required for MAPK signaling.* Proc Natl Acad Sci U S A 2008. **105**(19): p. 6870-6875.

138. Miralem T, L.-M.N., Gibbs PE, Jenkins JL, Heimiller C, Maines MD *Interaction of human biliverdin reductase with Akt/protein kinase B and phosphatidylinositol-dependent kinase 1 regulates glycogen synthase kinase 3 activity: a novel mechanism of Akt activation.* FASEB J 2016. **30**(8): p. 2926-2944.

139. Zhang Y, Z.W., Zhang L, Ma Y, Wang J *Protein kinase M zeta and the maintenance of long-term memory.* Neurochem Int, 2016. **99**: p. 215-220.

140. Barone E, D.D.F., Cenini G, Sultana R, Coccia R, Preziosi P, Perluigi M, Mancuso C and Butterfield DA., *Oxidative and nitrosative modifications of biliverdin reductase-A in the brain of subjects with Alzheimer's disease and amnestic mild cognitive impairment.* J Alzheimers Dis, 2011. **25**(4): p. 623-33.

141. Barone, E., et al., *Impairment of biliverdin reductase-A promotes brain insulin resistance in Alzheimer disease: A new paradigm.* Free Radic Biol Med, 2016. **91**: p. 127-42.

142. P.E. Gibbs, N.L.-M., A. Poulin, E. Farah, M.D. Maines, *Human biliverdin reductase-based peptides activate and inhibit glucose uptake*

through direct interaction with the kinase domain of insulin receptor,. FASEB J., 2014(28): p. 2478-2491.

143. Moloney AM, G.R., Timmons S, et al. , *Defects in IGF-1 receptor, insulin receptor and IRS-1/2 in Alzheimer's disease indicate possible resistance to IGF-1 and insulin signalling.* Neurobiol Aging, 2010. **31**: p. 224-43.

144. Liu Y, L.F., Grundke-Iqbal I, et al. , *Deficient brain insulin signalling pathway in Alzheimer's disease and diabetes.* J Pathol., 2011. **225**: p. 54-62.

145. Cheng D, N.J., Tang MX, et al. , *Type 2 diabetes and late-onset Alzheimer's disease.* Dement Geriatr Cogn Disord., 2011. **31**(424-30).

146. Luchsinger JA, R.C., Patel B, et al. , *Relation of diabetes to mild cognitive impairment. .* Arch Neurol., 2007. **64**: p. 570-5.

147. Profenno LA, P.A., Faraone SV. , *Meta-analysis of Alzheimer's disease risk with obesity, diabetes, and related disorders.* Biol Psychiatry, 2010. **67**: p. 505-12.

148. Craft S, N.J., Kanne S, Dagogo-Jack S, Cryer P, Sheline Y, Luby J, Dagogo-Jack A, Alderson A., *Memory improvement following induced hyperinsulinemia in Alzheimer's disease.* Neurobiol Aging. , 1996. **17**(1): p. 123-30.

149. Burns, J.K.M.J.M., *Insulin: An Emerging Treatment for Alzheimer's Disease Dementia?* Curr Neurol Neurosci Rep., 2012. **12**(5): p. 520-7.

150. Benedict C, F.W.n., Schiöth HB, Schultes B, Born J, Hallschmid M., *Intranasal insulin as a therapeutic option in the treatment of cognitive impairments.*
. Exp Gerontol., 2011. **46**(2-3): p. 112-5.

151. Liu XF1, F.J., Thorne RG, DeFor TA, Frey WH 2nd., *Intranasal administration of insulin-like growth factor-I bypasses the blood-brain barrier and protects against focal cerebral ischemic damage.* J Neurol Sci. , 2001. **187**(1-2): p. 91-7.

152. M., W., *NIH tackles major workforce issues.* Nature, 2012. **492**(7428): p. 167.

153. Reger MA, W.G., Frey WH, 2nd, Baker LD, Cholerton B, Keeling ML, Belongia DA, Fishel MA, Plymate SR, Schellenberg GD, Cherrier MM, Craft S (2006) . *Effects of intranasal insulin on cognition in memory-impaired older adults: modulation by APOE genotype.* Neurobiol Aging, 2006. **27**(3): p. 451-458.

154. Craft S, B.L., Montine TJ, Minoshima S, Watson GS, Claxton A, Arbuckle M, Callaghan M, Tsai E, Plymate SR, Green PS, Leverenz J, Cross D, Gerton B *Intranasal insulin therapy for Alzheimer disease and amnestic mild cognitive impairment: a pilot clinical trial.* Arch Neurol 2012. **69**(1): p. 29-38.

155. Apostolatos A, S.S., Acosta S, Peart M, Watson JE, Bickford P, Cooper DR, Patel NA *Insulin promotes neuronal survival via the alternatively spliced protein kinase CdeltaII isoform.* J Biol Chem 2012. **287**(12): p. 9299-9310.

156. Salameh TS, B.K., Hujoel IA, Niehoff ML, Wolden-Hanson T, Kim J, Morley JE, Farr SA, Banks WA *Central Nervous System Delivery of Intranasal Insulin: Mechanisms of Uptake and Effects on Cognition.* J Alzheimers Dis, 2015. **47**(3): p. 715-728.

157. Stanley M, M.S., Holtzman DM 213 (8):1375-1385., *Changes in insulin and insulin signaling in Alzheimer's disease: cause or consequence?* J Exp Med 2016. **213**(8): p. 1375-1385.

158. Stanley, M., S.L. Macauley, and D.M. Holtzman, *Changes in insulin and insulin signaling in Alzheimer's disease: cause or consequence?* J Exp Med, 2016. **213**(8): p. 1375-85.

159. D.J. Selkoe, D.S.B., M.B. Podlisny, D.L. Price, L.C. Cork, *Conservation of brain amyloid proteins in aged mammals and humans with Alzheimer's disease.* Science, 1987. **235**(873-877).

160. Head, E., et al., *Region-specific age at onset of beta-amyloid in dogs.* Neurobiol Aging, 2000. **21**(1): p. 89-96.

161. Oddo, S., et al., *Triple-transgenic model of Alzheimer's disease with plaques and tangles: intracellular Abeta and synaptic dysfunction.* Neuron, 2003. **39**(3): p. 409-21.

162. Cassano, T., et al., *Olfactory memory is impaired in a triple transgenic model of Alzheimer disease.* Behav Brain Res, 2011. **224**(2): p. 408-12.

163. Cassano, T., et al., *Glutamatergic alterations and mitochondrial impairment in a murine model of Alzheimer disease.* Neurobiol Aging, 2012. **33**(6): p. 1121 e1-12.

164. Bambico, F.R., et al., *Genetic deletion of fatty acid amide hydrolase alters emotional behavior and serotonergic transmission in the dorsal raphe, prefrontal cortex, and hippocampus.* Neuropsychopharmacology, 2010. **35**(10): p. 2083-100.

165. Romano, A., et al., *Depressive-like behavior is paired to monoaminergic alteration in a murine model of Alzheimer's disease.* Int J Neuropsychopharmacol, 2014. **18**(4).

166. Scuderi, C., et al., *Ultramicronized palmitoylethanolamide rescues learning and memory impairments in a triple transgenic mouse model of Alzheimer's disease by exerting anti-inflammatory and neuroprotective effects.* Transl Psychiatry, 2018. **8**(1): p. 32.

167. Giustino, A., et al., *Prenatal exposure to low concentrations of carbon monoxide alters habituation and non-spatial working memory in rat offspring.* Brain Res, 1999. **844**(1-2): p. 201-5.

168. Cenini, G., et al., *Effects of oxidative and nitrosative stress in brain on p53 proapoptotic protein in amnestic mild cognitive impairment and Alzheimer disease.* Free Radic Biol Med, 2008. **45**(1): p. 81-5.

169. Salim, M., B.A. Brown-Kipphut, and M.D. Maines, *Human biliverdin reductase is autophosphorylated, and phosphorylation is required for bilirubin formation.* J Biol Chem, 2001. **276**(14): p. 10929-34.

170. Lerner-Marmarosh, N., et al., *Human biliverdin reductase is an ERK activator; hBVR is an ERK nuclear transporter and is required for MAPK signaling.* Proc Natl Acad Sci U S A, 2008. **105**(19): p. 6870-5.

171. Barone, E., et al., *Oxidative and nitrosative modifications of biliverdin reductase-A in the brain of subjects with Alzheimer's disease and amnestic mild cognitive impairment.* J Alzheimers Dis, 2011. **25**(4): p. 623-33.

172. Barone, E., et al., *Biliverdin reductase--a protein levels and activity in the brains of subjects with Alzheimer disease and mild cognitive impairment.* Biochim Biophys Acta, 2011. **1812**(4): p. 480-7.

173. Mayer, C.M. and D.D. Belsham, *Central insulin signaling is attenuated by long-term insulin exposure via insulin receptor substrate-1 serine phosphorylation, proteasomal degradation, and lysosomal insulin receptor degradation.* Endocrinology, 2010. **151**(1): p. 75-84.

174. Gibbs, P.E., et al., *Human biliverdin reductase-based peptides activate and inhibit glucose uptake through direct interaction with the kinase domain of insulin receptor.* FASEB J, 2014. **28**(6): p. 2478-91.

175. Miralem, T., et al., *The human biliverdin reductase-based peptide fragments and biliverdin regulate protein kinase Cdelta activity: the peptides are inhibitors or substrate for the protein kinase C.* J Biol Chem, 2012. **287**(29): p. 24698-712.

176. Ripoli, C., et al., *Effects of different amyloid beta-protein analogues on synaptic function.* Neurobiol Aging, 2013. **34**(4): p. 1032-44.

177. Ripoli, C., et al., *Intracellular accumulation of amyloid-beta (Abeta) protein plays a major role in Abeta-induced alterations of glutamatergic synaptic transmission and plasticity.* J Neurosci, 2014. **34**(38): p. 12893-903.

178. Ryder, J., Y. Su, and B. Ni, *Akt/GSK3β serine/threonine kinases: evidence for a signalling pathway mediated by familial Alzheimer's disease mutations.* Cellular Signalling, 2004. **16**(2): p. 187-200.

179. Perluigi, M., et al., *Neuropathological role of PI3K/Akt/mTOR axis in Down syndrome brain.* Biochim Biophys Acta, 2014. **1842**(7): p. 1144-53.

180. Arnold, S.E., et al., *Brain insulin resistance in type 2 diabetes and Alzheimer disease: concepts and conundrums.* Nat Rev Neurol, 2018. **14**(3): p. 168-181.

181. Talbot, K., et al., *Demonstrated brain insulin resistance in Alzheimer's disease patients is associated with IGF-1 resistance, IRS-1 dysregulation, and cognitive decline.* J Clin Invest, 2012. **122**(4): p. 1316-38.

182. Tramutola, A., et al., *Alteration of mTOR signaling occurs early in the progression of Alzheimer disease (AD): analysis of brain from subjects with pre-clinical AD, amnestic mild cognitive impairment and late-stage AD.* J Neurochem, 2015. **133**(5): p. 739-49.

183. Spinelli, M., et al., *Brain insulin resistance impairs hippocampal synaptic plasticity and memory by increasing GluA1 palmitoylation through FoxO3a.* Nat Commun, 2017. **8**(1): p. 2009.

184. Di Domenico, F., et al., *HO-1/BVR-a system analysis in plasma from probable Alzheimer's disease and mild cognitive impairment subjects: a potential biochemical marker for the prediction of the disease.* J Alzheimers Dis, 2012. **32**(2): p. 277-89.

185. Butterfield, D.A. and E.R. Stadman, *Protein oxidation processes in aging brain.* Advances in Cell Aging and Gerontology, 1997. **S.T. Paula, E.E. Bittar (Eds.)**: p. 161–191.

186. Barone, E., et al., *Biliverdin reductase-A: a novel drug target for atorvastatin in a dog pre-clinical model of Alzheimer disease.* J Neurochem, 2012. **120**(1): p. 135-46.

187. Kapitulnik, J. and M.D. Maines, *Pleiotropic functions of biliverdin reductase: cellular signaling and generation of cytoprotective and cytotoxic bilirubin.* Trends Pharmacol Sci, 2009. **30**(3): p. 129-37.

188. Walter, J., et al., *Phosphorylation regulates intracellular trafficking of beta-secretase.* J Biol Chem, 2001. **276**(18): p. 14634-41.

189. Pastorino, L., et al., *The carboxyl-terminus of BACE contains a sorting signal that regulates BACE trafficking but not the formation of total A(beta).* Mol Cell Neurosci, 2002. **19**(2): p. 175-85.

190. Gibbs, P.E., et al., *Formation of ternary complex of human biliverdin reductase-protein kinase Cdelta-ERK2 protein is essential for ERK2-mediated activation of Elk1 protein, nuclear factor-kappaB, and inducible nitric-oxidase synthase (iNOS).* J Biol Chem, 2012. **287**(2): p. 1066-79.

191. Flajolet, M., et al., *Regulation of Alzheimer's disease amyloid-beta formation by casein kinase I.* Proc Natl Acad Sci U S A, 2007. **104**(10): p. 4159-64.

192. Chen, C., et al., *Up-regulation of casein kinase 1epsilon is involved in tau pathogenesis in Alzheimer's disease.* Sci Rep, 2017. **7**(1): p. 13478.

193. Yasojima, K., et al., *Casein kinase 1 delta mRNA is upregulated in Alzheimer disease brain.* Brain Res, 2000. **865**(1): p. 116-20.

194. Schwab, C., et al., *Casein kinase 1 delta is associated with pathological accumulation of tau in several neurodegenerative diseases.* Neurobiol Aging, 2000. **21**(4): p. 503-10.

195. Tan, J. and G. Evin, *Beta-site APP-cleaving enzyme 1 trafficking and Alzheimer's disease pathogenesis.* J Neurochem, 2012. **120**(6): p. 869-80.

196. Biessels, G.J. and L.P. Reagan, *Hippocampal insulin resistance and cognitive dysfunction.* Nat Rev Neurosci, 2015. **16**(11): p. 660-71.

197. Copps, K.D. and M.F. White, *Regulation of insulin sensitivity by serine/threonine phosphorylation of insulin receptor substrate proteins IRS1 and IRS2.* Diabetologia, 2012. **55**(10): p. 2565-2582.

198. Miralem, T., et al., *Interaction of human biliverdin reductase with Akt/protein kinase B and phosphatidylinositol-dependent kinase 1 regulates glycogen synthase kinase 3 activity: a novel mechanism of Akt activation.* FASEB J, 2016. **30**(8): p. 2926-44.

199. Lerner-Marmarosh, N., et al., *Human biliverdin reductase: a member of the insulin receptor substrate family with serine/threonine/tyrosine kinase activity.* Proc Natl Acad Sci U S A, 2005. **102**(20): p. 7109-14.

200. Arnold, S.E., et al., *Brain insulin resistance in type 2 diabetes and Alzheimer disease: concepts and conundrums.* Nat Rev Neurol, 2018.

201. King, G.L., K. Park, and Q. Li, *Selective Insulin Resistance and the Development of Cardiovascular Diseases in Diabetes: The 2015 Edwin Bierman Award Lecture.* Diabetes, 2016. **65**(6): p. 1462-71.

202. Ge, X., et al., *Chronic insulin treatment causes insulin resistance in 3T3-L1 adipocytes through oxidative stress.* Free Radic Res, 2008. **42**(6): p. 582-91.

203. Bell, G.A. and D.A. Fadool, *Awake, long-term intranasal insulin treatment does not affect object memory, odor discrimination, or reversal learning in mice.* Physiol Behav, 2017. **174**: p. 104-113.

204. Adzovic, L., et al., *Insulin improves memory and reduces chronic neuroinflammation in the hippocampus of young but not aged brains.* J Neuroinflammation, 2015. **12**: p. 63.

205. Lerner-Marmarosh, N., et al., *Regulation of TNF-alpha-activated PKC-zeta signaling by the human biliverdin reductase: identification of activating and inhibitory domains of the reductase.* FASEB J, 2007. **21**(14): p. 3949-62.

206. Tundo, G.R., et al., *Multiple functions of insulin-degrading enzyme: a metabolic crosslight?* Crit Rev Biochem Mol Biol, 2017. **52**(5): p. 554-582.

207. Steen, E., et al., *Impaired insulin and insulin-like growth factor expression and signaling mechanisms in Alzheimer's disease--is this type 3 diabetes?* J Alzheimers Dis, 2005. **7**(1): p. 63-80.

208. de la Monte, S.M., *Contributions of brain insulin resistance and deficiency in amyloid-related neurodegeneration in Alzheimer's disease.* Drugs, 2012. **72**(1): p. 49-66.

209. Watson, G.S., et al., *Insulin increases CSF Abeta42 levels in normal older adults.* Neurology, 2003. **60**(12): p. 1899-903.

210. Wang, D.S., D.W. Dickson, and J.S. Malter, *beta-Amyloid degradation and Alzheimer's disease.* J Biomed Biotechnol, 2006. **2006**(3): p. 58406.

211. Qiu, W.Q. and M.F. Folstein, *Insulin, insulin-degrading enzyme and amyloid-beta peptide in Alzheimer's disease: review and hypothesis.* Neurobiol Aging, 2006. **27**(2): p. 190-8.

212. Umegaki, H., *Insulin resistance in the brain: A new therapeutic target for Alzheimer's disease.* J Diabetes Investig, 2013. **4**(2): p. 150-1.

213. Zhao, W.Q., et al., *Amyloid beta oligomers induce impairment of neuronal insulin receptors.* FASEB J, 2008. **22**(1): p. 246-60.

214. De Felice, F.G., et al., *Protection of synapses against Alzheimer's-linked toxins: insulin signaling prevents the pathogenic binding of Abeta oligomers.* Proc Natl Acad Sci U S A, 2009. **106**(6): p. 1971-6.

215. De Felice, F.G. and C. Benedict, *A Key Role of Insulin Receptors in Memory.* Diabetes, 2015. **64**(11): p. 3653-5.

216. Bomfim, T.R., et al., *An anti-diabetes agent protects the mouse brain from defective insulin signaling caused by Alzheimer's disease-associated Abeta oligomers.* J Clin Invest, 2012. **122**(4): p. 1339-53.

217. Zhang, Y., et al., *Amyloid-beta induces hepatic insulin resistance by activating JAK2/STAT3/SOCS-1 signaling pathway.* Diabetes, 2012. **61**(6): p. 1434-43.

218. Schittek, B. and T. Sinnberg, *Biological functions of casein kinase 1 isoforms and putative roles in tumorigenesis.* Mol Cancer, 2014. **13**: p. 231.

219. Ghoshal, N., et al., *A new molecular link between the fibrillar and granulovacuolar lesions of Alzheimer's disease.* Am J Pathol, 1999. **155**(4): p. 1163-72.

220. Kannanayakal, T.J., et al., *Casein kinase-1 isoforms differentially associate with neurofibrillary and granulovacuolar degeneration lesions.* Acta Neuropathol, 2006. **111**(5): p. 413-21.

221. van der Heide, L.P., et al., *Insulin modulates hippocampal activity-dependent synaptic plasticity in a N-methyl-d-aspartate receptor and*

phosphatidyl-inositol-3-kinase-dependent manner. J Neurochem, 2005. **94**(4): p. 1158-66.

222. Chiu, S.L., C.M. Chen, and H.T. Cline, *Insulin receptor signaling regulates synapse number, dendritic plasticity, and circuit function in vivo.* Neuron, 2008. **58**(5): p. 708-19.

223. Lee, C.C., C.C. Huang, and K.S. Hsu, *Insulin promotes dendritic spine and synapse formation by the PI3K/Akt/mTOR and Rac1 signaling pathways.* Neuropharmacology, 2011. **61**(4): p. 867-79.

224. De Felice, F.G., *Alzheimer's disease and insulin resistance: translating basic science into clinical applications.* J Clin Invest, 2013. **123**(2): p. 531-9.

225. Benedict, C. and C.A. Grillo, *Insulin Resistance as a Therapeutic Target in the Treatment of Alzheimer's Disease: A State-of-the-Art Review.* Front Neurosci, 2018. **12**: p. 215.

226. Akter, K., et al., *Diabetes mellitus and Alzheimer's disease: shared pathology and treatment?* Br J Clin Pharmacol, 2011. **71**(3): p. 365-76.

227. Rivera, E.J., et al., *Insulin and insulin-like growth factor expression and function deteriorate with progression of Alzheimer's disease: link to brain reductions in acetylcholine.* J Alzheimers Dis, 2005. **8**(3): p. 247-68.

228. Ahmed, S., Z. Mahmood, and S. Zahid, *Linking insulin with Alzheimer's disease: emergence as type III diabetes.* Neurol Sci, 2015. **36**(10): p. 1763-9.

229. de la Monte, S.M., et al., *Therapeutic rescue of neurodegeneration in experimental type 3 diabetes: relevance to Alzheimer's disease.* J Alzheimers Dis, 2006. **10**(1): p. 89-109.

230. de la Monte, S.M., *Type 3 diabetes is sporadic Alzheimers disease: mini-review.* Eur Neuropsychopharmacol, 2014. **24**(12): p. 1954-60.

231. Schwartz, M.W., et al., *Insulin binding to brain capillaries is reduced in genetically obese, hyperinsulinemic Zucker rats.* Peptides, 1990. **11**(3): p. 467-72.

232. Wallum, B.J., et al., *Cerebrospinal fluid insulin levels increase during intravenous insulin infusions in man.* J Clin Endocrinol Metab, 1987. **64**(1): p. 190-4.

233. de la Monte, S.M., *Relationships between diabetes and cognitive impairment.* Endocrinol Metab Clin North Am, 2014. **43**(1): p. 245-67.

234. Watson, G.S. and S. Craft, *Modulation of memory by insulin and glucose: neuropsychological observations in Alzheimer's disease.* Eur J Pharmacol, 2004. **490**(1-3): p. 97-113.

235. Lourenco, M.V., et al., *TNF-alpha mediates PKR-dependent memory impairment and brain IRS-1 inhibition induced by Alzheimer's beta-amyloid oligomers in mice and monkeys.* Cell Metab, 2013. **18**(6): p. 831-43.

236. Velazquez, R., et al., *Central insulin dysregulation and energy dyshomeostasis in two mouse models of Alzheimer's disease.* Neurobiol Aging, 2017. **58**: p. 1-13.

237. Vandal, M., et al., *Age-dependent impairment of glucose tolerance in the 3xTg-AD mouse model of Alzheimer's disease.* FASEB J, 2015. **29**(10): p. 4273-84.

238. Head, E., *Neurobiology of the aging dog.* Age (Dordr), 2011. **33**(3): p. 485-96.

239. Siwak, C.T., P.D. Tapp, and N.W. Milgram, *Effect of age and level of cognitive function on spontaneous and exploratory behaviors in the beagle dog.* Learn Mem, 2001. **8**(6): p. 317-25.

240. Shimada, A., et al., *An immunohistochemical and ultrastructural study on age-related astrocytic gliosis in the central nervous system of dogs.* J Vet Med Sci, 1992. **54**(1): p. 29-36.

241. Kiatipattanasakul, W., et al., *Lectin histochemistry in the aged dog brain.* Acta Neuropathol, 1998. **95**(3): p. 261-8.

242. Pugliese, M., et al., *Canine cognitive deficit correlates with diffuse plaque maturation and S100beta (-) astrocytosis but not with insulin cerebrospinal fluid level.* Acta Neuropathol, 2006. **111**(6): p. 519-28.

243. Pugliese, M., et al., *Canine cognitive dysfunction and the cerebellum: acetylcholinesterase reduction, neuronal and glial changes.* Brain Res, 2007. **1139**: p. 85-94.

244. Hwang, I.K., et al., *Changes in glial fibrillary acidic protein immunoreactivity in the dentate gyrus and hippocampus proper of adult and aged dogs.* J Vet Med Sci, 2008. **70**(9): p. 965-9.

245. Swanson, K.S., et al., *Implications of age and diet on canine cerebral cortex transcription.* Neurobiol Aging, 2009. **30**(8): p. 1314-26.

246. Lowseth, L.A., et al., *The effects of aging on hematology and serum chemistry values in the beagle dog.* Vet Clin Pathol, 1990. **19**(1): p. 13-19.

247. Kaspar, L.V. and W.P. Norris, *Serum chemistry values of normal dogs (beagles): associations with age, sex, and family line.* Lab Anim Sci, 1977. **27**(6): p. 980-5.

248. Hinds, T.D., Jr., et al., *Biliverdin Reductase A Attenuates Hepatic Steatosis by Inhibition of Glycogen Synthase Kinase (GSK) 3beta Phosphorylation of Serine 73 of Peroxisome Proliferator-activated Receptor (PPAR) alpha.* J Biol Chem, 2016. **291**(48): p. 25179-25191.

249. O'Brien, L., et al., *Biliverdin reductase isozymes in metabolism.* Trends Endocrinol Metab, 2015. **26**(4): p. 212-20.

250. Fujimaki, S. and T. Kuwabara, *Diabetes-Induced Dysfunction of Mitochondria and Stem Cells in Skeletal Muscle and the Nervous System.* Int J Mol Sci, 2017. **18**(10).

251. Newsholme, P., C. Gaudel, and M. Krause, *Mitochondria and diabetes. An intriguing pathogenetic role.* Adv Exp Med Biol, 2012. **942**: p. 235-47.

252. Logan, S., et al., *Insulin-like growth factor receptor signaling regulates working memory, mitochondrial metabolism, and amyloid-beta uptake in astrocytes.* Mol Metab, 2018. **9**: p. 141-155.

253. Di Domenico, F., et al., *The Triangle of Death in Alzheimer's Disease Brain: The Aberrant Cross-Talk Among Energy Metabolism, Mammalian Target of Rapamycin Signaling, and Protein Homeostasis Revealed by Redox Proteomics.* Antioxid Redox Signal, 2017. **26**(8): p. 364-387.

254. Association, A.s., *Alzheimer's Disease Facts and Figures.* Alzheimers Dement, 2017. **13**: p. 325-373.

255. Diehl, T., R. Mullins, and D. Kapogiannis, *Insulin resistance in Alzheimer's disease.* Transl Res, 2017. **183**: p. 26-40.

256. Craft, S., et al., *Intranasal insulin therapy for Alzheimer disease and amnestic mild cognitive impairment: a pilot clinical trial.* Arch Neurol, 2012. **69**(1): p. 29-38.

257. Reger, M.A., et al., *Effects of intranasal insulin on cognition in memory-impaired older adults: modulation by APOE genotype.* Neurobiol Aging, 2006. **27**(3): p. 451-8.

258. Reger, M.A., et al., *Intranasal insulin administration dose-dependently modulates verbal memory and plasma amyloid-beta in memory-impaired older adults.* J Alzheimers Dis, 2008. **13**(3): p. 323-31.

259. Reger, M.A., et al., *Intranasal insulin improves cognition and modulates beta-amyloid in early AD.* Neurology, 2008. **70**(6): p. 440-8.

260. Benedict, C., et al., *Intranasal insulin improves memory in humans: superiority of insulin aspart.* Neuropsychopharmacology, 2007. **32**(1): p. 239-43.

261. Chapman, C.D., et al., *Intranasal treatment of central nervous system dysfunction in humans.* Pharm Res, 2013. **30**(10): p. 2475-84.

262. Buckner, R.L., et al., *Molecular, structural, and functional characterization of Alzheimer's disease: evidence for a relationship between default activity, amyloid, and memory.* J Neurosci, 2005. **25**(34): p. 7709-17.

263. Vlassenko, A.G., et al., *Spatial correlation between brain aerobic glycolysis and amyloid-beta (Abeta) deposition.* Proc Natl Acad Sci U S A, 2010. **107**(41): p. 17763-7.

264. Bero, A.W., et al., *Neuronal activity regulates the regional vulnerability to amyloid-beta deposition.* Nat Neurosci, 2011. **14**(6): p. 750-6.

265. Oh, H., et al., *Dynamic relationships between age, amyloid-beta deposition, and glucose metabolism link to the regional vulnerability to Alzheimer's disease.* Brain, 2016. **139**(Pt 8): p. 2275-89.

266. Willette, A.A., et al., *Insulin resistance predicts medial temporal hypermetabolism in mild cognitive impairment conversion to Alzheimer disease.* Diabetes, 2015. **64**(6): p. 1933-40.

267. Marks, D.R., et al., *Awake intranasal insulin delivery modifies protein complexes and alters memory, anxiety, and olfactory behaviors.* J Neurosci, 2009. **29**(20): p. 6734-51.

268. Bedse, G., et al., *Aberrant insulin signaling in Alzheimer's disease: current knowledge.* Front Neurosci, 2015. **9**: p. 204.

269. Carlson, C.J., M.F. White, and C.M. Rondinone, *Mammalian target of rapamycin regulates IRS-1 serine 307 phosphorylation.* Biochem Biophys Res Commun, 2004. **316**(2): p. 533-9.

270. Caccamo, A., et al., *Molecular interplay between mammalian target of rapamycin (mTOR), amyloid-beta, and Tau: effects on cognitive impairments.* J Biol Chem, 2010. **285**(17): p. 13107-20.

271. Caccamo, A., et al., *Naturally secreted amyloid-beta increases mammalian target of rapamycin (mTOR) activity via a PRAS40-mediated mechanism.* J Biol Chem, 2011. **286**(11): p. 8924-32.

272. Oddo, S., *The role of mTOR signaling in Alzheimer disease.* Front Biosci (Schol Ed), 2012. **4**: p. 941-52.

273. Bove, J., M. Martinez-Vicente, and M. Vila, *Fighting neurodegeneration with rapamycin: mechanistic insights.* Nat Rev Neurosci, 2011. **12**(8): p. 437-52.

274. Gratuze, M., et al., *Insulin deprivation induces PP2A inhibition and tau hyperphosphorylation in hTau mice, a model of Alzheimer's disease-like tau pathology.* Sci Rep, 2017. **7**: p. 46359.

275. van der Harg, J.M., et al., *Insulin deficiency results in reversible protein kinase A activation and tau phosphorylation.* Neurobiol Dis, 2017. **103**: p. 163-173.

276. Yang, Y., et al., *Intranasal insulin ameliorates tau hyperphosphorylation in a rat model of type 2 diabetes.* J Alzheimers Dis, 2013. **33**(2): p. 329-38.

277. Chen, Y., et al., *Intranasal insulin prevents anesthesia-induced hyperphosphorylation of tau in 3xTg-AD mice.* Front Aging Neurosci, 2014. **6**: p. 100.

278. Gispen, W.H. and G.J. Biessels, *Cognition and synaptic plasticity in diabetes mellitus.* Trends Neurosci, 2000. **23**(11): p. 542-9.

279. Skeberdis, V.A., et al., *Insulin promotes rapid delivery of N-methyl-D- aspartate receptors to the cell surface by exocytosis.* Proc Natl Acad Sci U S A, 2001. **98**(6): p. 3561-6.

10. APPENDIX

APPENDIX A

BBA - Molecular Basis of Disease 1864 (2018) 3181–3194

Contents lists available at ScienceDirect

BBA - Molecular Basis of Disease

journal homepage: www.elsevier.com/locate/bbadis

Biliverdin reductase-A impairment links brain insulin resistance with increased Aβ production in an animal model of aging: Implications for Alzheimer disease

Francesca Triani[a], Antonella Tramutola[a], Fabio Di Domenico[a], Nidhi Sharma[a], D. Allan Butterfield[b,c], Elizabeth Head[c,d], Marzia Perluigi[a], Eugenio Barone[a,c,*]

[a] Department of Biochemical Sciences "A. Rossi-Fanelli", Sapienza University of Rome, Piazzale A. Moro 5, 00185 Roma, Italy
[b] Department of Chemistry, Markey Cancer Center, and Sanders-Brown Center on Aging, University of Kentucky, Lexington, KY 40506-0055, USA
[c] University of Kentucky, Sanders-Brown Center on Aging, 800 South Limestone Street, Lexington, KY 40536, United States
[d] University of Kentucky, Department of Pharmacology & Nutritional Sciences, Lexington, KY 40536, United States
[e] Universidad Autónoma de Chile, Instituto de Ciencias Biomédicas, Facultad de Salud, Avenida Pedro de Valdivia 425, Providencia, Santiago, Chile

ARTICLE INFO

Keywords:
Alzheimer disease
BACE1
Biliverdin reductase-A
Canine
Dog
Insulin resistance

ABSTRACT

Brain insulin resistance is associated with an increased Aβ production in AD although the molecular mechanisms underlying this link are still largely unknown. Biliverdin reductase-A (BVR-A) is a unique Ser/Thr/Tyr kinase regulating insulin signalling. Studies from our group, demonstrated that BVR-A impairment is among the earliest events favoring brain insulin resistance development. Furthermore, reported a negative association between BVR-A protein levels/activation and BACE1 protein levels in the parietal cortex of aged beagles (an animal model of AD), thus suggesting a possible interaction. Therefore, we aimed to demonstrate that BVR-A impairment is a molecular bridge linking brain insulin resistance with increased Aβ production. Age-associated changes of BVR-A, BACE1, insulin signalling cascade and APP processing were evaluated in the parietal cortex of beagles and experiments to confirm the hypothesized mechanism(s) have been performed in vitro in HEK293APPswe cells. Our results show that BVR-A impairment occurs early with age and is associated with brain insulin resistance. Furthermore, we demonstrate that BVR-A impairment favors CK1-mediated Ser phosphorylation of BACE1 (known to mediate BACE1 recycling to plasma membrane) along with increased Aβ production in the parietal cortex, with age. Overall, our results suggest that the impairment of BVR-A is an early molecular event contributing to both (I) the onset of brain insulin resistance and (II) the increased Aβ production observed in AD. We, therefore, suggest that by targeting BVR-A activity it could be possible to delay the onset of brain insulin resistance along with an improved regulation of the APP processing.

1. Introduction

Alzheimer disease (AD) is the most common cause of dementia and a primary age-related neurodegenerative disorder [1]. Aβ is thought to play a central role in the pathogenesis of AD: (i) high levels of Aβ small oligomers markedly reduce synaptic plasticity, thus favoring learning and memory deficits [2,3] (ii) accumulation of Aβ peptides into fibrillar deposits is associated with extensive neuronal loss [4] and (iii) Aβ impairs mitochondrial redox activity, increases the generation of reactive oxygen (ROS) and reactive nitrogen species (RNS), which in turn contribute to lipid and protein damage [5,6]. Impairment of brain insulin signalling, known as brain insulin resistance, has been proposed to have a role in the production and accumulation of Aβ in AD [7–10]. Consequently, as in a vicious cycle, increased Aβ oligomer generation, further exacerbates brain insulin resistance through the down-regulation the of the insulin receptor (IR) [11]. Subsequently, the activation of neuronal tumor necrosis factor-alpha (TNF-α) receptor along with the aberrant activation of stress-regulated kinases leads to insulin receptor substrate 1 (IRS1) inhibition [12,13].

From a molecular point of view, Aβ is generated following the sequential cleavage of the amyloid precursor protein (APP) by two enzymes, i.e., β-site APP cleaving enzyme 1 (BACE 1) and γ-secretase, which drive the amyloidogenic pathway [14,15]. BACE1 is the rate-limiting enzyme in the process leading to Aβ generation [15]. Among the mechanisms proposed to regulate BACE1 activity, it has been reported that mature BACE1 is internalized from the cell surface to early

* Corresponding author at: Department of Biochemical Sciences "A. Rossi-Fanelli", Sapienza University of Rome, Piazzale A. Moro 5, 00185 Rome, Italy.
E-mail address: eugenio.barone@uniroma1.it (E. Barone).

https://doi.org/10.1016/j.bbadis.2018.07.005
Received 19 May 2018; Received in revised form 21 June 2018; Accepted 3 July 2018
Available online 05 July 2018
0925-4439/

APPENDIX B

Molecular Neurobiology
https://doi.org/10.1007/s12035-018-1231-5

Biliverdin Reductase-A Mediates the Beneficial Effects of Intranasal Insulin in Alzheimer Disease

Eugenio Barone[1,2] · Antonella Tramutola[1] · Francesca Triani[1] · Silvio Calcagnini[3] · Fabio Di Domenico[1] · Cristian Ripoli[4] · Silvana Gaetani[3] · Claudio Grassi[4,5] · D Allan Butterfield[6] · Tommaso Cassano[7] · Marzia Perluigi[1]

Received: 1 May 2018 / Accepted: 10 July 2018

Abstract
Impairment of biliverdin reductase-A (BVR-A) is an early event leading to brain insulin resistance in AD. Intranasal insulin (INI) administration is under evaluation as a strategy to alleviate brain insulin resistance; however, the molecular mechanisms underlying INI beneficial effects are still unclear. We show that INI improves insulin signaling activation in the hippocampus and cortex of adult and aged 3×Tg-AD mice by ameliorating BVR-A activation. These changes were associated with a reduction of nitrosative stress, Tau phosphorylation, and Aβ oligomers in brain, along with improved cognitive functions. The role of BVR-A was strengthened by showing that cells lacking BVR-A: (i) develop insulin resistance if treated with insulin and (ii) can be recovered from insulin resistance only if treated with a BVR-A-mimetic peptide. These novel findings shed light on the mechanisms underlying INI treatment effects and suggest BVR-A as potential therapeutic target to prevent brain insulin resistance in AD.

Keywords Alzheimer disease · Biliverdin reductase-A · Insulin resistance · Intranasal · Neuroprotection

Introduction

As populations age, the chronic diseases of older adults become increasingly important, not least to health systems and economies. Alzheimer disease (AD) has no proven preventative or behavioral intervention, and the currently approved pharmacological treatments are only modestly effective. The failure of insulin signaling, known as brain insulin resistance, heavily impacts the core pathological processes of AD since insulin regulates brain metabolism, cognitive functions, and life span [1, 2]. Examination of postmortem AD and amnestic mild cognitive impairment brain uncovered key signs of brain insulin resistance, i.e., reduced insulin receptor (IR) and increased serine phosphorylation (inhibitory) of insulin receptor substrate 1 (IRS1), particularly in the hippocampus, cortex, and hypothalamus [1–3]. Higher levels of insulin resistance markers are associated with poorer performance on cognitive tests of episodic and working memory, independent of the senile plaques and tangles load, thus suggesting a role for insulin signaling in neuronal functions [2].

Electronic supplementary material The online version of this article (https://doi.org/10.1007/s12035-018-1231-5) contains supplementary material, which is available to authorized users.

✉ Tommaso Cassano
tommaso.cassano@unifg.it

✉ Marzia Perluigi
marzia.perluigi@uniroma1.it

[1] Department of Biochemical Sciences "A. Rossi-Fanelli", Sapienza University of Rome, Piazzale A. Moro 5, 00185 Rome, Italy

[2] Instituto de Ciencias Biomédicas, Facultad de Salud, Universidad Autónoma de Chile, Avenida Pedro de Valdivia 425, Providencia, Santiago, Chile

[3] Department of Physiology and Pharmacology "V. Erspamer", Sapienza University of Rome, Piazzale A. Moro 5, 00185 Rome, Italy

[4] Institute of Human Physiology, Università Cattolica Medical School, 00168 Rome, Italy

[5] Fondazione Policlinico Universitario A. Gemelli, 00168 Rome, Italy

[6] Department of Chemistry, Markey Cancer Center, and Sanders-Brown Center on Aging, University of Kentucky, Lexington, KY 40506-0055, USA

[7] Department of Clinical and Experimental Medicine, University of Foggia, Via L. Pinto, 71122 Foggia, Italy

Published online: 02 August 2018

APPENDIX C

Neurobiology of Disease 118 (2018) 129–141

Contents lists available at ScienceDirect

Neurobiology of Disease

journal homepage: www.elsevier.com/locate/ynbdi

Poly-ubiquitin profile in Alzheimer disease brain

Antonella Tramutola[a], Francesca Triani[a], Fabio Di Domenico[a], Eugenio Barone[a], Jian Cai[b], Jon B. Klein[b], Marzia Perluigi[a], D. Allan Butterfield[c,d,*]

[a] Department of Biochemical Sciences, Sapienza University of Rome, Italy
[b] Department of Nephrology and Proteomics Center, University of Louisville, Louisville, KY, USA
[c] Sanders-Brown Center on Aging, University of Kentucky, Lexington, KY, USA
[d] Department of Chemistry, University of Kentucky, Lexington, KY, USA

ARTICLE INFO

Keywords:
Polyubiquitinylation
Alzheimer disease brain
Proteomics
Contribution to neurodegeneration

ABSTRACT

Alzheimer disease (AD) is a neurodegenerative disorder characterized by progressive loss of memory, reasoning and other cognitive functions. Pathologically, patients with AD are characterized by deposition of senile plaques (SPs), formed by β-amyloid (Aβ), and neurofibrillary tangles (NTFs) that consist of aggregated hyperphosphorylated tau protein. The accumulation of insoluble protein aggregates in AD brain can be associated with an impairment of degradative systems. This current study investigated if the disturbance of protein poly-ubiquitination is associated with AD neurodegeneration. By using a novel proteomic approach, we found that 13 brain proteins are increasingly polyubiquitinated in AD human brain compared to age-matched controls. Moreover, the majority of the identified proteins were previously found to be oxidized in our prior proteomics, and these proteins are mainly involved in protein quality control and glucose metabolism. This is the first study showing alteration of the poly-ubiquitin profile in AD brain compared with healthy controls. Understanding the onset of the altered ubiquitin profile in AD brain may contribute to identification of key molecular regulators of cognitive decline. In AD, deficits of the proteolytic system may further exacerbate the accumulation of oxidized/misfolded/polyubiquitinated proteins that are not efficiently degraded and may become harmful to neurons and contribute to AD neuropathology and cognitive decline.

1. Introduction

Alzheimer disease (AD) is the most prevalent form of dementia in the elderly. The symptoms of AD include a progressive decline in memory and other cognitive functions. Histologically, AD cases present extensive neurodegeneration and loss of synaptic connections, resulting in progressive atrophy of the temporal, frontal and parietal lobes of the cerebral cortex, areas that are especially critical for learning and memory formation. The two pathophysiological hallmarks of AD are deposition of intracellular, filamentous aggregates mainly consisting of hyperphosphorylated tau (neurofibrillary tangles, NFTs) and extracellular plaques rich in amyloid-beta (Aβ) (Glabe, 2005). Degradation of Aβ or tau by the ubiquitin–proteasome system (UPS), as the main intracellular proteolytic pathway in eukaryotic cells, has been gaining attention in AD research field (Grimm et al., 2011; Stadtman and Levine, 2000). Several studies demonstrate that UPS integrity is required for normal lifespan, and the identification of ubiquitin-dependent degradation pathways that specifically control the "steady-state" levels of lifespan regulators further highlights a key role of the UPS in the aging process and age-related diseases (Dantuma and Bott, 2014). Keller et al. demonstrated decreased proteasome activities in AD brain (Keller et al., 2000). An impairment of the UPS can be a principal cause of protein aggregation and accumulation in the brain of persons with AD, and all these features can lead to extensive neurodegeneration and loss of synaptic connections.

Most proteins designated for destruction by UPS are first tagged by a polyubiquitin chain (Goldberg, 2003). Ubiquitinylated forms of tau and Aβ are well known and probably are among the major components of the protein aggregates noted in AD (Perry et al., 1987). This highly regulated process, divided in three steps (activation, conjugation and ligation), adds ubiquitin to target lysine residues on the substrate, and these same processes can also add other ubiquitin molecules onto lysine of a ubiquitin already conjugated to a protein substrate. By this process, ubiquitin chains of varying lengths and composition can be formed. The elongation of ubiquitin chains can occur at any of ubiquitin's own seven lysines, resulting in the formation of different linkage types (Peng et al., 2003). Although all possible linkage types are present in cells, their precise functions remain only partially understood. Polyubiquitination

* Corresponding author at: Department of Chemistry and Sanders-Brown Center on Aging, University of Kentucky, Lexington, KY 40506, USA.
E-mail address: dabcns@uky.edu (D.A. Butterfield).

https://doi.org/10.1016/j.nbd.2018.07.006
Received 6 September 2017; Received in revised form 23 June 2018; Accepted 4 July 2018
Available online 09 July 2018
0969-9961/

APPENDIX D

Protein nitration profile of $CD3^+$ lymphocytes from Alzheimer disease patients: Novel hints on immunosenescence and biomarker detection.

Antonella Tramutola[a1], Giulia Abate[b1], Chiara Lanzillotta[a], Francesca Triani[a], Eugenio Barone[a], Federica Iavarone[c], Federica Vincenzoni[c], Massimo Castagnola[c], Mariagrazia Marziano[b], Maurizio Memo[b], Emirena Garrafa[b], D. Allan Butterfield[d], Marzia Perluigi[a], Fabio Di Domenico[*a23], Daniela Uberti[b24]

[a]Department of Biochemical Sciences, Sapienza University of Rome, Rome, Italy
[b]Department of Biomedical Sciences and Biotechnologies, University of Brescia, Brescia, Italy
[c]Istituto di Biochimica e Biochimica Clinica, Università Cattolica, and/or Dip. di Diagnostica di Laboratorio e Malattie Infettive, Fondazione Policlinico Universitario A. Gemelli, IRCCS, Rome-Italy
[d]Department of Chemistry and Sanders-Brown Center on Aging, University of Kentucky, Lexington, KY, USA

[*]**Corresponding Authors.**

ABSTRACT:

Alzheimer's disease (AD) is a progressive form of dementia characterized by increased production of amyloid-β plaques and hyperphosphorylated tau protein, mitochondrial dysfunction, elevated oxidative stress, reduced protein clearance, among other. Several studies showed systemic modifications of immune and inflammatory systems due, in part, to decreased levels of $CD3^+$ lymphocytes in peripheral blood in AD. Considering that oxidative stress, both in the brain and in the periphery, can influence the activation and differentiation of T-cells, we investigated the 3-nitrotyrosine (3-NT)

[1] Authors contributed equally to this work
[2] Co-corresponding authors
[3] PhD, Department of Biochemical Sciences, Sapienza University of Rome, P.le Aldo Moro 5, Rome, Italy, 00185 fabio.didomenico@uniroma1.it
[4] PhD, Department of Molecular and Translational Medicine, University of Brescia, 25123 Brescia, Italy; daniela.uberti@unibs.it

Dopo 3 anni questo percorso ricco di emozioni e dispiaceri è giunto alla fine. Ovviamente in ogni percorso ci sono persone che hanno avuto un ruolo molto importante alle quali vorrei dire grazie.

Eugenio, mi sembra giusto iniziare da te, anche se abbiamo avuto un rapporto molto altalenante soprattutto nell'ultimo periodo, sei stato un ottimo "MENTORE". Mi hai sempre spronato a fare di più e sei sempre stato disponibile. Se sono diventata quello che sono è anche merito tuo.

Liz, thank you so much for this amazing opportunity. You made me feel as a component of your group from the first day, making me feel at home and very welcome. You have made me grow so much both from a personal and professional point of view. I will treasure your advices forever.

Vorrei ringraziare Marzia per avermi accolta nel suo gruppo e Fabio, la tua passione per la ricerca e la tua umiltà non sai quanto mi hanno spronato.

Un grazie speciale va ad Antonella, Chiara e Andrea per l'aiuto che mi hanno dato in questi anni passati insieme.

Ringrazio tutti i ragazzi che hanno frequentato il lab 316 e condiviso con me questo percorso (Nidhi, Anna, Andrea (Scoma) e Graziella) e le Professoresse del 3° piano.

Gina, ho trovato in te un'amica. Ti auguro il meglio perché te lo meriti e sai anche che a casa mia ci sarà sempre uno spazzolino per te.

Maria e Flavia, un semplice grazie non racchiuderebbe tutto quello che avete fatto per me. Siete e sarete sempre la mia ancóra ovunque il destino ci porterà.

Giorgina, che dirti? La nostra amicizia è stata un po' come un uragano, in un secondo ci siamo ritrovate amiche senza neanche accorgercene. Grazie per aver sempre creduto in me e incoraggiata a fare del mio meglio.

Alex, Margo and Katie thank you for making my experience in Head Lab fabulous.

Diana, sei stata la mia piccola famiglia nella “ridente” Lexington. Hai fatto tanto per me e per questo te ne sarò per sempre grata.
Ringrazio la mia famiglia che mi è sempre stata accanto e mi ha sempre supportato in tutte le scelte fatte in questi anni.
Il grazie più grande va a te Alessandro.

Francesca